FAST CALCULATION OF FLOW ENSEMBLES

by

Nan Jiang

B.S. in Information & Computing Science,

Xi'an Jiaotong University, 2010

Submitted to the Graduate Faculty of

the Kenneth P. Dietrich Graduate School of Arts and Sciences in

partial fulfillment

of the requirements for the degree of

Doctor of Philosophy

University of Pittsburgh

2014

UNIVERSITY OF PITTSBURGH

DIETRICH GRADUATE SCHOOL OF ARTS AND SCIENCES

This dissertation was presented

by

Nan Jiang

It was defended on

December 3, 2014

and approved by

Prof. William Layton, Dept. of Mathematics, University of Pittsburgh

Prof. Ivan Yotov, Dept. of Mathematics, University of Pittsburgh

Prof. Catalin Trenchea, Dept. of Mathematics, University of Pittsburgh

Prof. Paolo Zunino, Dept. of Mechanical Engineering and Materials Science, University of Pittsburgh

Dissertation Director: Prof. William Layton, Dept. of Mathematics, University of Pittsburgh

FAST CALCULATION OF FLOW ENSEMBLES

Nan Jiang, PhD

University of Pittsburgh, 2014

Computing Ensembles occurs frequently in the simulation of complex flows to increase forecasting skill, quantify uncertainty and estimate flow sensitivity. The main issue with ensemble calculation is its high demand of computer resources vs. the limited computer resources existing. Generally computing a large ensemble is prohibitive due to the high computational cost of numerical simulation of nonlinear dynamical systems. Moreover, to compute ensembles of moderate/small size, resolution is very often sacrificed to reduce computation time. In this thesis, we study an efficient ensemble simulation algorithm that can reduce the computing cost significantly making computing a large ensemble or an ensemble of high resolution possible.

The motivation for the new algorithm is that for linearly implicit methods, the linear solve is a large contributor to overall complexity and it is far cheaper in both storage and solution time to solve linear systems with the same coefficient matrix than with different coefficient matrices. We present this algorithm with different ensemble time stepping methods. These methods are carefully derived and both theoretically and numerically investigated.

Computing an ensemble simultaneously allows each realization to access ensemble data and the use of means and fluctuations in numerical regularizations for each realization. We put forth two ensemble eddy viscosity regularizations that remove severe timestep condition for high Reynolds number flows. The study of the ensemble eddy viscosity regularizations also suggests reconsidering an old but not as well developed definition of the mixing length. This mixing length vanishes at solid walls without van Driest damping, increases stability and improves flow predictions in our preliminary tests.

The goal of conventional turbulence models is to produce a model that accurately predicts time averaged or ensemble averaged flow statistics. In this thesis, we develop a new family of ensemble based turbulence models and study their convergence by analyzing the evolution of model variance. For these new turbulence models from the calculated ensemble (at low cost), the kinetic energy in fluctuations can be directly calculated without additional modeling, reducing the computing cost while increasing the physical fidelity of the models.

Keywords: Navier-Stokes equations, ensemble calculation, numerical regularization, eddy viscosity, turbulence modeling.

TABLE OF CONTENTS

LIST OF TABLES

LIST OF FIGURES

PREFACE

First and foremost, I would like to express my most sincere gratitude to my advisor, Dr. William Layton, for his enthusiastic support and guidance through every step of my graduate studies. I have learned so much from his unique perspective on research and his personal integrity and expectations of excellence. His door was always open whenever I ran into a trouble spot with my research and he has always been patient and inspiring. I am so glad to have him as my advisor and enjoy very much working with him.

I am also deeply grateful to Dr. Catalin Trenchea for his support and many valuable discussions and suggestions in my research. I would also like to thank Dr. Ivan Yotov for his stimulating lectures on various topics in computational fluid dynamics, from which my research has greatly benefited. I also wish to thank Dr. Paolo Zunino for his insightful comments on this thesis and suggestions on the future directions of my research.

I wish to express my thanks to my fellow graduate students, Nick Hurl, Michaela Kubacki, Yong Li, Marina Moraiti, Aziz Takhirov, Hoang Tran and Xin Xiong. I have enjoyed our time together studying mathematics and doing research. Besides, I have obtained so much support from them along the way.

A special thank to Dr. Mike Sussman for spending time reading my numerical results and providing help with programming.

Last but not the least, I would like to thank my parents Qiuxiang Zhao and Zhijie Jiang, for their constant love and encouragement. Without their support, this thesis could not have been possible.

1.0 INTRODUCTION

There are many uncertainties inherent in predicting flow motion by numerical simulations. A major source of uncertainty is the imperfect initial conditions. Due to the nonlinear nature of dynamic systems that are of most interest to engineers and scientists, tiny errors in the initial state will be amplified and grows quickly as time advances. The imperfection of the numerical models used, such as the inaccurate model parameters, will also introduce errors. Computing ensembles deals with these uncertainties. Instead of running just a single forecast, the computer model is run a number of times from slightly different starting conditions (and/or different model parameters, which is application dependent). The predicted ensemble provides important statistics to quantify uncertainties and a basis for decision-making. For instance, today ensemble forecasting is an indispensable modern numerical weather prediction method and plays an important role in determining the forecast of the possible future tracks of developing depressions that may evolve into hurricanes.

Performing ensemble calculation leads to an inevitable increase in computational cost. Computing a large ensemble is not practicable in most flows of engineering interest, yet highly desirable in some applications. Even to compute ensembles of moderate size, resolution is very often sacrificed to reduce computation time. For geophysical problems with large computational domains, the current computational resources can only allow computing a very small ensemble even with resolution reduced at certain time intervals. An efficient ensemble simulation algorithm that can reduce the computing cost significantly is thus highly desirable.

The fundamental dynamics of fluid motion is described by the Navier-Stokes equations. In this thesis, we study an efficient algorithm for fast calculation of Navier-Stokes equations. The algorithm results in linear systems with the same coefficient matrix at each timestep,

which allows the use of special methods, such as the block generalized CG method, reducing both storage and computing time significantly. We propose and study ensemble simulation methods for both small and large Reynolds number flows. For high Reynolds number flow, we study two ensemble eddy viscosity regularizations that relax/remove severe timestep condition.

Turbulence is ubiquitous in nature and engineering applications. In principle, it is simply a solution to the Navier-Stokes equations. However, direct numerical simulation (DNS) is not feasible for most turbulent flows due to the extremely small-scales motion featured in turbulence. Engineering models seek to predict the averaged properties of the flow without resolving the chaotic, small-scale motion. Based on different averaging operators, there are various approaches to turbulence modeling (Reynolds Averaged Navier-Stokes equations (RANS), turbulent viscosity models (e.g. $k-\epsilon$ model), large eddy simulation, e.g., [57, 3, 76, 85]). The goal of conventional turbulence models (CTMs) (such as RANS and $k-\epsilon$) is to produce a model that accurately predicts time or ensemble averaged flow statistics, [12]. Thus a CTM should quickly converge (in time) to statistical equilibrium that captures averaged flow behavior. This differs from large eddy simulation models that seek to represent the essentially dynamic behavior of local spacial averages. The latter contains more information but also requires many more degrees of freedom. We develop a new family of turbulence models and algorithms for their solutions and study their convergence to statistical equilibrium by analyzing the evolution of model variance.

In Chapter 2 we introduce some fundamental concepts and common notations used extensively in this thesis.

In Chapter 3 we present an efficient algorithm for computing an ensemble of Navier-Stokes equations. The solutions are found, at each timestep, by solving a linear system with one shared coefficient matrix and multiple right hand sides, reducing both storage required and computational cost of the solution process. The price that must be paid is a timestep condition involving the timestep and the size of the fluctuations about the ensemble mean. Since the method is a one step method and the timestep condition involves only known quantities, it can be imposed to adapt the next timestep. We give a comprehensive stability analysis, an error estimate and some first tests. The material in this chapter is based on the

paper [53].

In Chapter 4 we analyze an efficient ensemble regularization algorithm for under-resolved and convection dominated flows (including ones at higher Reynolds numbers). Computing an ensemble simultaneously allows each realization to access ensemble data. This allows use of means and fluctuations in regularizations used for each realization. The combined approach of ensemble time stepping and ensemble regularizations allows direct calculation of the turbulent viscosity coefficient and gives an unconditionally stable algorithm. It also suggests reconsidering an old but not as well developed definition of the mixing length. This mixing length vanishes at solid walls without van Driest damping, increases stability and improves flow predictions in our preliminary tests. The material in this chapter is based on the paper [54].

In Chapter 5 we present an efficient, higher order method for fast calculation of an ensemble of solutions of the Navier-Stokes equations. We give a complete stability and convergence analysis of the method for laminar flows and an extension to turbulent flows. For high Reynolds number flows, we propose and analyze an eddy viscosity regularization method. This method depends on an ensemble mean compatible with the higher order method. We show the regularization method has superior stability, also demonstrated in numerical tests. We also give tests showing the potential of the new method for exploring flow problems to compute turbulence intensities, effective Lyapunov exponents, windows of predictability and to verify the selective decay principle. The material in this chapter is based on the paper [55].

In Chapter 6 we develop an ensemble or statistical eddy viscosity model. The model is parameterized by an ensemble of solutions of an ensemble-Leray regularization. The combined approach of ensemble time stepping and ensemble eddy viscosity modeling allows direct parametrization of the turbulent viscosity coefficient that gives an unconditionally stable algorithm. We prove that the model's solution approaches statistical equilibrium as $t \to \infty$; the model's variance $\to 0$ as $t \to \infty$. The ensemble method is used to interrogate a rotating flow, testing its predictability by computing effective averaged Lyapunov exponents. The material in this chapter is based on the paper [56].

2.0 MATHEMATICAL PRELIMINARIES

In this chapter we are going to provided mathematical preliminaries on Navier-Stokes equations and related analysis tools in finite element methods.

2.1 THE NAVIER-STOKES EQUATIONS

The dynamic law that governs an incompressible, viscous fluid is the Navier-Stokes equations. In a bounded region Ω in R^2 or R^3, the fluid velocity and pressure satisfy

$$\begin{aligned} u_t + u \cdot \nabla u - \nu \Delta u + \nabla p &= f(x,t) \text{ in } \Omega, \\ \nabla \cdot u &= 0 \text{ in } \Omega, \\ u(x,0) &= u_0(x) \text{ in } \Omega. \end{aligned} \tag{2.1.1}$$

Here $u = u(x,t)$ is the fluid velocity, $p = p(x,t)$ is the pressure (normalized by the constant density ρ), ν $(= \mu/\rho$, where μ is the dynamic viscosity) is the kinematic viscosity, $\triangle$ is the Laplacian operator, i.e. $\sum_{i=1}^{N} \partial_i \partial_i$, and f is the external force (also normalized by ρ). We will use no-slip boundary condition ($u = 0$ on $\partial\Omega$) throughout this thesis. The first equation in (2.1.1) is derived by conservation of linear momentum and the second equation by conservation of mass. The Navier−Stokes equations are nonlinear partial differential equations. The nonlinearity makes most problems difficult or impossible to solve and is the main contributor to the turbulence that the equations govern.

Introduced over 180 years ago by French engineer Claude Louis Marie Henri Navier, the Navier-Stokes equations are nowadays the foundations of many branches of applied sciences,

including Meteorology, Oceanography, Geology, Oil Industry, Biology and Medicine. Over decades, these equations have seen their undisputed success in providing accurate, simple modeling of physical and engineering phenomena. Despite these success, up to the present time, there are still a number of basic mathematical questions remain unresolved, most of which are for 3d flows. The most famous one is that of proving or disproving the existence of global 3d regular flow for smooth data of any size. This is often referred to the global regularity problem. To date, the 3d regular flows are known to exist either for all times but for small data, or for data of any size but for only a finite interval of time. Properly formulated, the global regularity problem is listed as one of Clay prize problems.

Now let us non-dimensionalize the Navier-Stokes equations by rescaling the variables

$$\tilde{u} = u/U, \tilde{p} = p/U^2, \tilde{x} = x/L, \text{ and } \tilde{t} = tU/L. \tag{2.1.2}$$

Here L is the characteristic length of the domain and U is the characteristic velocity. Then the Navier-Stokes equations become

$$\begin{aligned} \tilde{u}_t + \tilde{u} \cdot \nabla \tilde{u} - \frac{1}{Re} \Delta \tilde{u} + \nabla \tilde{p} &= \frac{L}{U^2} f(x,t) \text{ in } \Omega, \\ \nabla \cdot \tilde{u} &= 0 \text{ in } \Omega, \end{aligned} \tag{2.1.3}$$

where

$$Re = \frac{LU}{\nu}.$$

It is called the Reynolds number. In fluid dynamics, the Reynolds number plays an important role to help predict similar flow patterns in different fluid flow situations. It is roughly defined as the ratio of inertial forces to viscous forces. If Re is small, then the viscous forces are dominate and the flow tends to be smooth and move slowly (laminar flow). For very large Re the flow is dominated by the inertial forces and featured by instabilities and chaotic, small-scales motion (turbulence).

2.2 ANALYSIS TOOLS

Let Ω be an open, regular domain in R^d ($d = 2$ or 3). The $L^2(\Omega)$ norm and the inner product are $\|\cdot\|$ and $(\cdot,\cdot)$. Likewise, the $L^p(\Omega)$ norms and the Sobolev $W_p^k(\Omega)$ norms are $\|\cdot\|_{L^p}$ and $\|\cdot\|_{W_p^k}$ respectively. $H^k(\Omega)$ is the Sobolev space $W_2^k(\Omega)$, with norm $\|\cdot\|_k$. For functions $v(x,t)$ defined on $(0,T)$, we define ($1 \le m < \infty$)

$$\|v\|_{\infty,k} := EssSup_{[0,T]}\|v(t,\cdot)\|_k, \text{ and } \|v\|_{m,k} := \left(\int_0^T \|v(t,\cdot)\|_k^m dt\right)^{1/m}.$$

The space $H^{-k}(\Omega)$ is the dual space of bounded linear functions on $H_0^k(\Omega)$. A norm for $H^{-1}(\Omega)$ is given by

$$\|f\|_{-1} = \sup_{0 \neq v \in H_0^1(\Omega)} \frac{(f,v)}{\|\nabla v\|}.$$

We base our analysis on the finite element method (FEM) for the spacial discretization. The results also extend to many other variational methods. Let X be the velocity space and Q be the pressure space:

$$X := (H_0^1(\Omega))^d, \; Q := L_0^2(\Omega).$$

For $v \in X$ the usual $H^{1/2}(\Omega)$ norm satisfies the interpolation inequality

$$\|v\|_{1/2} \le C\sqrt{\|v\|\|\nabla v\|}.$$

The space of divergence free functions is

$$V := \{v \in X \; : (\nabla \cdot v, q) = 0 \; , \forall q \in Q\}.$$

A weak formulation of (2.1.1) is: Find $u : [0,T] \to X$, $p : [0,T] \to Q$ for a.e. $t \in (0,T]$ satisfying:

$$(u_t, v) + (u \cdot \nabla u, v) + \nu(\nabla u, \nabla v) - (p, \nabla \cdot v) = (f, v) \; , \forall v \in X$$
$$u(x,0) = u^0(x) \text{ in X and } (\nabla \cdot u, q) = 0, \forall q \in Q.$$

Conforming velocity, pressure finite element spaces based on an edge to edge triangulation (if $d = 2$) or tetrahedralization (if $d = 3$) of Ω with maximum element diameter h are denoted by

$$X_h \subset X \ , \ Q_h \subset Q.$$

We assume the finite element spaces $(X_h,\ Q_h)$ satisfy the usual discrete inf-sup $/LBB^h$ condition for stability of the discrete pressure, see [38] for more on this condition. Taylor-Hood elements, e.g., [7], [38], are one such choice used in the tests in Section 6. The discretely divergence free subspace of X_h is

$$V_h : \ = \{v_h \in X_h : (\nabla \cdot v_h, q_h) = 0 \ , \ \forall q_h \in Q_h\}.$$

We assume the mesh and finite element spaces satisfy the following standard inequalities (typical for locally quasi-uniform meshes and standard FEM spaces, see, e.g., [7]): for all $v_h \in X_h$

$$h\|\nabla v_h\| \leq C_{(inv)}\|v_h\|, \qquad \text{(Inverse Ineq)}$$

$$\|v_h\|_\infty \leq C|\ln h|^{1/2}\|\nabla v_h\|, \text{ in dimension } d = 2. \qquad \text{(Discrete Sobolev)}$$

Define the usual explicitly skew symmetric trilinear form

$$b^*(u, v, w) := \frac{1}{2}(u \cdot \nabla v, w) - \frac{1}{2}(u \cdot \nabla w, v).$$

In both 3D and 2D, for all $u, v, w \in X$, $b^*(u, v, w)$ satisfies

$$|b^*(u, v, w)| \leq C(\Omega)\|\nabla u\|\|\nabla v\|\|\nabla w\|, \tag{2.2.1}$$

and two sharper bounds (improvable in 2D)

$$|b^*(u, v, w)| \leq C(\Omega)\|\nabla u\|^{1/2}\|u\|^{1/2}\|\nabla v\|\|\nabla w\|, \tag{2.2.2}$$

$$|b^*(u, v, w)| \leq C(\Omega)\|\nabla u\|\|\nabla v\|\|\nabla w\|^{1/2}\|w\|^{1/2}. \tag{2.2.3}$$

Lemma 1. *For any $u_h, v_h, w_h \in X_h$,*

$$b^*(u_h, v_h, w_h) = \int_\Omega u_h \cdot \nabla v_h \cdot w_h \ dx + \frac{1}{2}\int_\Omega (\nabla \cdot u_h)(v_h \cdot w_h) \ dx.$$

Proof.

$$b^*(u_h, v_h, w_h) := \frac{1}{2}(u_h \cdot \nabla v_h, w_h) - \frac{1}{2}(u_h \cdot \nabla w_h, v_h).$$

Integrating by parts the second term and using $u_h|_{\partial\Omega} = 0$:

$$-(u_h \cdot \nabla w_h, v_h) = (u_h \cdot \nabla v_h, w_h) + (\nabla \cdot u_h, v_h \cdot w_h).$$

□

C represents a positive constant independent of ν, the solution u, the time step Δt and the mesh width h. Its value may vary from situation to situation.

3.0 AN ALGORITHM FOR FAST CALCULATION OF FLOW ENEEMBLES

There are many uncertainties inherent in numerical simulation of fluid flows. Calculation of an ensemble of J solutions deals with these inherent uncertainties to increase the window of predictability (by averaging), e.g., [89], [67], [60], to estimate solution sensitivities, e.g., [75], [94] and to estimate the uncertainty in the result (by calculation of a PDF of the resulting solution), e.g., [35], [17]. Further, the bred-vectors algorithm, [89], used to select a minimal set of ensemble members capturing maximal spread of the resulting forecast itself involves repeated ensemble flow simulations. One common way to calculate these ensembles is to treat them as separate tasks, requiring computational effort and memory J-times the amount required for one simulation. If available memory is sufficient to treat the tasks in parallel, then the turnaround time is not increased, while if not then the turnaround time is multiplied by J. In this Chapter we explore a new approach ((BEFE-Ensemble) below) intermediate between these two extremes which requires a negligible storage increase over one simulation (J solution vectors) and could have run time reduced over J successive simulations, depending on the block solver used and the timestep condition required for stability. Thus the method is a new way to rebalance "the competition between high-resolution, single deterministic forecasts and ensembles" (Stensrud [86], p. 401). The motivation for the new method is that for linearly implicit methods, the linear solve is a large contributor to overall complexity and it is far cheaper in both storage and solution time to solve J linear systems with the same coefficient matrix than with J different coefficient matrices. For example, block generalized CG methods compute J residuals at each step but compensate in speed of convergence by producing approximations optimized over a $J \times (\#steps)$ dimensional Krylov subspace, e.g., [78], [29], [39], [32].

3.1 METHOD DESCRIPTIONS

Accordingly, we consider a discretization of an ensemble of J solutions of the NSE requiring solution of one linear system with the same coefficient matrix and J RHS[1]. To begin, consider J Navier-Stokes equations with J slightly different initial conditions and body forces, u_j^0, f_j, on a bounded domain subject to no slip boundary conditions, for $j = 1, ..., J$:

$$\begin{aligned} u_{j,t} + u_j \cdot \nabla u_j - \nu \triangle u_j + \nabla p_j &= f_j(x,t), \text{ in } \Omega, \\ \nabla \cdot u_j &= 0, \text{ in } \Omega, \\ u_j &= 0, \text{ on } \partial\Omega, \\ u_j(x,0) &= u_j^0(x), \text{ in } \Omega. \end{aligned} \tag{3.1.1}$$

We denote the ensemble mean by

$$< u >^n := \frac{1}{J} \sum_{j=1}^{J} u_j^n.$$

To present the idea, suppress the spacial discretization. Using an implicit-explicit time discretization and keeping the resulting coefficient matrix independent of the ensemble member, leads to the method:

$$\begin{aligned} &\frac{u_j^{n+1} - u_j^n}{\Delta t} + < u >^n \cdot \nabla u_j^{n+1} + (u_j^n - < u >^n) \cdot \nabla u_j^n \\ &+ \nabla p_j^{n+1} - \nu \Delta u_j^{n+1} = f_j^{n+1}, \\ &\nabla \cdot u_j^{n+1} = 0. \end{aligned} \tag{BEFE-Ensemble}$$

Since the resulting coefficient matrix multiplying each u_j^{n+1} is independent of j, (ensemble number), advancing one step we solve one linear system with J RHS. Naturally, if the number of ensemble members is large enough, it can be subdivided into sub-ensembles, balancing memory, communication and computations, and (BEFE-Ensemble) applied to each. Further, the choice of the ensemble data u_j^0 and f_j is application dependent.

[1] One easy method to do this is simply to lag the nonlinear terms and pay the price in the associated and severe Re dependent timestep restriction.

The ensemble mean equation. Taking the ensemble mean of (BEFE-Ensemble), $< u >^n$ satisfies

$$\begin{aligned} &\frac{< u >^{n+1} - < u >^n}{\Delta t} + < u >^n \cdot \nabla < u >^{n+1} + \nabla < p >^{n+1} - \nu \Delta < u >^{n+1} \\ &\quad + [< u \cdot \nabla u >^n - < u >^n \nabla < u >^n] =< f >^{n+1} , \text{ and} \\ &\nabla \cdot < u >^{n+1} = 0, \end{aligned} \tag{3.1.2}$$

which is a discretized variant on the usual ensemble averaged NSE.

Timestep conditions. Since (BEFE-Ensemble) involves an explicit discretization of a stretching term, a timestep restriction is necessary for long time, nonlinear stability. With an FEM spacial discretization with mesh size h, we prove in Section 3.2 that in both 2d and 3d (BEFE-Ensemble) is stable under

$$C \frac{\Delta t}{\nu h} \| \nabla (u_{j,h}^n - < u_h >^n) \|^2 \leq 1. \tag{3.1.3}$$

Thus, as long as the deviation of each ensemble member from the ensemble mean at each time step is not too big, the method is stable. When the deviation increases, the timestep must decrease according to (3.1.3). In Section 3.3 we give improvements of this condition. For example, in 2d we prove stability under

$$\frac{C ln(1/h) \Delta t}{\nu} \| \nabla (u_{j,h}^n - < u_h >^n) \|^2 \leq 1 \ .$$

We also give a condition valid for locally refined meshes, useful in cases when local mesh widths are cut to balance locally large gradients.

3.2 STABILITY OF THE ENSEMBLE METHOD

The fully discrete approximation we study of (3.1.1) is: Given $u_{j,h}^n$, find $u_{j,h}^{n+1} \in X_h$, $p_{j,h}^{n+1} \in Q_h$ satisfying

$$\begin{aligned}(\frac{u_{j,h}^{n+1}-u_{j,h}^n}{\Delta t}, v_h) + b^*(< u_h >^n, u_{j,h}^{n+1}, v_h) + b^*(u_{j,h}^n - < u_h >^n, u_{j,h}^n, v_h)\\ -(p_{j,h}^{n+1}, \nabla \cdot v_h) + \nu(\nabla u_{j,h}^{n+1}, \nabla v_h) = (f_j^{n+1}, v_h), \qquad \forall v_h \in X_h,\\ (\nabla \cdot u_{j,h}^{n+1}, q_h) = 0, \qquad \forall q_h \in Q_h.\end{aligned} \tag{3.2.1}$$

We begin by proving unconditional, nonlinear, long time stability of (3.2.1) under the first timestep condition:

$$C\frac{\Delta t}{\nu h}\|\nabla(u_{j,h}^n - < u_h >^n)\|^2 \le 1, \qquad j = 1, \cdots, J\ . \tag{3.2.2}$$

Since (3.2.2) is based on known quantities and (3.2.1) is a 1-step method, (3.2.2) can be applied to adapt $\triangle t$ at every timestep to compute u_j^{n+1} stably. Improvements of (3.2.2) in special cases are developed in Section 3.3.

Theorem 1 (Stability of BEFE-Ensemble)**.** *Consider the method (3.2.1). Suppose the condition (3.2.2) holds. Then, for any $N \ge 1$*

$$\begin{aligned}&\frac{1}{2}\|u_{j,h}^N\|^2 + \frac{1}{4}\sum_{n=0}^{N-1}\|u_{j,h}^{n+1} - u_{j,h}^n\|^2 + \frac{\nu\Delta t}{4}\|\nabla u_{j,h}^N\|^2 + \frac{\nu\Delta t}{4}\sum_{n=0}^{N-1}\|\nabla u_{j,h}^{n+1}\|^2\\ &\le \sum_{n=0}^{N-1}\frac{\Delta t}{2\nu}\|f_j^{n+1}\|_{-1}^2 + \frac{1}{2}\|u_{j,h}^0\|^2 + \frac{\nu\Delta t}{4}\|\nabla u_{j,h}^0\|^2, \qquad j = 1, ..., J\ .\end{aligned}$$

Proof. Set $v_h = u_{j,h}^{n+1}$ in (3.2.1). This gives:

$$\begin{aligned}&\frac{1}{2}\|u_{j,h}^{n+1}\|^2 - \frac{1}{2}\|u_{j,h}^n\|^2 + \frac{1}{2}\|u_{j,h}^{n+1} - u_{j,h}^n\|^2\\ &+\Delta t b^*(u_{j,h}^n - < u_h >^n, u_{j,h}^n, u_{j,h}^{n+1}) + \nu\Delta t\|\nabla u_{j,h}^{n+1}\|^2 = \Delta t(f_j^{n+1}, u_{j,h}^{n+1})\ .\end{aligned} \tag{3.2.3}$$

Applying Young's inequality to the right hand side gives

$$\begin{aligned}
&\frac{1}{2}\|u_{j,h}^{n+1}\|^2-\frac{1}{2}\|u_{j,h}^{n}\|^2+\frac{1}{2}\|u_{j,h}^{n+1}-u_{j,h}^{n}\|^2\\
&+\Delta t b^*(u_{j,h}^{n}-<u_h>^n,u_{j,h}^{n},u_{j,h}^{n+1}-u_{j,h}^{n})+\nu\Delta t\|\nabla u_{j,h}^{n+1}\|^2\\
&\leq \frac{\nu\Delta t}{2}\|\nabla u_{j,h}^{n+1}\|^2+\frac{\Delta t}{2\nu}\|f_j^{n+1}\|_{-1}^2\ .
\end{aligned}\tag{3.2.4}$$

Next, we bound the trilinear term using Lemma 1, the interpolation and inverse inequalities.

$$\begin{aligned}
&-\Delta t b^*(u_{j,h}^{n}-<u_h>^n,u_{j,h}^{n},u_{j,h}^{n+1}-u_{j,h}^{n})\\
&\leq C\Delta t\|\nabla(u_{j,h}^{n}-<u_h>^n)\|\|\nabla u_{j,h}^{n}\|\|u_{j,h}^{n+1}-u_{j,h}^{n}\|_{\frac{1}{2}}\\
&+\frac{1}{2}C\Delta t\|\nabla\cdot(u_{j,h}^{n}-<u_h>^n)\|\|u_{j,h}^{n}\cdot(u_{j,h}^{n+1}-u_{j,h}^{n})\|\\
&\leq C\Delta t\|\nabla(u_{j,h}^{n}-<u_h>^n)\|\|\nabla u_{j,h}^{n}\|\|u_{j,h}^{n+1}-u_{j,h}^{n}\|_{\frac{1}{2}}\\
&+\frac{1}{2}C\Delta t\|\nabla\cdot(u_{j,h}^{n}-<u_h>^n)\|\|\nabla u_{j,h}^{n}\|\|u_{j,h}^{n+1}-u_{j,h}^{n}\|^{\frac{1}{2}}\|\nabla(u_{j,h}^{n+1}-u_{j,h}^{n})\|^{\frac{1}{2}}\\
&\leq C\Delta t\|\nabla(u_{j,h}^{n}-<u_h>^n)\|\|\nabla u_{j,h}^{n}\|(Ch^{-\frac{1}{2}})\|u_{j,h}^{n+1}-u_{j,h}^{n}\|\\
&+\frac{1}{2}C\Delta t\|\nabla(u_{j,h}^{n}-<u_h>^n)\|\|\nabla u_{j,h}^{n}\|(Ch^{-\frac{1}{2}})\|u_{j,h}^{n+1}-u_{j,h}^{n}\|\ .
\end{aligned}\tag{3.2.5}$$

Using Young's inequality again gives

$$\begin{aligned}
&-\Delta t b^*(u_{j,h}^{n}-<u_h>^n,u_{j,h}^{n},u_{j,h}^{n+1}-u_{j,h}^{n})\\
&\leq C\frac{\Delta t^2}{h}\|\nabla(u_{j,h}^{n}-<u_h>^n)\|^2\|\nabla u_{j,h}^{n}\|^2+\frac{1}{4}\|u_{j,h}^{n+1}-u_{j,h}^{n}\|^2\ .
\end{aligned}\tag{3.2.6}$$

Combining like terms, (3.2.4) becomes

$$\begin{aligned}
&\frac{1}{2}\|u_{j,h}^{n+1}\|^2-\frac{1}{2}\|u_{j,h}^{n}\|^2+\frac{1}{4}\|u_{j,h}^{n+1}-u_{j,h}^{n}\|^2+\frac{\nu\Delta t}{2}\|\nabla u_{j,h}^{n+1}\|^2\\
&\leq \frac{\Delta t}{2\nu}\|f_j^{n+1}\|_{-1}^2+C\frac{\Delta t^2}{h}\|\nabla(u_{j,h}^{n}-<u_h>^n)\|^2\|\nabla u_{j,h}^{n}\|^2\ .
\end{aligned}\tag{3.2.7}$$

Adding and subtracting $\frac{\nu\Delta t}{4}\|\nabla u_{j,h}^n\|^2$ gives

$$\frac{1}{2}\|u_{j,h}^{n+1}\|^2-\frac{1}{2}\|u_{j,h}^n\|^2+\frac{1}{4}\|u_{j,h}^{n+1}-u_{j,h}^n\|^2+\frac{\nu\Delta t}{4}\{\|\nabla u_{j,h}^{n+1}\|^2-\|\nabla u_{j,h}^n\|^2\} \tag{3.2.8}$$
$$+\frac{\nu\Delta t}{4}\{\|\nabla u_{j,h}^{n+1}\|^2+(1-\frac{C\Delta t}{\nu h}\|\nabla(u_{j,h}^n-<u_h>^n)\|^2)\|\nabla u_{j,h}^n\|^2\}\leq\frac{\Delta t}{2\nu}\|f_j^{n+1}\|_{-1}^2\ .$$

With the restriction (3.2.2) assumed, we have

$$\frac{\nu\Delta t}{4}(1-\frac{C\Delta t}{\nu h}\|\nabla(u_{j,h}^n-<u_h>^n)\|^2)\|\nabla u_{j,h}^n\|^2\geq 0\ .$$

Equation (3.2.8) reduces to

$$\frac{1}{2}\|u_{j,h}^{n+1}\|^2-\frac{1}{2}\|u_{j,h}^n\|^2+\frac{1}{4}\|u_{j,h}^{n+1}-u_{j,h}^n\|^2 \tag{3.2.9}$$
$$+\frac{\nu\Delta t}{4}\{\|\nabla u_{j,h}^{n+1}\|^2-\|\nabla u_{j,h}^n\|^2\}+\frac{\nu\Delta t}{4}\|\nabla u_{j,h}^{n+1}\|^2\leq\frac{\Delta t}{2\nu}\|f_j^{n+1}\|_{-1}^2\ .$$

Summing up (3.2.9) from $n=0$ to $n=N-1$ results in

$$\frac{1}{2}\|u_{j,h}^N\|^2+\frac{1}{4}\sum_{n=0}^{N-1}\|u_{j,h}^{n+1}-u_{j,h}^n\|^2+\frac{\nu\Delta t}{4}\|\nabla u_{j,h}^N\|^2+\frac{\nu\Delta t}{4}\sum_{n=0}^{N-1}\|\nabla u_{j,h}^{n+1}\|^2$$
$$\leq\sum_{n=0}^{N-1}\frac{\Delta t}{2\nu}\|f_j^{n+1}\|_{-1}^2+\frac{1}{2}\|u_{j,h}^0\|^2+\frac{\nu\Delta t}{4}\|\nabla u_{j,h}^0\|^2\ . \tag{3.2.10}$$

This concludes the proof of stability. □

3.3 SHARPENING THE TIMESTEP CONDITION

We have derived a global condition on the timestep that is sufficient for stability in 2d and 3d. There are many important cases where this condition is improvable:

$$\frac{C|ln(h)|\Delta t}{\nu}\|\nabla(u_{j,h}^n-<u_h>^n)\|^2\leq 1,\ \ 2\text{d}\ , \tag{2d C1}$$

$$\frac{C\Delta t}{\nu h^2}(\|u_{j,h}^n-<u_h>^n\|^2+\|\nabla\cdot(u_{j,h}^n-<u_h>^n)\|^2)\leq 1,\ \ 2\text{d}\ , \tag{2d C2}$$

$$\frac{C\Delta t}{\nu h^2}\|u_{j,h}^n-<u_h>^n\|_{L^3}^2\leq 1,\ 3\text{d - no derivatives of fluctuations}, \tag{3d, L3}$$

$$\max_e\frac{C\Delta t}{\nu h_e}\|\nabla(u_{j,h}^n-<u_h>^n)\|_{L^2(e)}^2\leq 1,\ \ 3\text{d-locally refined meshes}. \tag{Local}$$

3.3.1 The case of 2d domains

In 2d, embedding estimates improve and this improvement leads to an improvement of the timestep condition.

Theorem 2 (2d domains)**.** *Consider the method (3.2.1). Suppose the condition (2d C1) or (2d C2) holds. Then, for any* $N \geq 1$

$$\frac{1}{2}\|u_{j,h}^N\|^2 + \frac{1}{4}\sum_{n=0}^{N-1}\|u_{j,h}^{n+1} - u_{j,h}^n\|^2 + \frac{\nu\Delta t}{4}\|\nabla u_{j,h}^N\|^2 + \frac{\nu\Delta t}{4}\sum_{n=0}^{N-1}\|\nabla u_{j,h}^{n+1}\|^2$$
$$\leq \sum_{n=0}^{N-1}\frac{\Delta t}{2\nu}\|f_j^{n+1}\|_{-1}^2 + \frac{1}{2}\|u_{j,h}^0\|^2 + \frac{\nu\Delta t}{4}\|\nabla u_{j,h}^0\|^2, \qquad j = 1, ..., J\ .$$

Proof. In 2d we have

$$\begin{aligned}
&\Delta t b^*(u_{j,h}^n - < u_h >^n, u_{j,h}^n, u_{j,h}^{n+1} - u_{j,h}^n)\\
&\leq C\Delta t\|u_{j,h}^n - < u_h >^n\|_\infty\|\nabla u_{j,h}^n\|\|u_{j,h}^{n+1} - u_h^n\|\\
&+\frac{1}{2}C\Delta t\|\nabla\cdot(u_{j,h}^n - < u_h >^n)\|\|u_{j,h}^n\|_\infty\|u_{j,h}^{n+1} - u_h^n\| \qquad (3.3.1)\\
&\leq C\sqrt{|ln(h)|}\Delta t\|\nabla(u_{j,h}^n - < u_h >^n)\|\|\nabla u_{j,h}^n\|\|u_{j,h}^{n+1} - u_{j,h}^n\|\\
&+\frac{1}{2}C\sqrt{|ln(h)|}\Delta t\|\nabla(u_{j,h}^n - < u_h >^n)\|\|\nabla u_{j,h}^n\|\|u_{j,h}^{n+1} - u_{j,h}^n\|\\
&\leq C|ln(h)|\Delta t^2\|\nabla(u_{j,h}^n - < u_h >^n)\|^2\|\nabla u_{j,h}^n\|^2 + \frac{1}{4}\|u_{j,h}^{n+1} - u_{j,h}^n\|^2\ ,
\end{aligned}$$

or,

$$\begin{aligned}
&\Delta t b^*(u_{j,h}^n - < u_h >^n, u_{j,h}^n, u_{j,h}^{n+1} - u_{j,h}^n)\\
&\leq C\Delta t\|u_{j,h}^n - < u_h >^n\|_\infty\|\nabla u_{j,h}^n\|\|u_{j,h}^{n+1} - u_{j,h}^n\|\\
&+\frac{1}{2}C\Delta t\|\nabla\cdot(u_{j,h}^n - < u_h >^n)\|\|u_{j,h}^n\|_\infty\|u_{j,h}^{n+1} - u_h^n\|\\
&\leq Ch^{-1}\Delta t\|u_{j,h}^n - < u_h >^n\|\|\nabla u_{j,h}^n\|\|u_{j,h}^{n+1} - u_{j,h}^n\| \qquad (3.3.2)\\
&+\frac{1}{2}Ch^{-1}\Delta t\|\nabla\cdot(u_{j,h}^n - < u_h >^n)\|\|\nabla u_{j,h}^n\|\|u_{j,h}^{n+1} - u_{j,h}^n\|\\
&\leq C\frac{\Delta t^2}{h^2}(\|u_{j,h}^n - < u_h >^n\|^2 + \|\nabla\cdot(u_{j,h}^n - < u_h >^n)\|^2)\|\nabla u_{j,h}^n\|^2\\
&+\frac{1}{4}\|u_{j,h}^{n+1} - u_{j,h}^n\|^2\ .
\end{aligned}$$

Thus,

$$\begin{aligned}
&\frac{1}{2}\|u_{j,h}^{n+1}\|^2-\frac{1}{2}\|u_{j,h}^{n}\|^2+\frac{1}{4}\|u_{j,h}^{n+1}-u_{j,h}^{n}\|^2\\
&+\frac{\nu\Delta t}{4}\{\|\nabla u_{j,h}^{n+1}\|^2-\|\nabla u_{j,h}^{n}\|^2\}+\frac{\nu\Delta t}{4}\{\|\nabla u_{j,h}^{n+1}\|^2\\
&+(1-\frac{C|ln(h)|\Delta t}{\nu}\|\nabla(u_{j,h}^{n}-<u_h>^n)\|^2)\|\nabla u_{j,h}^{n}\|^2\}\leq\frac{\Delta t}{2\nu}\|f_j^{n+1}\|_{-1}^2\ ,
\end{aligned}\tag{3.3.3}$$

or,

$$\begin{aligned}
&\frac{1}{2}\|u_{j,h}^{n+1}\|^2-\frac{1}{2}\|u_{j,h}^{n}\|^2+\frac{1}{4}\|u_{j,h}^{n+1}-u_{j,h}^{n}\|^2\\
&+\frac{\nu\Delta t}{4}\{\|\nabla u_{j,h}^{n+1}\|^2-\|\nabla u_{j,h}^{n}\|^2\}+\frac{\nu\Delta t}{4}\{\|\nabla u_{j,h}^{n+1}\|^2\\
&+(1-\frac{C\Delta t}{\nu h^2}(\|u_{j,h}^{n}-<u_h>^n\|^2+\|\nabla\cdot(u_{j,h}^{n}-<u_h>^n)\|^2))\|\nabla u_{j,h}^{n}\|^2\}\\
&\leq\frac{\Delta t}{2\nu}\|f_j^{n+1}\|_{-1}^2\ .
\end{aligned}\tag{3.3.4}$$

□

3.3.2 L^3 estimate on the fluctuating part

Theorem 3 (L3 estimate)**.** *Consider the method (3.2.1). Suppose the condition (3d, L3 norms) holds. Then, for any* $N\geq 1$

$$\begin{aligned}
&\frac{1}{2}\|u_{j,h}^{N}\|^2+\frac{1}{4}\sum_{n=0}^{N-1}\|u_{j,h}^{n+1}-u_{j,h}^{n}\|^2+\frac{\nu\Delta t}{4}\|\nabla u_{j,h}^{N}\|^2+\frac{\nu\Delta t}{4}\sum_{n=0}^{N-1}\|\nabla u_{j,h}^{n+1}\|^2\\
&\leq\sum_{n=0}^{N-1}\frac{\Delta t}{2\nu}\|f_j^{n+1}\|_{-1}^2+\frac{1}{2}\|u_{j,h}^{0}\|^2+\frac{\nu\Delta t}{4}\|\nabla u_{j,h}^{0}\|^2,\qquad j=1,...,J\ .
\end{aligned}$$

Proof. By *Hölders'* inequality, we have

$$\begin{aligned}
&\Delta t b^*(u^n_{j,h} - < u^n_{j,h} >, u^n_{j,h}, u^{n+1}_{j,h} - u^n_{j,h}) \\
&\leq \frac{1}{2}\Delta t \|(u^n_{j,h} - < u_h >^n)\|_{L^3} \|\nabla u^n_{j,h}\|_{L^2} \|u^{n+1}_{j,h} - u^n_{j,h}\|_{L^6} \\
&+\frac{1}{2}\Delta t \|(u^n_{j,h} - < u_h >^n)\|_{L^3} \|u^n_{j,h}\|_{L^6} \|\nabla(u^{n+1}_{j,h} - u^n_{j,h})\|_{L^2}.
\end{aligned} \tag{3.3.5}$$

Using the Sobolev embedding theorem and the inverse estimate on the $(u^{n+1}_{j,h} - u^n_{j,h})$ terms give

$$\begin{aligned}
\|\nabla(u^{n+1}_{j,h} - u^n_{j,h})\|_{L^2} &\leq Ch^{-1}\|u^{n+1}_{j,h} - u^n_{j,h}\| \\
\|u^{n+1}_{j,h} - u^n_{j,h}\|_{L^6} &\leq Ch^{-1}\|u^{n+1}_{j,h} - u^n_{j,h}\| \ .
\end{aligned}$$

Thus, for any $\epsilon > 0$,

$$\begin{aligned}
&\Delta t b^*(u^n_{j,h} - < u_h >^n, u^n_{j,h}, u^{n+1}_{j,h} - u^n_{j,h}) \\
&\leq Ch^{-1}\Delta t \|(u^n_{j,h} - < u_h >^n)\|_{L^3} \|\nabla u^n_{j,h}\| \|u^{n+1}_{j,h} - u^n_{j,h}\| \\
&\leq \frac{\epsilon \Delta t}{2}\|u^{n+1}_{j,h} - u^n_{j,h}\|^2 + \frac{C\Delta t}{2\epsilon h^2}\|(u^n_{j,h} - < u_h >^n)\|^2_{L^3}\|\nabla u^n_{j,h}\|^2.
\end{aligned} \tag{3.3.6}$$

We use this estimate with $\epsilon = \frac{1}{2}\Delta t^{-1}$. This gives

$$\begin{aligned}
&\frac{1}{2}\|u^{n+1}_{j,h}\|^2 - \frac{1}{2}\|u^n_{j,h}\|^2 + \frac{1}{4}\|u^{n+1}_{j,h} - u^n_{j,h}\|^2 + \frac{\nu\Delta t}{4}\{\|\nabla u^{n+1}_{j,h}\|^2 - \|\nabla u^n_{j,h}\|^2\} \\
&+\frac{\nu\Delta t}{4}\{\|\nabla u^{n+1}_{j,h}\|^2 + (1 - \frac{C\Delta t}{\nu h^2}\|u^n_{j,h} - < u_h >^n \|^2_{L^3})\|\nabla u^n_{j,h}\|^2\} \leq \frac{\Delta t}{2\nu}\|f^{n+1}_j\|^2_{-1} \ .
\end{aligned} \tag{3.3.7}$$

□

3.3.3 Locally refined meshes:

Often meshes are locally refined in regions of sharp gradients. We show that a sufficient condition is that Δt satisfies the following for all elements e:

$$\frac{C\Delta t}{\nu h_e}\|\nabla(u^n_{j,h} - < u_h >^n)\|^2_{L^2(e)} \leq 1.$$

For the local condition we perform the same steps (locally on the element e) as in the proof of Theorem 1 noting that (i) $H\ddot{o}lders'$ inequality can be applied locally (with no dependence on $diam(e)$ therefrom), (ii) the inverse inequality holds locally, with $h_e = diam(e)$ and constant depending only on the shape (h_e/ρ_e, ρ_e is the diameter of the largest ball that can be inscribed in e) of the element, [92], and (iii) the Sobolev embedding theorem holds locally with absolute constant independent of h_e.

From the stability proof we observe the following.

Lemma 2. *The conclusion of Theorem 1 (on stability) holds provided at every timestep:*

$$\frac{1}{4}\|u^{n+1}_{j,h} - u^n_{j,h}\|^2 + \frac{\nu\Delta t}{4}\|\nabla u^n_{j,h}\|^2$$
$$+\Delta t b^*(u^n_{j,h} - < u_h >^n, u^n_{j,h}, u^{n+1}_{j,h} - u^n_{j,h}) \geq 0 \ .$$

The same conclusion holds if, on every element e,

$$\int_e \{\frac{1}{4}|u^{n+1}_{j,h} - u^n_{j,h}|^2 + \frac{\nu\Delta t}{4}|\nabla u^n_{j,h}|^2$$
$$+\Delta t[(u^n_{j,h} - < u_h >^n)\cdot\nabla u^n_{j,h}\cdot(u^{n+1}_{j,h} - u^n_{j,h})$$
$$+\frac{1}{2}(\nabla\cdot(u^n_{j,h} - < u_h >^n)\cdot(u^n_{j,h}\cdot(u^{n+1}_{j,h} - u^n_{j,h})))]\}dx \geq 0 \ .$$

Theorem 4 (Locally refined meshes)**.** *Consider the method (3.2.1). Suppose the locally refined meshes condition holds. Then, for any $N \geq 1$*

$$\frac{1}{2}\|u^N_{j,h}\|^2 + \frac{1}{4}\sum_{n=0}^{N-1}\|u^{n+1}_{j,h} - u^n_{j,h}\|^2 + \frac{\nu\Delta t}{4}\|\nabla u^N_{j,h}\|^2 + \frac{\nu\Delta t}{4}\sum_{n=0}^{N-1}\|\nabla u^{n+1}_{j,h}\|^2$$
$$\leq \sum_{n=0}^{N-1}\frac{\Delta t}{2\nu}\|f^{n+1}_j\|^2_{-1} + \frac{1}{2}\|u^0_{j,h}\|^2 + \frac{\nu\Delta t}{4}\|\nabla u^0_{j,h}\|^2, \qquad j = 1, ..., J \ .$$

Proof. We have

$$
\begin{aligned}
&|\int_e \Delta t[(u_{j,h}^n - < u_h >^n)\cdot\nabla u_{j,h}^n\cdot(u_{j,h}^{n+1}-u_{j,h}^n)\\
&+\frac{1}{2}(\nabla\cdot(u_{j,h}^n - < u_h >^n)\cdot(u_{j,h}^n\cdot(u_{j,h}^{n+1}-u_{j,h}^n)))]\ dx|\\
&\le C\Delta t\|\nabla(u_{j,h}^n - < u_h >^n)\|_{L^2(e)}\|\nabla u_{j,h}^n\|_{L^2(e)}\\
&\cdot\|u_{j,h}^{n+1}-u_{j,h}^n\|_{L^2(e)}^{\frac{1}{2}}\|\nabla(u_{j,h}^{n+1}-u_{j,h}^n)\|_{L^2(e)}^{\frac{1}{2}}\\
&+\frac{1}{2}C\Delta t\|\nabla\cdot(u_{j,h}^n - < u_h >^n)\|_{L^2(e)}\|u_{j,h}^n\cdot(u_{j,h}^{n+1}-u_{j,h}^n)\|_{L^2(e)} \qquad (3.3.8)\\
&\le C\Delta t\|\nabla(u_{j,h}^n - < u_h >^n)\|_{L^2(e)}\|\nabla u_{j,h}^n\|_{L^2(e)}\\
&\cdot\|u_{j,h}^{n+1}-u_{j,h}^n\|_{L^2(e)}^{\frac{1}{2}}\|\nabla(u_{j,h}^{n+1}-u_{j,h}^n)\|_{L^2(e)}^{\frac{1}{2}}\\
&+\frac{1}{2}C\Delta t\|\nabla\cdot(u_{j,h}^n - < u_h >^n)\|_{L^2(e)}\|\nabla u_{j,h}^n\|_{L^2(e)}\\
&\cdot\|u_{j,h}^{n+1}-u_{j,h}^n\|_{L^2(e)}^{\frac{1}{2}}\|\nabla(u_{j,h}^{n+1}-u_{j,h}^n)\|_{L^2(e)}^{\frac{1}{2}}\\
&\le C\Delta t\|\nabla(u_{j,h}^n - < u_h >^n)\|_{L^2(e)}\|\nabla u_{j,h}^n\|_{L^2(e)}(Ch_e^{-\frac{1}{2}})\|u_{j,h}^{n+1}-u_{j,h}^n\|_{L^2(e)}\\
&+\frac{1}{2}C\Delta t\|\nabla(u_{j,h}^n - < u_h >^n)\|_{L^2(e)}\|\nabla u_{j,h}^n\|_{L^2(e)}(Ch_e^{-\frac{1}{2}})\|u_{j,h}^{n+1}-u_{j,h}^n\|_{L^2(e)}\ .
\end{aligned}
$$

Using Young's inequality gives

$$
\begin{aligned}
&|\int_e \Delta t[(u_{j,h}^n - < u_h >^n)\cdot\nabla u_{j,h}^n\cdot(u_{j,h}^{n+1}-u_{j,h}^n)\\
&+\frac{1}{2}(\nabla\cdot(u_{j,h}^n - < u_h >^n)\cdot(u_{j,h}^n\cdot(u_{j,h}^{n+1}-u_{j,h}^n)))]\ dx| \qquad (3.3.9)\\
&\le C\frac{\Delta t^2}{h_e}\|\nabla(u_{j,h}^n - < u_h >^n)\|_{L^2(e)}^2\|\nabla u_{j,h}^n\|_{L^2(e)}^2+\frac{1}{4}\|u_{j,h}^{n+1}-u_{j,h}^n\|_{L^2(e)}^2\ .
\end{aligned}
$$

Thus, under the locally refined meshes condition,

$$
\begin{aligned}
&\int_e\{\frac{1}{4}|u_{j,h}^{n+1}-u_{j,h}^n|^2+\frac{\nu\Delta t}{4}|\nabla u_{j,h}^n|^2\\
&+\Delta t[(u_{j,h}^n - < u_h >^n)\cdot\nabla u_{j,h}^n\cdot(u_{j,h}^{n+1}-u_{j,h}^n)\\
&+(u_{j,h}^n - < u_h >^n)\cdot\nabla(u_{j,h}^{n+1}-u_{j,h}^n)\cdot u_{j,h}^n]\}dx \qquad (3.3.10)\\
&\ge\frac{\nu\Delta t}{4}(1-\frac{C\Delta t}{\nu h_e}\|\nabla(u_{j,h}^n - < u_h >^n)\|_{L^2(e)}^2)\|\nabla u_{j,h}^n\|_{L^2(e)}^2\ge 0.
\end{aligned}
$$

Then, by Lemma 2, we obtain stability. □

3.4 ERROR ANALYSIS FOR THE ENSEMBLE METHOD

In this section we give a detailed error analysis of the proposed method under the 3d stability condition. This analysis can be elaborated to analogous results in the cases of the other, sharpened stability conditions. Assume X_h and Q_h satisfy the usual (LBB^h) condition, then the method is equivalent to: *For* $n = 0, 1, ..., N_T$, *find* $u_{j,h}^{n+1} \in V_h$ *such that*

$$(\frac{u_{j,h}^{n+1} - u_{j,h}^{n}}{\Delta t}, v_h) + b^*(< u_h >^n, u_{j,h}^{n+1}, v_h) + b^*(u_{j,h}^n - < u_{j,h} >^n, u_{j,h}^n, v_h) \tag{3.4.1}$$
$$+\nu(\nabla u_{j,h}^{n+1}, \nabla v_h) = (f_j^{n+1}, v_h) \ , \ \forall v_h \in V_h.$$

Let $t^n = n\Delta t, n = 0, 1, 2, ..., N_T$, and $T := N_T \Delta t$. Denote $u_j^n = u_j(t^n)$, $j = 1, ..., J$. We introduce the following discrete norms:

$$|||v|||_{m,k} := (\sum_{n=0}^{N_T} ||v^n||_k^m \Delta t)^{1/m}, |||v|||_{\infty,k} = \max_{0 \le n \le N_T} \|v^n\|_k.$$

To analyze the rate of convergence of the approximation we assume that the following regularity

$$u_j \in L^\infty(0, T; H^{k+1}(\Omega)) \cap H^1(0, T; H^{k+1}(\Omega)) \cap H^2(0, T; L^2(\Omega)),$$
$$p_j \in L^2(0, T; H^{s+1}(\Omega)), \text{and } f_j \in L^2(0, T; L^2(\Omega)).$$

Let $e_j^n = u_j^n - u_{j,h}^n$ be the error between the true solution and the approximation, then we have the following error estimates.

Theorem 5 (Convergence of (BEFE-Ensemble))**.** *Consider the method (3.4.1). Suppose that for any* $0 \le n \le N_T$, *the condition (1.3) holds*

$$C\frac{\Delta t}{\nu h}\|\nabla(u_{j,h}^n - < u_h >^n)\|^2 \le 1 \ , \qquad j = 1, ..., J.$$

Then, for any $0 \le t^N \le T$, there is a positive constant C independent of the mesh width and timestep such that

$$\begin{aligned}
&\frac{1}{2}\|e_j^N\|^2 + \sum_{n=0}^{N-1}\frac{1}{4}\|e_j^{n+1}-e_j^n\|^2 + \frac{\nu\Delta t}{8}\|\nabla e_j^N\|^2 + C\Delta t\sum_{n=0}^{N-1}\nu\|\nabla e_j^{n+1}\|^2 \\
&\le exp(C\frac{T}{\nu^2})\{\frac{1}{2}\|e_j^0\|^2 + \frac{\nu\Delta t}{8}\|\nabla e_j^0\|^2 + C\frac{h^{2k}}{\nu}|||\nabla u_j|||^2_{\infty,0}|||u_j|||^2_{2,k+1} \\
&\quad + C\frac{\Delta t^2}{\nu}|||\nabla u_j|||^2_{\infty,0}|||\nabla u_{j,t}|||^2_{2,0} + C\frac{h^{2k}}{\nu^2}|||u_j|||^2_{2,k+1} \\
&\quad + C\frac{h^{2k+1}}{\Delta t}|||u_j|||^2_{2,k+1} + Ch\Delta t|||\nabla u_{j,t}|||^2_{2,0} \\
&\quad + C\frac{h^{2s+2}}{\nu}|||p_j|||^2_{2,s+1} + C\frac{h^{2k+2}}{\nu}|||u_{j,t}|||^2_{2,k+1} \\
&\quad + C\nu h^{2k}|||u_j|||^2_{2,k+1} + \frac{C\Delta t^2}{\nu}|||u_{j,tt}|||^2_{2,0}\} \ .
\end{aligned} \tag{3.4.2}$$

For $k=2, s=1$, Taylor-Hood elements, i.e. C^0 piecewise quadratic velocity space X_h and C^0 piecewise linear pressure space Q_h, we have the following estimate.

Corollary 1. *Under the assumptions of Theorem 5, with e_j^0 taken to be 0, $\Delta t/h$ fixed to be a constant C, (X_h, Q_h) given by the Taylor-Hood approximation elements, we have*

$$\frac{1}{2}\|e_j^N\|^2 + \sum_{n=0}^{N-1}\frac{1}{4}\|e_j^{n+1}-e_j^n\|^2 + \frac{\nu\Delta t}{8}\|\nabla e_j^N\|^2 + C\Delta t\sum_{n=0}^{N-1}\nu\|\nabla e_j^{n+1}\|^2 \le Ch^2 \ .$$

Proof. The true solutions of the NSE u_j satisfy

$$\begin{aligned}
&(\frac{u_j^{n+1}-u_j^n}{\Delta t}, v_h) + b^*(u_j^{n+1}, u_j^{n+1}, v_h) + \nu(\nabla u_j^{n+1}, \nabla v_h) - (p_j^{n+1}, \nabla\cdot v_h) \\
&\qquad = (f_j^{n+1}, v_h) + Intp(u_j^{n+1}; v_h) \ , \qquad \text{for all } v_h \in V_h \ .
\end{aligned} \tag{3.4.3}$$

where $Intp(u_j^{n+1}; v_h)$ is defined as

$$Intp(u_j^{n+1}; v_h) = (\frac{u_j^{n+1}-u_j^n}{\Delta t} - u_{j,t}(t^{n+1}), v_h) \ .$$

Let

$$e_j^n = u_j^n - u_{j,h}^n = (u_j^n - I_h u_j^n) + (I_h u_j^n - u_{j,h}^n) = \eta_j^n + \xi_{j,h}^n \ , \qquad j = 1, ..., J \ .$$

where $I_h u_j^n \in V_h$ is an interpolant of u_j^n in V_h. Denote

$$U_j^n = u_{j,h}^n - < u_h >^n \quad .$$

Subtracting (3.4.1) from (3.4.3) gives

$$\begin{aligned}
&(\frac{\xi_{j,h}^{n+1} - \xi_{j,h}^n}{\Delta t}, v_h) + \nu(\nabla \xi_{j,h}^{n+1}, \nabla v_h) + b^*(u_j^{n+1}, u_j^{n+1}, v_h) \\
&-b^*(u_{j,h}^n - U_j^n, u_{j,h}^{n+1}, v_h) - b^*(U_j^n, u_{j,h}^n, v_h) - (p_j^{n+1}, \nabla \cdot v_h) \\
&= -(\frac{\eta_j^{n+1} - \eta_j^n}{\Delta t}, v_h) - \nu(\nabla \eta_j^{n+1}, \nabla v_h) + Intp(u_j^{n+1}; v_h) \ .
\end{aligned} \tag{3.4.4}$$

Set $v_h = \xi_{j,h}^{n+1} \in V_h$, and rearrange the nonlinear terms, then we have

$$\begin{aligned}
&\frac{1}{\Delta t}(\frac{1}{2}||\xi_{j,h}^{n+1}||^2 - \frac{1}{2}||\xi_{j,h}^n||^2 + \frac{1}{2}\|\xi_{j,h}^{n+1} - \xi_{j,h}^n\|^2) + \nu||\nabla \xi_{j,h}^{n+1}||^2 \\
&= -b^*(u_j^{n+1}, u_j^{n+1}, \xi_{j,h}^{n+1}) + b^*(u_{j,h}^n, u_{j,h}^{n+1}, \xi_{j,h}^{n+1}) \\
&-b^*(U_j^n, u_{j,h}^{n+1} - u_{j,h}^n, \xi_{j,h}^{n+1}) + (p_j^{n+1}, \nabla \cdot \xi_{j,h}^{n+1}) \\
&-(\frac{\eta_j^{n+1} - \eta_j^n}{\Delta t}, \xi_{j,h}^{n+1}) - \nu(\nabla \eta_j^{n+1}, \nabla \xi_{j,h}^{n+1}) + Intp(u_j^{n+1}; \xi_{j,h}^{n+1}) \ .
\end{aligned} \tag{3.4.5}$$

Now we bound the right hand side of the equation above. First, for the nonlinear term, adding and subtracting both $b^*(u_j^{n+1}, u_{j,h}^{n+1}, \xi_{j,h}^{n+1})$ and $b^*(U_j^n, u_j^{n+1} - u_j^n, \xi_{j,h}^{n+1})$, we have

$$\begin{aligned}
&-b^*(u_j^{n+1}, u_j^{n+1}, \xi_{j,h}^{n+1}) + b^*(u_{j,h}^n, u_{j,h}^{n+1}, \xi_{j,h}^{n+1}) \\
&+b^*(U_j^n, u_{j,h}^{n+1} - u_{j,h}^n, \xi_{j,h}^{n+1}) \\
&= -b^*(u_j^{n+1}, e_j^{n+1}, \xi_{j,h}^{n+1}) - b^*(u_j^{n+1} - u_j^n, u_{j,h}^{n+1}, \xi_{j,h}^{n+1}) \\
&-b^*(e_j^n, u_{j,h}^{n+1}, \xi_{j,h}^{n+1}) + b^*(U_j^n, u_{j,h}^{n+1} - u_{j,h}^n, \xi_{j,h}^{n+1}) \\
&= -b^*(u_j^{n+1}, \eta_j^{n+1}, \xi_{j,h}^{n+1}) - b^*(u_j^{n+1} - u_j^n, u_{j,h}^{n+1}, \xi_{j,h}^{n+1}) \\
&-b^*(\eta_j^n, u_{j,h}^{n+1}, \xi_{j,h}^{n+1}) - b^*(\xi_{j,h}^n, u_{j,h}^{n+1}, \xi_{j,h}^{n+1}) \\
&-b^*(U_j^n, e_j^{n+1} - e_j^n, \xi_{j,h}^{n+1}) + b^*(U_j^n, u_j^{n+1} - u_j^n, \xi_{j,h}^{n+1}) \\
&= -b^*(u_j^{n+1}, \eta_j^{n+1}, \xi_{j,h}^{n+1}) - b^*(u_j^{n+1} - u_j^n, u_{j,h}^{n+1}, \xi_{j,h}^{n+1}) \\
&-b^*(\eta_j^n, u_{j,h}^{n+1}, \xi_{j,h}^{n+1}) - b^*(\xi_{j,h}^n, u_{j,h}^{n+1}, \xi_{j,h}^{n+1}) \\
&-b^*(U_j^n, \eta_j^{n+1}, \xi_{j,h}^{n+1}) + b^*(U_j^n, \eta_j^n, \xi_{j,h}^{n+1}) \\
&+b^*(U_j^n, \xi_{j,h}^n, \xi_{j,h}^{n+1}) + b^*(U_j^n, u_j^{n+1} - u_j^n, \xi_{j,h}^{n+1}) \ .
\end{aligned} \tag{3.4.6}$$

We estimate the nonlinear terms as follows

$$
\begin{aligned}
b^*(u_j^{n+1},\eta_j^{n+1},\xi_{j,h}^{n+1}) &\le C\|\nabla u_j^{n+1}\|\|\nabla\eta_j^{n+1}\|\|\nabla\xi_{j,h}^{n+1}\| \\
&\le \frac{\nu}{64}\|\nabla\xi_{j,h}^{n+1}\|^2 + C\nu^{-1}\|\nabla u_j^{n+1}\|^2\|\nabla\eta_j^{n+1}\|^2 \ ,
\end{aligned} \tag{3.4.7}
$$

$$
\begin{aligned}
b^*(u_j^{n+1}-u_j^n,u_{j,h}^{n+1},\xi_{j,h}^{n+1}) &\le C\|\nabla(u_j^{n+1}-u_j^n)\|\|\nabla u_{j,h}^{n+1}\|\|\nabla\xi_{j,h}^{n+1}\| \\
&\le \frac{\nu}{64}\|\nabla\xi_{j,h}^{n+1}\|^2 + C\nu^{-1}\|\nabla(u_j^{n+1}-u_j^n)\|^2\|\nabla u_{j,h}^{n+1}\|^2 \\
&\le \frac{\nu}{64}\|\nabla\xi_{j,h}^{n+1}\|^2 + \frac{C\Delta t^2}{\nu}\|\nabla\frac{u_j^{n+1}-u_j^n}{\Delta t}\|^2\|\nabla u_{j,h}^{n+1}\|^2 \\
&= \frac{\nu}{64}\|\nabla\xi_{j,h}^{n+1}\|^2 + \frac{C\Delta t^2}{\nu}(\int_\Omega(\frac{1}{\Delta t}\int_{t^n}^{t^{n+1}}(\nabla u_{j,t})dt)^2d\Omega)\|\nabla u_{j,h}^{n+1}\|^2 \\
&\le \frac{\nu}{64}\|\nabla\xi_{j,h}^{n+1}\|^2 + \frac{C\Delta t^2}{\nu}(\int_\Omega(\frac{1}{\Delta t}\int_{t^n}^{t^{n+1}}|\nabla u_{j,t}|^2dt)d\Omega)\|\nabla u_{j,h}^{n+1}\|^2 \\
&\le \frac{\nu}{64}\|\nabla\xi_{j,h}^{n+1}\|^2 + \frac{C\Delta t}{\nu}(\int_{t^n}^{t^{n+1}}\|\nabla u_{j,t}\|^2dt)\|\nabla u_{j,h}^{n+1}\|^2 \ ,
\end{aligned} \tag{3.4.8}
$$

$$
\begin{aligned}
b^*(\eta_j^n,u_{j,h}^{n+1},\xi_{j,h}^{n+1}) &\le C\|\nabla\eta_j^n\|\|\nabla u_{j,h}^{n+1}\|\|\nabla\xi_{j,h}^{n+1}\| \\
&\le \frac{\nu}{64}\|\nabla\xi_{j,h}^{n+1}\|^2 + C\nu^{-1}\|\nabla\eta_j^n\|^2\|\nabla u_{j,h}^{n+1}\|^2,
\end{aligned} \tag{3.4.9}
$$

$$
\begin{aligned}
b^*(\xi_{j,h}^n,u_{j,h}^{n+1},\xi_{j,h}^{n+1}) &\le C\|\nabla\xi_{j,h}^n\|^{\frac{1}{2}}\|\xi_{j,h}^n\|^{\frac{1}{2}}\|\nabla u_{j,h}^{n+1}\|\|\nabla\xi_{j,h}^{n+1}\| \\
&\le C\|\nabla\xi_{j,h}^n\|^{\frac{1}{2}}\|\xi_{j,h}^n\|^{\frac{1}{2}}\|\nabla\xi_{j,h}^{n+1}\| \\
&\le C(\epsilon\|\nabla\xi_{j,h}^{n+1}\|^2 + \frac{1}{\epsilon}\|\nabla\xi_{j,h}^n\|\|\xi_{j,h}^n\|) \\
&\le C(\epsilon\|\nabla\xi_{j,h}^{n+1}\|^2 + \frac{1}{\epsilon}(\delta\|\nabla\xi_{j,h}^n\|^2 + \frac{1}{\delta}\|\xi_{j,h}^n\|) \\
&\le (\frac{\nu}{64}\|\nabla\xi_{j,h}^{n+1}\|^2 + \frac{\nu}{8}\|\nabla\xi_{j,h}^n\|^2) + \frac{C}{\nu^2}\|\xi_{j,h}^n\|^2,
\end{aligned} \tag{3.4.10}
$$

$$
\begin{aligned}
b^*(U_j^n,\eta_j^{n+1},\xi_{j,h}^{n+1}) &\le C\|\nabla U_j^n\|\|\nabla\eta_j^{n+1}\|\|\nabla\xi_{j,h}^{n+1}\| \\
&\le \frac{\nu}{64}\|\nabla\xi_{j,h}^{n+1}\|^2 + C\nu^{-1}\|\nabla U_j^n\|^2\|\nabla\eta_j^{n+1}\|^2 \ ,
\end{aligned} \tag{3.4.11}
$$

$$b^*(U_j^n, \eta_j^n, \xi_{j,h}^{n+1}) \le C\|\nabla U_j^n\|\|\nabla \eta_j^n\|\|\nabla \xi_{j,h}^{n+1}\| \tag{3.4.12}$$
$$\le \frac{\nu}{64}\|\nabla \xi_{j,h}^{n+1}\|^2 + C\nu^{-1}\|\nabla U_j^n\|^2\|\nabla \eta_j^n\|^2 \ .$$

The next term, $b^*(U_j^n, \xi_{j,h}^n, \xi_{j,h}^{n+1})$, is the key term in the error analysis. Note that by skew symmetry and Lemma 1

$$b^*(U_j^n, \xi_{j,h}^n, \xi_{j,h}^{n+1}) = b^*(U_j^n, \xi_{j,h}^n - \xi_{j,h}^{n+1}, \xi_{j,h}^{n+1}) =$$
$$= -(U_j^n \cdot \nabla \xi_{j,h}^{n+1}, \xi_{j,h}^n - \xi_{j,h}^{n+1}) - \frac{1}{2}(\nabla \cdot U_j^n, \left(\xi_{j,h}^n - \xi_{j,h}^{n+1}\right) \cdot \xi_{j,h}^{n+1}).$$

Using standard estimates for each additive term (with $\varepsilon = 1/(2\triangle t)$) and an inverse inequality gives

$$b^*(U_j^n, \xi_{j,h}^n, \xi_{j,h}^{n+1}) \le C\|\nabla U_j^n\|\|\nabla \xi_{j,h}^{n+1}\|\|\xi_{j,h}^{n+1} - \xi_{j,h}^n\|_{1/2} + C\|\nabla \cdot U_j^n\|\|\xi_{j,h}^{n+1} \cdot (\xi_{j,h}^{n+1} - \xi_{j,h}^n)\|$$
$$\le C\|\nabla U_j^n\|\|\nabla \xi_{j,h}^{n+1}\|\|\xi_{j,h}^{n+1} - \xi_{j,h}^n\|_{1/2} + C\|\nabla \cdot U_j^n\|\|\nabla \xi_{j,h}^{n+1}\|\|\xi_{j,h}^{n+1} - \xi_{j,h}^n\|_{1/2}$$
$$\le C\|\nabla U_j^n\|\|\nabla \xi_{j,h}^{n+1}\|\|\xi_{j,h}^{n+1} - \xi_{j,h}^n\|_{1/2} \le C\|\nabla U_j^n\|\|\nabla \xi_{j,h}^{n+1}\|h^{-1/2}\|\xi_{j,h}^{n+1} - \xi_{j,h}^n\|$$
$$\le \frac{1}{4\triangle t}\|\xi_{j,h}^{n+1} - \xi_{j,h}^n\|^2 + \left(C\frac{\triangle t}{h}\|\nabla U_j^n\|^2\right)\|\nabla \xi_{j,h}^{n+1}\|^2. \tag{3.4.13}$$

For the next terms we have

$$b^*(U_j^n, u_j^{n+1} - u_j^n, \xi_{j,h}^{n+1}) \le C\|\nabla U_j^n\|\|\nabla (u_j^{n+1} - u_j^n)\|\|\nabla \xi_{j,h}^{n+1}\|$$
$$\le \frac{\nu}{64}\|\nabla \xi_{j,h}^{n+1}\|^2 + C\nu^{-1}\|\nabla U_j^n\|^2\|\nabla (u_j^{n+1} - u_j^n)\|^2 \tag{3.4.14}$$
$$\le \frac{\nu}{64}\|\nabla \xi_{j,h}^{n+1}\|^2 + \frac{C\Delta t}{\nu}\|\nabla U_j^n\|^2(\int_{t^n}^{t^{n+1}} \|\nabla u_{j,t}\|^2 \ dt) \ .$$

Next, consider the pressure term. Since $\xi_{j,h}^{n+1} \in V_h$ we have

$$(p_j^{n+1}, \nabla \cdot \xi_{j,h}^{n+1}) = (p_j^{n+1} - q_{j,h}^{n+1}, \nabla \cdot \xi_{j,h}^{n+1})$$
$$\le \|p_j^{n+1} - q_{j,h}^{n+1}\|\|\nabla \cdot \xi_{j,h}^{n+1}\| \tag{3.4.15}$$
$$\le \frac{\nu}{64}\|\nabla \xi_{j,h}^{n+1}\|^2 + C\nu^{-1}\|p_j^{n+1} - q_{j,h}^{n+1}\|^2 \ .$$

The other terms, are bounded as

$$
\begin{aligned}
(\frac{\eta_j^{n+1}-\eta_j^n}{\Delta t}, \xi_{j,h}^{n+1}) &\leq C\|\frac{\eta_j^{n+1}-\eta_j^n}{\Delta t}\|\|\nabla\xi_{j,h}^{n+1}\| \\
&\leq C\nu^{-1}\|\frac{\eta_j^{n+1}-\eta_j^n}{\Delta t}\|^2 + \frac{\nu}{64}\|\nabla\xi_{j,h}^{n+1}\|^2 \\
&\leq C\nu^{-1}\|\frac{1}{\Delta t}\int_{t^n}^{t^{n+1}} \eta_{j,t}\ dt\|^2 + \frac{\nu}{64}\|\nabla\xi_{j,h}^{n+1}\|^2 \\
&\leq \frac{C}{\nu\Delta t}\int_{t^n}^{t^{n+1}} \|\eta_{j,t}\|^2\ dt + \frac{\nu}{64}\|\nabla\xi_{j,h}^{n+1}\|^2\ .
\end{aligned}
\tag{3.4.16}
$$

$$
\begin{aligned}
\nu(\nabla\eta_j^{n+1}, \nabla\xi_{j,h}^{n+1}) &\leq \nu\|\nabla\eta_j^{n+1}\|\|\nabla\xi_{j,h}^{n+1}\| \\
&\leq C\nu\|\nabla\eta_j^{n+1}\|^2 + \frac{\nu}{64}\|\nabla\xi_{j,h}^{n+1}\|^2\ .
\end{aligned}
\tag{3.4.17}
$$

Finally,

$$
\begin{aligned}
Intp(u_j^{n+1}; \xi_{j,h}^{n+1}) &= (\frac{u_j^{n+1}-u_j^n}{\Delta t} - u_{j,t}(t^{n+1}), \xi_{j,h}^{n+1}) \\
&\leq C\|\frac{u_j^{n+1}-u_j^n}{\Delta t} - u_{j,t}(t^{n+1})\|\|\nabla\xi_{j,h}^{n+1}\| \\
&\leq \frac{\nu}{64}\|\nabla\xi_{j,h}^{n+1}\|^2 + \frac{C}{\nu}\|\frac{u_j^{n+1}-u_j^n}{\Delta t} - u_{j,t}(t^{n+1})\|^2 \\
&\leq \frac{\nu}{64}\|\nabla\xi_{j,h}^{n+1}\|^2 + \frac{C\Delta t}{\nu}\int_{t^n}^{t^{n+1}} \|u_{j,tt}\|^2 dt\ .
\end{aligned}
\tag{3.4.18}
$$

Combining, we now have the following inequality:

$$\begin{aligned}
&\frac{1}{\Delta t}(\frac{1}{2}||\xi_{j,h}^{n+1}||^2-\frac{1}{2}||\xi_{j,h}^{n}||^2+\frac{1}{4}\|\xi_{j,h}^{n+1}-\xi_{j,h}^{n}\|^2)+\frac{\nu}{8}(\|\nabla\xi_{j,h}^{n+1}\|^2-\|\nabla\xi_{j,h}^{n}\|^2)\\
&\qquad+(\frac{\nu}{4}-C\frac{\triangle t}{h}\|\nabla U_j^n\|^2)\|\nabla\xi_{j,h}^{n+1}\|^2\\
&\leq C\nu^{-1}\|\nabla u_j^{n+1}\|^2\|\nabla\eta_j^{n+1}\|^2+\frac{C\Delta t}{\nu}(\int_{t^n}^{t^{n+1}}\|\nabla u_{j,t}\|^2dt)\|\nabla u_{j,h}^{n+1}\|^2\\
&+C\nu^{-1}\|\nabla\eta_j^{n}\|^2\|\nabla u_{j,h}^{n+1}\|^2+\frac{C}{\nu^2}\|\xi_{j,h}^{n}\|^2+C\nu^{-1}\|\nabla U_j^n\|^2\|\nabla\eta_j^{n+1}\|^2\\
&\qquad+C\nu^{-1}\|\nabla U_j^n\|^2\|\nabla\eta_j^{n}\|^2\\
&\qquad+\frac{C\Delta t}{\nu}\|\nabla U_j^n\|^2(\int_{t^n}^{t^{n+1}}\|\nabla u_{j,t}\|^2dt)+C\nu^{-1}\|p_j^{n+1}-q_{j,h}^{n+1}\|^2\\
&\qquad+\frac{C}{\nu\Delta t}\int_{t^n}^{t^{n+1}}\|\eta_{j,t}\|^2dt+C\nu\|\nabla\eta_j^{n+1}\|^2+\frac{C\Delta t}{\nu}\int_{t^n}^{t^{n+1}}\|u_{j,tt}\|^2dt\ .
\end{aligned}\tag{3.4.19}$$

By the timestep condition $\frac{\nu}{4}-C\frac{\triangle t}{h}\|\nabla U_j^n\|^2\geq C\nu>0$. Take the sum of (3.4.19) from n=1 to n=N-1 and multiply through by Δt

$$\begin{aligned}
&\frac{1}{2}||\xi_{j,h}^{N}||^2+\frac{\nu\Delta t}{8}||\nabla\xi_{j,h}^{N}||^2+\sum_{n=0}^{N-1}\frac{1}{4}\|\xi_{j,h}^{n+1}-\xi_{j,h}^{n}\|^2+C\Delta t\sum_{n=0}^{N-1}\nu\|\nabla\xi_{j,h}^{n+1}\|^2\\
&\qquad\leq\frac{1}{2}||\xi_{j,h}^{0}||^2+\frac{\nu\Delta t}{8}||\nabla\xi_{j,h}^{0}||^2+\Delta t\sum_{n=0}^{N-1}\frac{C}{\nu^2}\|\xi_{j,h}^{n}\|^2\\
&\qquad+\Delta t\sum_{n=0}^{N-1}\{C\nu^{-1}\|\nabla u_j^{n+1}\|^2\|\nabla\eta_j^{n+1}\|^2\\
&+\frac{C\Delta t}{\nu}(\int_{t^n}^{t^{n+1}}\|\nabla u_{j,t}\|^2\ dt)\|\nabla u_j^{n+1}\|^2+C\nu^{-1}\|\nabla\eta_j^{n}\|^2\|\nabla u_{j,h}^{n+1}\|^2\\
&\qquad+C\nu^{-1}\|\nabla U_j^n\|^2\|\nabla\eta_j^{n+1}\|^2+C\nu^{-1}\|\nabla U_j^n\|^2\|\nabla\eta_j^{n}\|^2\\
&\qquad+\frac{C\Delta t}{\nu}\|\nabla U_j^n\|^2(\int_{t^n}^{t^{n+1}}\|\nabla u_{j,t}\|^2dt)+C\nu^{-1}\|p_j^{n+1}-q_{j,h}^{n+1}\|^2\\
&+\frac{C}{\nu\Delta t}\int_{t^n}^{t^{n+1}}\|\eta_{j,t}\|^2dt+C\nu\|\nabla\eta_j^{n+1}\|^2+\frac{C\Delta t}{\nu}\int_{t^n}^{t^{n+1}}\|u_{j,tt}\|^2\ dt\}\ .
\end{aligned}\tag{3.4.20}$$

Applying interpolation inequalities gives

$$\begin{aligned}
&\frac{1}{2}||\xi_{j,h}^N||^2 + \sum_{n=0}^{N-1}\frac{1}{4}\|\xi_{j,h}^{n+1} - \xi_{j,h}^n\|^2 + \frac{\nu\Delta t}{8}||\nabla\xi_{j,h}^N||^2 + C\Delta t\sum_{n=0}^{N-1}\nu\|\nabla\xi_{j,h}^{n+1}\|^2 \\
&\qquad \leq \frac{1}{2}||\xi_{j,h}^0||^2 + \frac{\nu\Delta t}{8}||\nabla\xi_{j,h}^0||^2 + \Delta t\sum_{n=0}^{N-1}\frac{C}{\nu^2}\|\xi_{j,h}^n\|^2 \\
&\quad + C\frac{h^{2k}}{\nu}|||\nabla u_j|||_{\infty,0}^2|||u_j|||_{2,k+1}^2 + C\frac{\Delta t^2}{\nu}|||\nabla u_j|||_{\infty,0}^2|||\nabla u_{j,t}|||_{2,0}^2 \\
&\quad + C\frac{h^{2k}}{\nu^2}|||u_j|||_{2,k+1}^2 + C\frac{h^{2k+1}}{\Delta t}|||u_j|||_{2,k+1}^2 + Ch\Delta t|||\nabla u_{j,t}|||_{2,0}^2 \\
&\qquad + C\frac{h^{2s+2}}{\nu}|||p_j|||_{2,s+1}^2 + C\frac{h^{2k+2}}{\nu}|||u_{j,t}|||_{2,k+1}^2 \\
&\qquad + C\nu h^{2k}|||u_j|||_{2,k+1}^2 + \frac{C\Delta t^2}{\nu}|||u_{j,tt}|||_{2,0}^2 \ .
\end{aligned} \tag{3.4.21}$$

The next step will be the application of the discrete Gronwall inequality (Girault and Raviart [37], p. 176).

$$\begin{aligned}
&\frac{1}{2}\|\xi_{j,h}^N\|^2 + \sum_{n=0}^{N-1}\frac{1}{4}\|\xi_{j,h}^{n+1} - \xi_{j,h}^n\|^2 + \frac{\nu\Delta t}{8}\|\nabla\xi_{j,h}^N\|^2 + C\Delta t\sum_{n=0}^{N-1}\nu\|\nabla\xi_{j,h}^{n+1}\|^2 \\
&\leq exp(\frac{CN\Delta t}{\nu^2})\{\frac{1}{2}\|\xi_{j,h}^0\|^2 + \frac{\nu\Delta t}{8}||\nabla\xi_{j,h}^0||^2 + C\frac{h^{2k}}{\nu}|||\nabla u_j|||_{\infty,0}^2|||u_j|||_{2,k+1}^2 \\
&\qquad + C\frac{\Delta t^2}{\nu}|||\nabla u_j|||_{\infty,0}^2|||\nabla u_{j,t}|||_{2,0}^2 + C\frac{h^{2k}}{\nu^2}|||u_j|||_{2,k+1}^2 \\
&\qquad + C\frac{h^{2k+1}}{\Delta t}|||u_j|||_{2,k+1}^2 + Ch\Delta t|||\nabla u_{j,t}|||_{2,0}^2 \\
&\qquad + C\frac{h^{2s+2}}{\nu}|||p_j|||_{2,s+1}^2 + C\frac{h^{2k+2}}{\nu}|||u_{j,t}|||_{2,k+1}^2 \\
&\qquad + C\nu h^{2k}|||u_j|||_{2,k+1}^2 + \frac{C\Delta t^2}{\nu}|||u_{j,tt}|||_{2,0}^2\} \ .
\end{aligned} \tag{3.4.22}$$

Recall that $e_j^n = \eta_j^n + \xi_{j,h}^n$. Use the triangle inequality on the error equation to split the error terms into terms of η_j^n and $\xi_{j,h}^n$.

$$\frac{1}{2}\|e_j^N\|^2 + \sum_{n=0}^{N-1}\frac{1}{4}\|e_j^{n+1}-e_j^n\|^2 + \frac{\nu\Delta t}{8}\|\nabla e_j^N\|^2 + C\Delta t\sum_{n=0}^{N-1}\nu\|\nabla e_j^{n+1}\|^2$$
$$\leq \frac{1}{2}\|\xi_{j,h}^N\|^2 + \sum_{n=0}^{N-1}\frac{1}{4}\|\xi_{j,h}^{n+1}-\xi_{j,h}^n\|^2 + \frac{\nu\Delta t}{8}\|\nabla\xi_{j,h}^N\|^2 + C\Delta t\sum_{n=0}^{N-1}\nu\|\nabla\xi_{j,h}^{n+1}\|^2 \tag{3.4.23}$$
$$+\frac{1}{2}\|\eta_j^N\|^2 + \sum_{n=0}^{N-1}\frac{1}{4}\|\eta_j^{n+1}-\eta_j^n\|^2 + \frac{\nu\Delta t}{8}\|\nabla\eta_{j,h}^N\|^2 + C\Delta t\sum_{n=0}^{N-1}\nu\|\nabla\eta_j^{n+1}\|^2 .$$

Applying inequality (3.4.21), using the previous bounds for η_j^n terms,and absorbing constants into a new constant C, we have Theorem 2. □

3.5 NUMERICAL EXPERIMENTS

We present numerical experiments of the algorithm (BEFE-Ensemble). Our initial tests are simple with only $J = 2$ ensemble members verifying accuracy on an academic problem and the various stability conditions on a more interesting one. For the first test, using a perturbation of the Green-Taylor vortex, [40], [87], that leads to perturbed initial conditions and boundary conditions, we confirm the predicted convergence rates. Next we study a rotating flow involving offset cylinders. Adapting the timestep we show that stability is preserved, as predicted and measured by energy, enstrophy, and aggregate angular momentum. As the Reynolds number is increased, the rate of separation of nearby trajectories in the continuous problem is expected to increase, leading to a decrease in Δt under (3.1.3). This is indeed observed. We use FreeFEM++ [50], with Taylor-Hood elements (continuous piecewise quadratic polynomials for the velocity and continuous linear polynomials for the pressure) in all tests.

3.5.1 Convergence Experiment

The Green-Taylor vortex is a commonly used problem for convergence rates, since the true solution is known, e.g. [16], [88], [52], [13], [8]. In $\Omega = (0,1)^2$, the exact solution of the

Green-Taylor vortex is

$$
\begin{aligned}
u(x,y,t) &= -\cos(\omega\pi x)\sin(\omega\pi y)e^{-2\omega^2\pi^2 t/\tau}\,,\\
v(x,y,t) &= \sin(\omega\pi x)\cos(\omega\pi y)e^{-2\omega^2\pi^2 t/\tau}\,,\\
p(x,y,t) &= -\frac{1}{4}(\cos(2\omega\pi x)+\cos(2\omega\pi y))e^{-4\omega^2\pi^2 t/\tau}\,.
\end{aligned}
$$

Given $\tau = Re$, this is a solution of the NSE consisting of an $\omega \times \omega$ array of oppositely signed vortices that decay as $t \to \infty$. The initial condition is

$$
u^0 = (-\cos(\omega\pi x)\sin(\omega\pi y), \sin(\omega\pi x)\cos(\omega\pi y))^T\,.
$$

We take $\omega = 1$, $\tau = Re = 100$, $T = 1$, $h = 1/m$ and $\Delta t/h = 1/10$. Convergence rates are calculated from the error at two successive values of h in the usual manner by postulating $e(h) = Ch^\beta$ and solving for β via $\beta = \ln(e(h_1)/e(h_2))/\ln(h_1/h_2)$. The boundary condition on the problem is taken to be inhomogeneous Dirichlet: $u_h = u_{true}$, on $\partial\Omega$.

Generation of the initial conditions. The generation of ensemble members is necessarily dependent on the application and the question asked. In the first test, we consider an ensemble of two members u_1, u_2, which are the solutions corresponding to two different initial conditions $u_1^0 = (1+\epsilon_1)u^0$, $u_2^0 = (1+\epsilon_2)u^0$ respectively. This simple choice implies u_1, u_2 have a closed form $u_{1,2} = (1+\epsilon_{1,2})u_{exact}$ so errors can be calculated. Here $\epsilon_1 = 10^{-3}$, $\epsilon_2 = -10^{-3}$ are small perturbations on the initial condition u^0. Denote $u_{exact} = (u(x,y,t), v(u,y,t))^T$ and $p_{exact} = p(x,y,t)$. Adjusting body forces and boundary conditions for each ensemble member, we have $u_1 = (1+\epsilon_1)u_{exact}$, $p_1 = (1+\epsilon_1)^2 p_{exact}$, $u_2 = (1+\epsilon_2)u_{exact}$, $p_2 = (1+\epsilon_2)^2 p_{exact}$, see [95] for explanations. From the tables we can see the convergence rate for u_1 and u_2 is first order as predicted. u_{ave} is expected to converge to $0.5*(u_1+u_2)$, which in this test is equal to u_{exact}.

m	$\|u_1 - u_{1,h}\|_{\infty,0}$	rate	$\|\nabla u_1 - \nabla u_{1,h}\|_{2,0}$	rate
$\frac{3}{2} \cdot 27$	$8.45557 \cdot 10^{-6}$	–	$2.41940 \cdot 10^{-3}$	–
$(\frac{3}{2})^2 \cdot 27$	$2.26251 \cdot 10^{-6}$	3.2515	$9.21029 \cdot 10^{-4}$	2.3819
$(\frac{3}{2})^3 \cdot 27$	$1.09082 \cdot 10^{-6}$	1.7993	$3.65861 \cdot 10^{-4}$	2.2770
$(\frac{3}{2})^4 \cdot 27$	$6.90354 \cdot 10^{-7}$	1.1283	$1.56884 \cdot 10^{-4}$	2.0883
$(\frac{3}{2})^5 \cdot 27$	$4.57036 \cdot 10^{-7}$	1.0172	$6.85081 \cdot 10^{-5}$	2.0435

Table 1: Errors and convergence rates for the first ensemble member

3.5.2 Stability Verification

We test the timestep condition for stability of our algorithm on a problem of flow between two offset circles, motivated by the classic problem of flow between rotating cylinders. The domain is a disk with a smaller off center obstacle inside. Let $r_1 = 1$, $r_2 = 0.1$, $c = (c_1, c_2) = (\frac{1}{2}, 0)$, then the domain is given by

$$\Omega = \{(x, y) : x^2 + y^2 \leq r_1^2 \text{ and } (x - c_1)^2 + (y - c_2)^2 \geq r_2^2\}.$$

The flow is driven by a counterclockwise rotational body force

$$f(x, y, t) = (-4y * (1 - x^2 - y^2), 4x * (1 - x^2 - y^2))^T$$

with no-slip boundary conditions suppressed on both circles. Note that the rotational force $f \equiv 0$ at the outer circle so most of the interesting structures are expected to be due to the interaction of the flow with the inner circle. The flow rotates about $(0, 0)$ and interacts with the immersed circle $(x-c_1)^2+(y-c_2)^2 \leq r_2^2$ which induces a von Kármán vortex street. This vortex street rotates and itself re-interacts with the immersed circle, creating more complex structures. The mesh is parameterized by the number of mesh points (n=40) around the outer circle and the mesh points (m=10) around the immersed circle, and extended to all of Ω as a Delaunay mesh. As Re increases, this flow will be underresolved. Thus we give tests of stability but neither expect nor test accuracy.

m	$\|u_2 - u_{2,h}\|_{\infty,0}$	rate	$\|\nabla u_2 - \nabla u_{2,h}\|_{2,0}$	rate
$(\frac{3}{2}) \cdot 27$	$8.42864 \cdot 10^{-6}$	–	$2.41223 \cdot 10^{-3}$	–
$(\frac{3}{2})^2 \cdot 27$	$2.25806 \cdot 10^{-6}$	3.2484	$9.18647 \cdot 10^{-4}$	2.3810
$(\frac{3}{2})^3 \cdot 27$	$1.09000 \cdot 10^{-6}$	1.7963	$3.65017 \cdot 10^{-4}$	2.2763
$(\frac{3}{2})^4 \cdot 27$	$6.89994 \cdot 10^{-7}$	1.1277	$1.56547 \cdot 10^{-4}$	2.0879
$(\frac{3}{2})^5 \cdot 27$	$4.56809 \cdot 10^{-7}$	1.0171	$6.83669 \cdot 10^{-5}$	2.0433

Table 2: Errors and convergence rates for the second ensemble member

Generation of the initial conditions. In the second test, we generate perturbations of the initial conditions that are incompressible and satisfy no-slip boundary conditions by solving steady Stokes problem on the same geometry with body forces perturbed. Let

$$f_1(x,y,t) = f(x,y,t) + \epsilon_1 * (sin(3\pi x)sin(3\pi y), cos(3\pi x)cos(3\pi y))^T,$$

$$f_2(x,y,t) = f(x,y,t) + \epsilon_2 * (sin(3\pi x)sin(3\pi y), cos(3\pi x)cos(3\pi y))^T,$$

where $\epsilon_1 = 10^{-3}$, $\epsilon_2 = -10^{-3}$. In this way, we generate $u_j^0, j = 1, 2$, satisfying the no-slip condition. The solutions of the steady Stokes problem corresponding to these two body forces are our perturbed initial conditions, which are denoted by u_1^0 and u_2^0.

We solve Navier-Stokes equations using our algorithm with these two initial conditions, which gives us u_1, u_2, and u_{ave}. We also solve the steady Stokes problem using $f(x,y,t)$ and get the initial condition u_0^0 to do a comparison. The solution of NSE with u_0^0 is denoted by u_0 (marked as 'no perturbation' in the figures).

Test 1: Taking $Re = 200$, we give plots over $0 \le t \le 10$ of the following quantities:

$$|\text{Angular Momentum}| = |\int_\Omega \vec{x} \times \vec{u}\ d\vec{x}|$$

$$\text{Enstrophy} = \frac{1}{2}\nu\|\nabla \times \vec{u}\|^2$$

$$\text{Energy} = \frac{1}{2}\|u\|^2$$

To ensure the algorithm is stable, we first cut Δt to enforce

$$C\frac{\Delta t}{\nu h}||\nabla(u_{j,h}^n - < u_h >^n)||^2 \le 1, \qquad (j = 1, \cdots, J) \tag{3.5.1}$$

m	$\|u_{exact} - u_{ave,h}\|_{\infty,0}$	rate	$\|\nabla u_{exact} - \nabla u_{ave,h}\|_{2,0}$	rate
$(\frac{3}{2}) \cdot 27$	$8.44211 \cdot 10^{-6}$	–	$2.41582 \cdot 10^{-3}$	–
$(\frac{3}{2})^2 \cdot 27$	$2.26028 \cdot 10^{-6}$	3.2500	$9.19838 \cdot 10^{-4}$	2.3815
$(\frac{3}{2})^3 \cdot 27$	$1.09041 \cdot 10^{-6}$	1.7978	$3.65439 \cdot 10^{-4}$	2.2766
$(\frac{3}{2})^4 \cdot 27$	$6.90174 \cdot 10^{-7}$	1.1280	$1.56715 \cdot 10^{-4}$	2.0881
$(\frac{3}{2})^5 \cdot 27$	$4.56923 \cdot 10^{-7}$	1.0172	$6.84375 \cdot 10^{-5}$	2.0434

Table 3: Errors and convergence rates for the average of ensemble members

In practise, the constant C can be determined by a few pre-computations. In our test, we cut Δt to enforce the condition

$$\frac{\Delta t}{h}||\nabla(u^n_{j,h} - < u_h >^n)||^2 \leq \frac{1200}{Re}, \qquad (j = 1, 2) \tag{3.5.2}$$

Once this condition is violated, we update the time step with $dt^{new} = dt^{old}/2$ and keep doing this until the condition is satisfied again. Note that in this first test we cut Δt but do not increase Δt. Figure 1-3 show that the condition (3.5.2) is, as predicted, sufficient for stability of our algorithm for $Re = 200$. Figure 4 shows a comparison of time step evolution with respect to 3d condition (3.5.2) and 2d condition (2d C1) with the same constant $C = \frac{1}{1200}$. Figure 5 shows snapshots of the flow, which is complex (some complexity from the flow and some from the underresolved mesh) and seems to be pulsating. Figure 6 shows snapshots of the contours ($|Vor|/|Vor|.max > 0.1$) of vorticity.

Test 2: Taking $Re = 800$, we test the 2d condition (2d C1).

Case 1: Timestep halving only.

$$|ln(h)|\Delta t||\nabla(u^n_{j,h} - < u_h >^n)||^2 \leq \frac{1200}{Re}$$

Figure 10 shows that as Re increases, Δt decreases.

m	$\|\nabla p_1 - \nabla p_{1,h}\|_{2,0}$	rate	$\|\nabla p_2 - \nabla p_{2,h}\|_{2,0}$	rate
$(\frac{3}{2}) \cdot 27$	$5.93247 \cdot 10^{-2}$	–	$5.91504 \cdot 10^{-2}$	–
$(\frac{3}{2})^2 \cdot 27$	$3.97196 \cdot 10^{-2}$	0.9894	$3.94309 \cdot 10^{-2}$	1.0002
$(\frac{3}{2})^3 \cdot 27$	$2.64583 \cdot 10^{-2}$	1.0020	$2.59944 \cdot 10^{-2}$	1.0276
$(\frac{3}{2})^4 \cdot 27$	$1.81013 \cdot 10^{-2}$	0.9362	$1.73880 \cdot 10^{-2}$	0.9917
$(\frac{3}{2})^5 \cdot 27$	$1.26636 \cdot 10^{-2}$	0.8811	$1.15926 \cdot 10^{-2}$	0.9999

Table 4: Errors and convergence rates for pressure

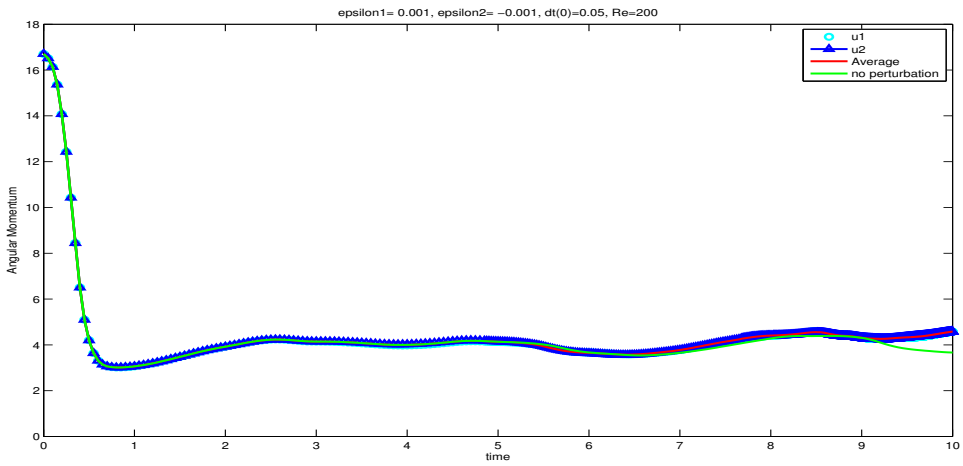

Figure 1: Stability: Angular Momentum, $\nu = 1/200$

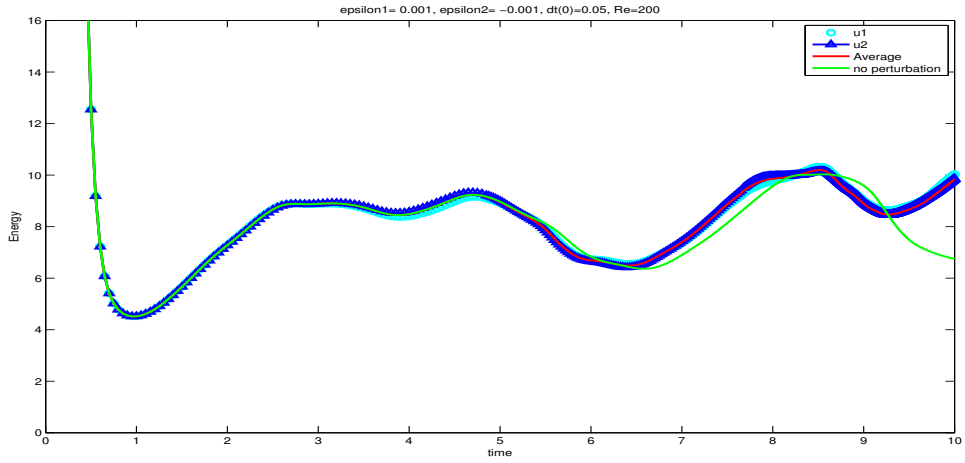

Figure 2: Stability: Energy with $\nu = 1/200$

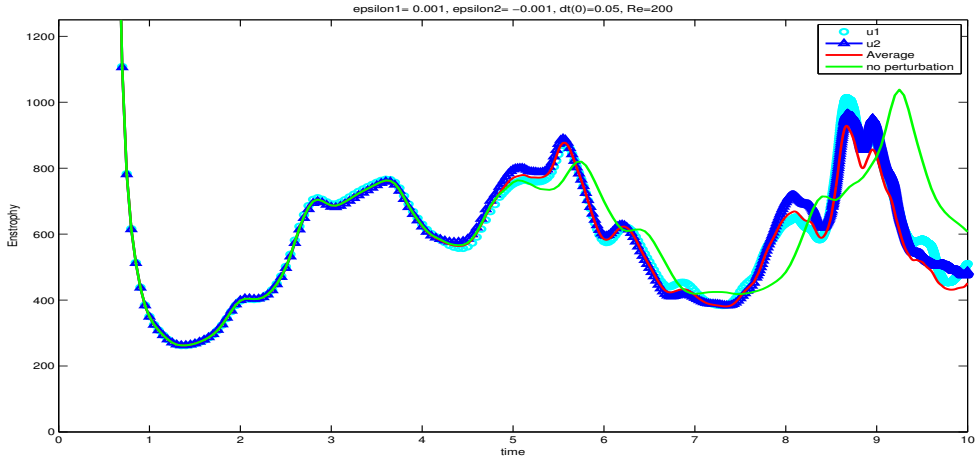

Figure 3: Stability: Enstrophy, $\nu = 1/200$

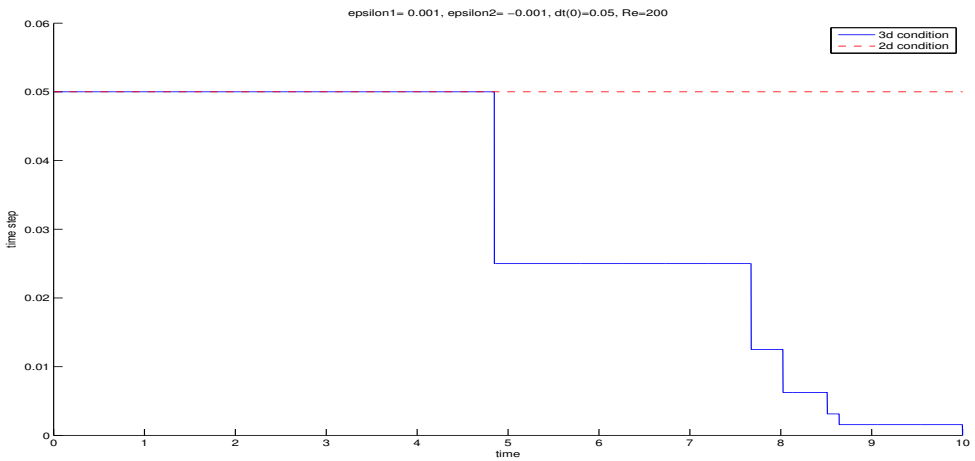

Figure 4: Timestep evolution, $\nu = 1/200$

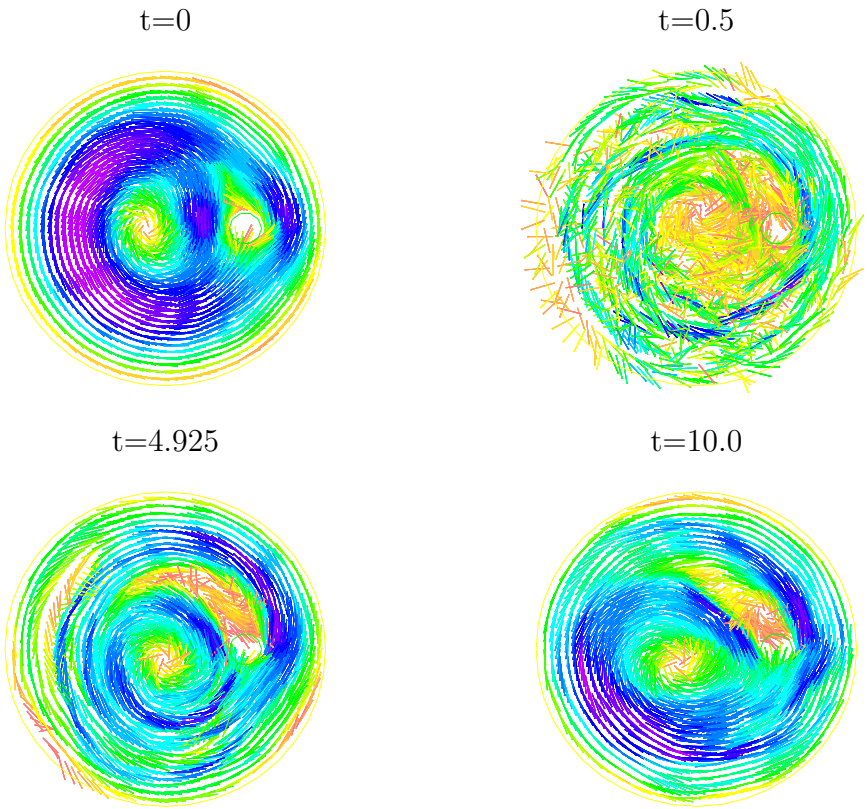

Figure 5: Velocity, $\nu = 1/200$

t=0

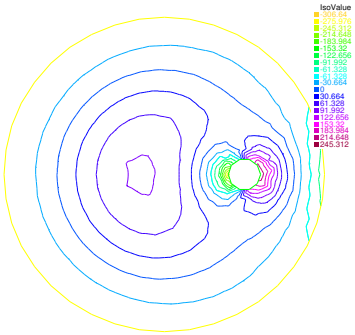

t=0.5

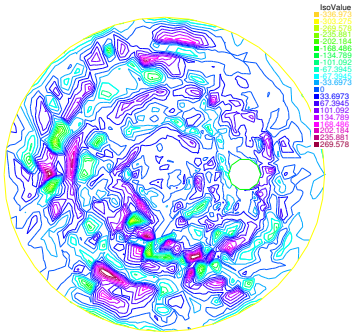

t=4.925

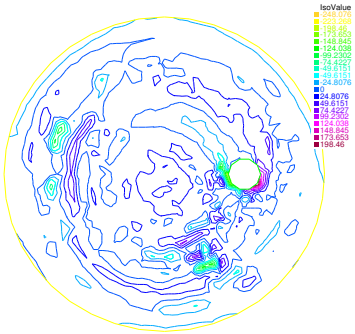

t=10.0

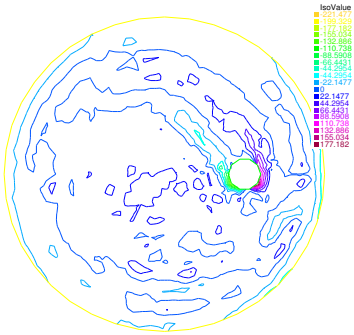

Figure 6: Contours of Vorticity, $\nu = 1/200$

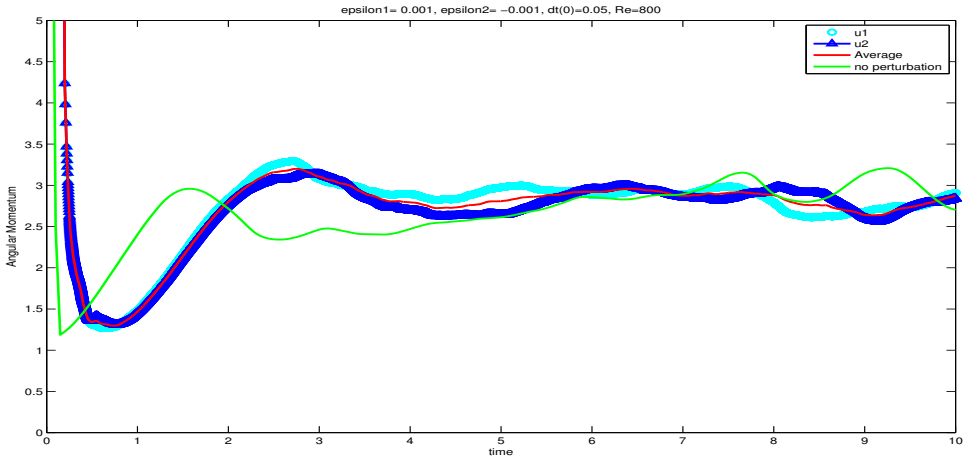

Figure 7: 2d-condition (timestep halving): Angular Momentum, $\nu = 1/800$

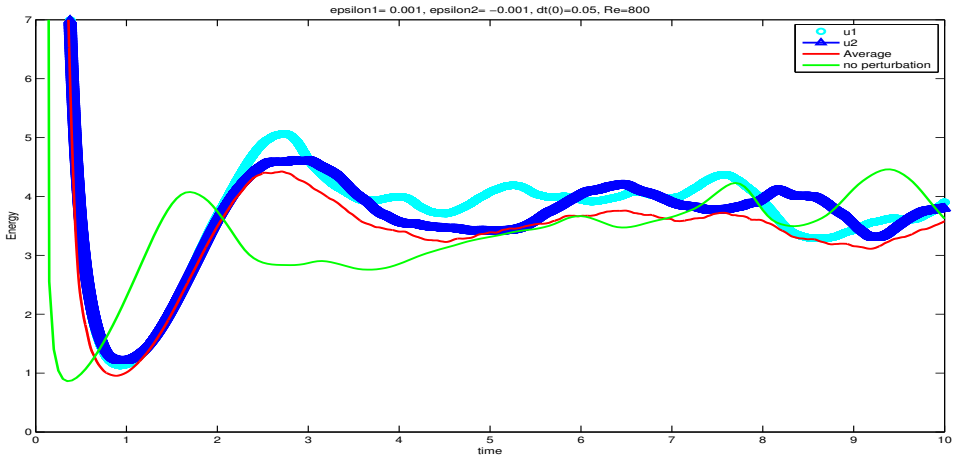

Figure 8: 2d-condition (timestep halving): Energy, $\nu = 1/800$

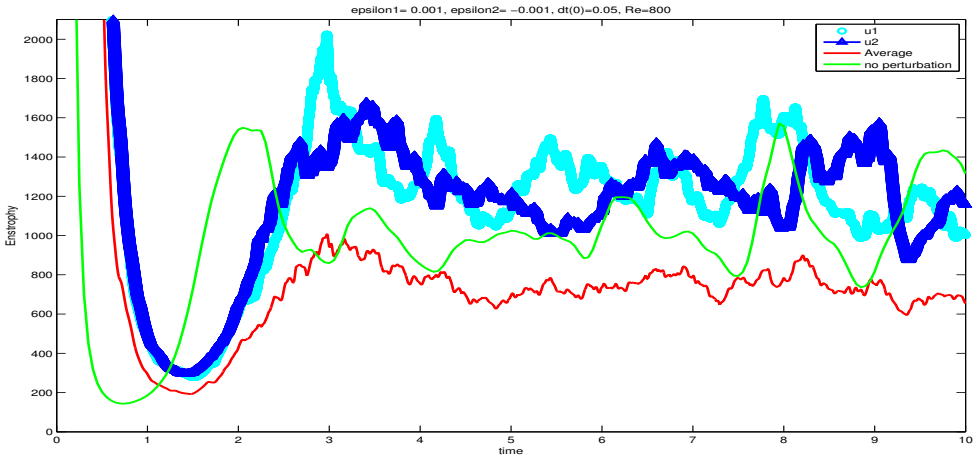

Figure 9: 2d-condition (timestep halving): Enstrophy, $\nu = 1/800$

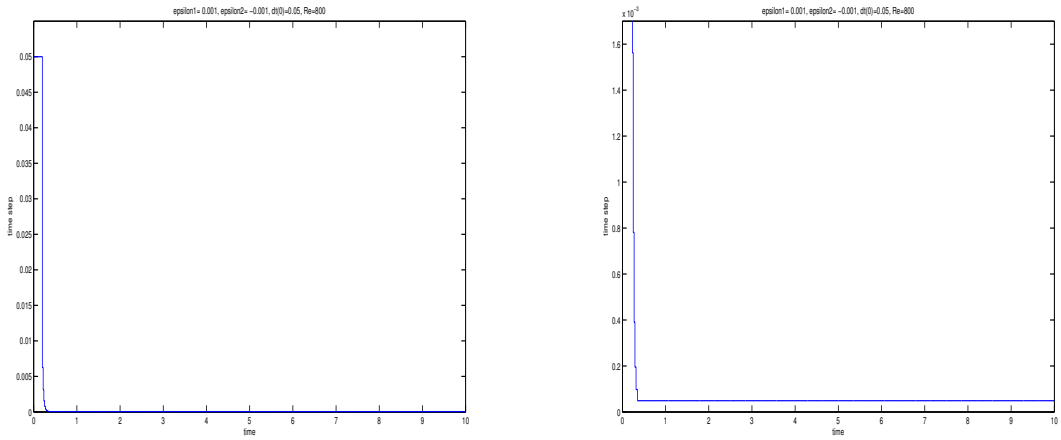

Figure 10: Timestep Halving: Timestep evolution (left), Zoom in (right), $\nu = 1/800$

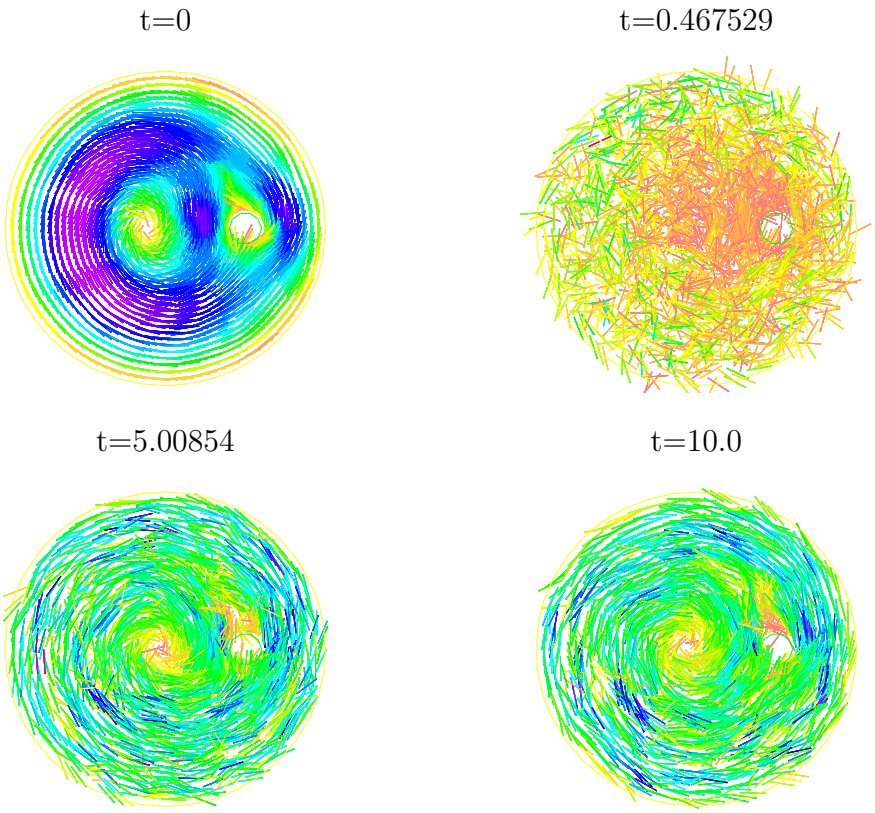

Figure 11: Velocity (timestep halving), $\nu = 1/800$

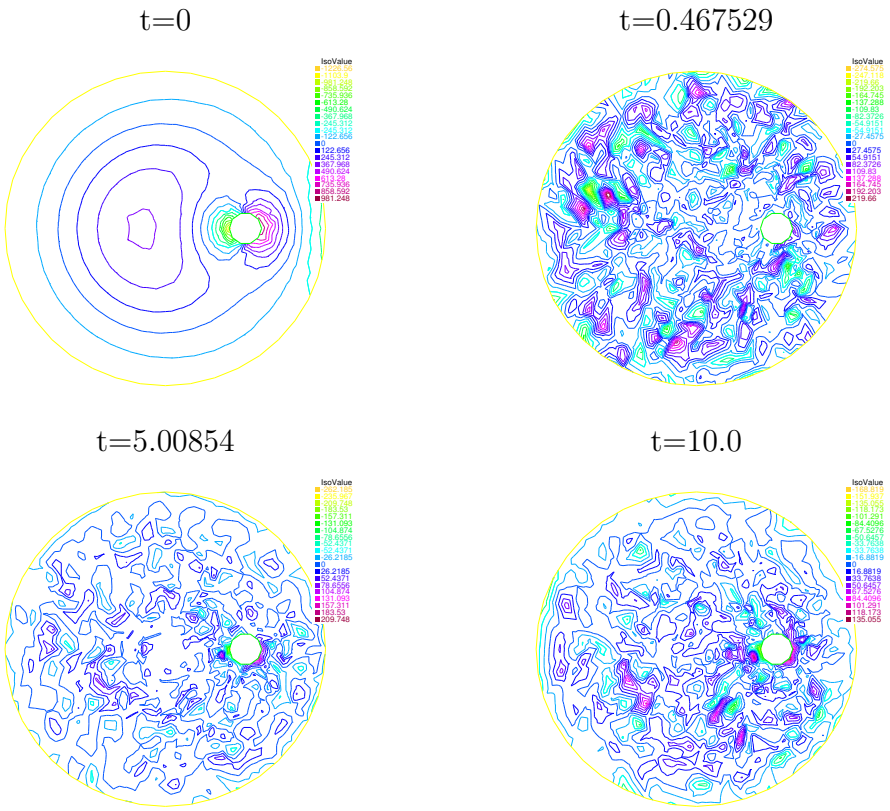

Figure 12: Contours of Vorticity (timestep halving), $\nu = 1/800$

Case 2: Timestep halving and doubling.

$$|ln(h)|\Delta t||\nabla(u^n_{j,h} - < u_h >^n)||^2 \leq \frac{1200}{Re}$$

and $$|ln(h)|\Delta t||\nabla(u^n_{j,h} - < u_h >^n)||^2 \geq 0.5 * \frac{1200}{Re}$$

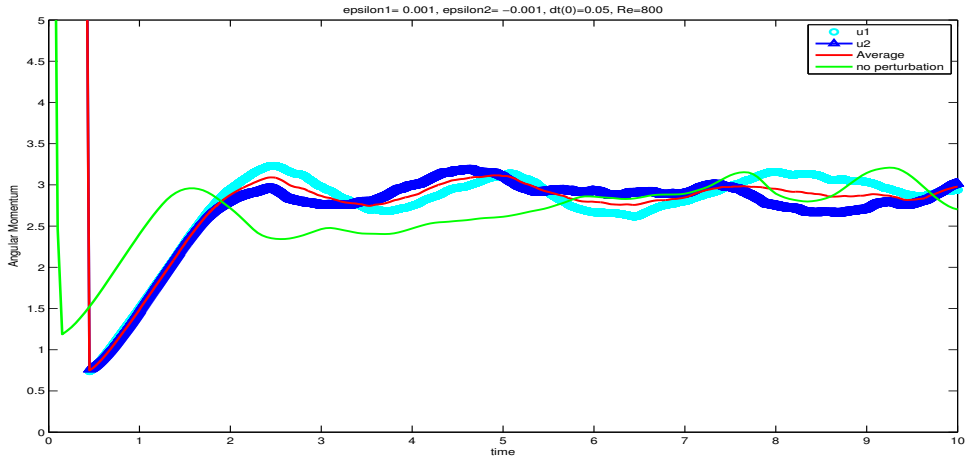

Figure 13: 2d-condition (timestep halving and doubling): Angular Momentum, $\nu = 1/800$

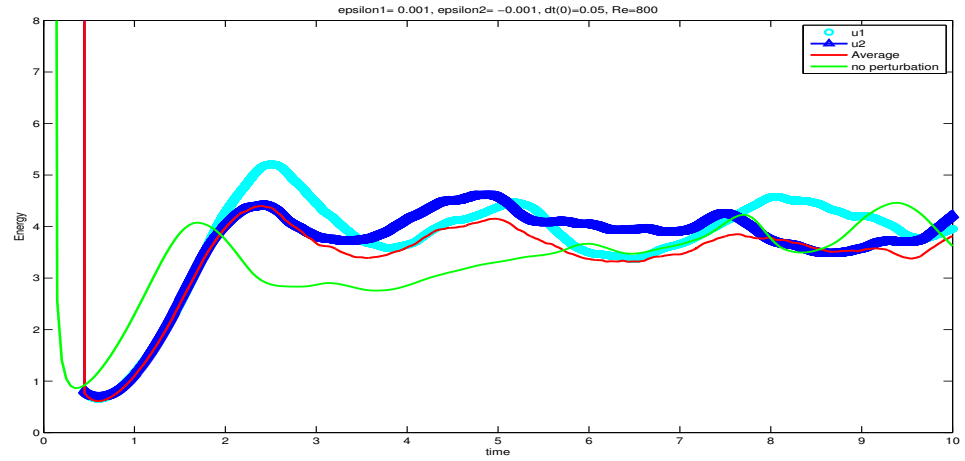

Figure 14: 2d-condition(timestep halving and doubling): Energy, $\nu = 1/800$

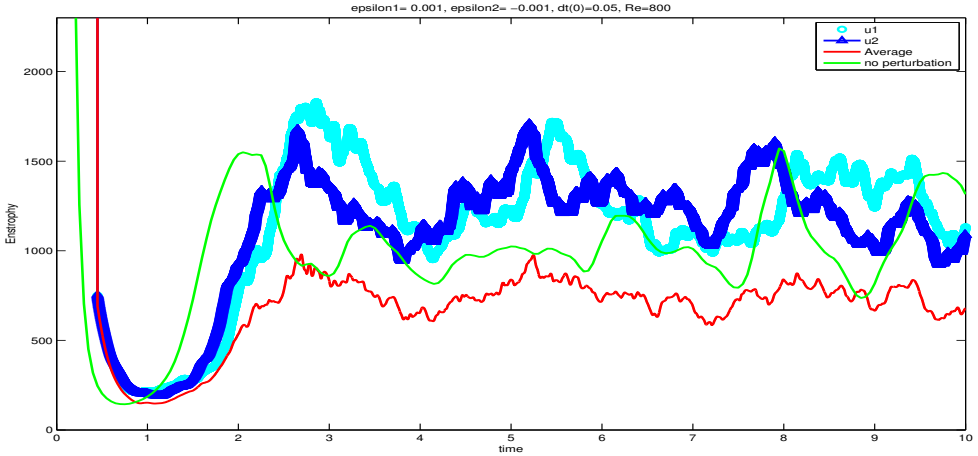

Figure 15: 2d-condition(timestep halving and doubling): Enstrophy, $\nu = 1/800$

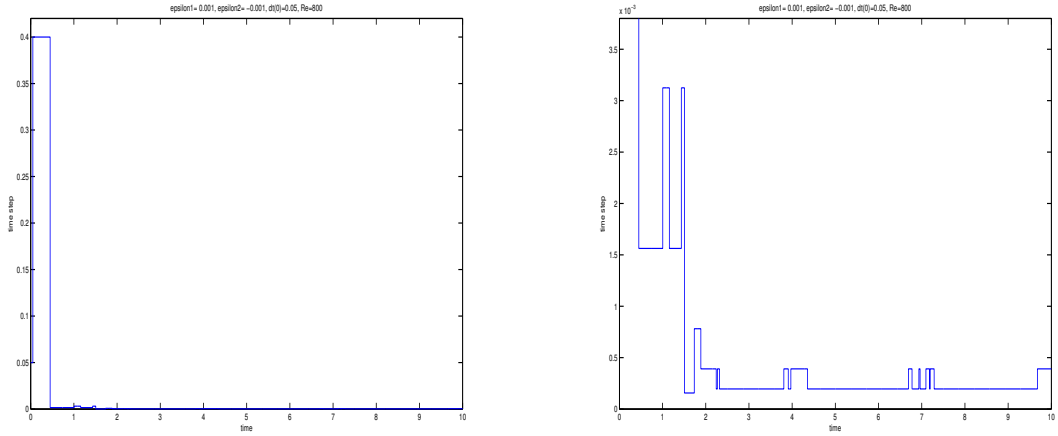

Figure 16: Timestep Halving and Doubling: Timestep evolution, $\nu = 1/800$,

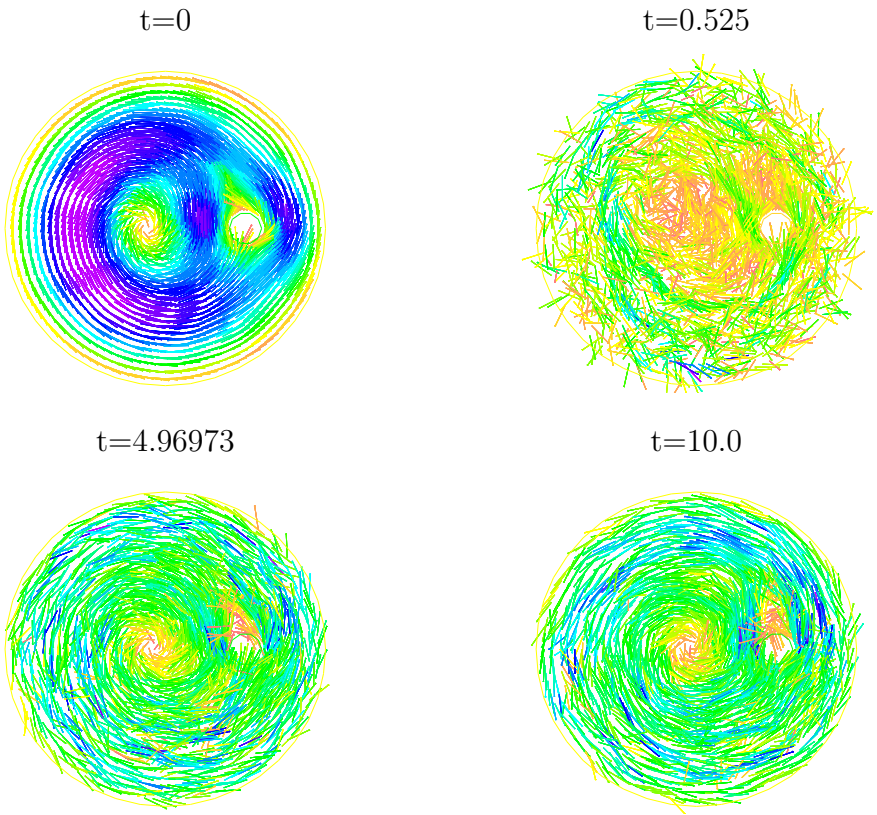

Figure 17: 2d-condition (timestep halving and doubling): Velocity, $\nu = 1/800$

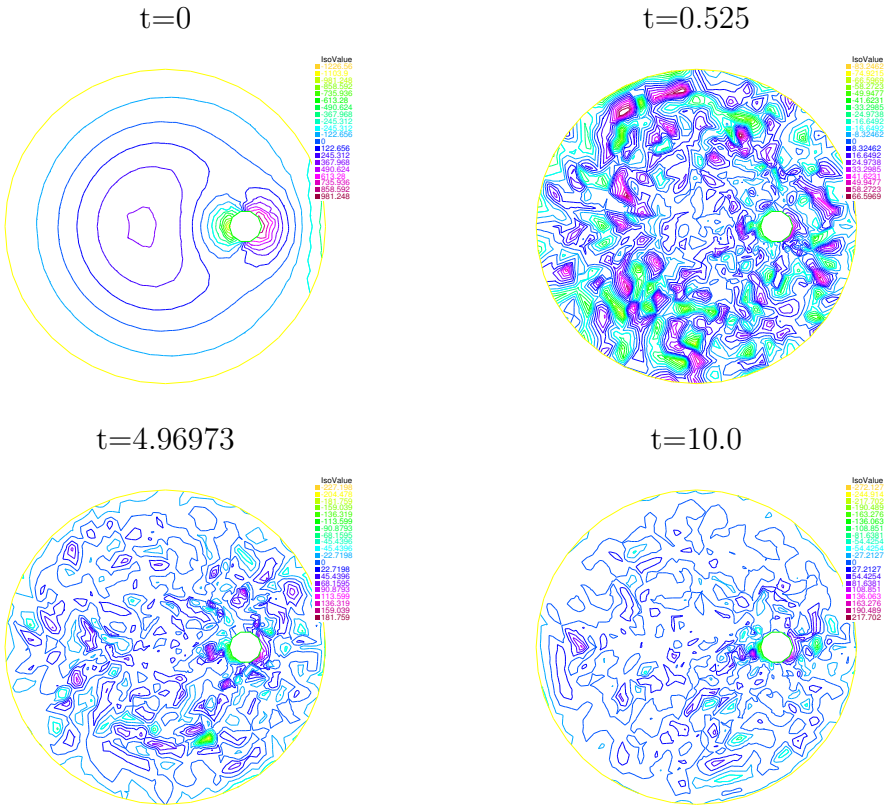

Figure 18: 2d-condition (timestep halving and doubling): Contours of Vorticity, $\nu = 1/800$

3.6 CONCLUSIONS

The need for ensemble calculations arises in calculation of sensitivities by differences [75], uncertainty quantification [67], stochastic NSE simulations [73], generation of bred vectors and their use in improving forecasting skill, Kalnay [89]. The most efficient way to calculate such an ensemble will vary widely depending on the application, flow, computational resources and code used. This chapter has presented and analyzed an algorithm for computation of an ensemble of solutions such that each step requires the solution of one linear system with multiple right hand sides. Stability requires a timestep condition that can easily be imposed step by step. Experimental verification of stability under the condition is given.

4.0 NUMERICAL ANALYSIS OF TWO ENSEMBLE EDDY VISCOSITY NUMERICAL REGULARIZATIONS OF FLUID MOTION

In the numerical simulation of flows with incomplete data, quantification of uncertainty, increasing forecasting skill, quantification of flow sensitivities and other issues lead to the problem of computing ensembles, u_j, p_j, of solutions of the Navier-Stokes equations. Many studies have computed flow ensembles of various turbulence models for various applications (e.g., [18], [15], [62], [67], [75]). Herein algorithms are considered that compute an ensemble at one pass aiming at methods that are unconditionally, nonlinearly, long time stable and have computational cost and storage only modestly increased over that of one realization. These new algorithms also allow each realization access to data on the size of fluctuations. This chapter also studies the use of this newly available ensemble data for numerical regularization in each realization. The use of ensemble data to parametrize a turbulence model for each realization was previously presented in the interesting paper of Carati, Roberts and Wray [15].

The number of realizations required (J) varies with application. For many, a small ensemble number often suffices. For example, [15] found that by reducing the simulation time window by the number of ensemble members (under the hypothesis of equivalence of time and ensemble averaging) simulation costs were reduced and the statistics studied changed little for more than $J = 16$ realizations. It may also be that only $J = 3$ realizations suffice for providing error bars when the realizations are initialized by the Bred-Vectors algorithm of Toth and Kalnay [89] (described in Remark 2 below) which gives at low cost ensemble data with maximal forecast spread. In Bred-Vectors algorithm, bred vectors are generated by subtracting the control (the one with no perturbation in its initial condition) from each realization after integrating the numerical model over some time. Then the bred vectors are

scaled to have the same size of the initial perturbations and added to the control providing a new ensemble of realizations. This process is repeated periodically and usually in a short time it can generate perturbations dominated by the fastest growing errors of the model . However large or small the ensemble number, there arises inevitably the competition between computing ensembles of solutions vs. high resolution, [86], that is, between J parallel, low resolution simulations and (more commonly) J sequential, high resolution ones. In [53] a third possibility was advanced for laminar flows and extended herein.

The key to efficiency in the ensemble algorithm presented in Chapter 3 is that, after spacial discretization, each time step requires the solution of one linear system with the same, shared coefficient matrix:

$$A \left[\begin{array}{c|c|c} u_1 & \cdots & u_J \\ p_1 & \cdots & p_J \end{array} \right] = [RHS_1 \,|\cdots|\, RHS_J]\,. \tag{4.0.1}$$

This form allows the use of special projective, [30], or block iterative methods, e.g., [79], [31], [4], [39], reducing required storage and work to advance in time.

The method *without numerical regularization* requires a timestep condition $C\frac{\Delta t}{\nu \triangle x}\|\nabla u'\|^2 \leq 1$ ($||\cdot|| = L^2$ norm, $\langle u\rangle$ = mean and u' = fluctuation) that begins mild but degrades quickly as fluctuations grow for either under resolved simulations or increasing Re. This need for numerical regularization as Re increases / ν decreases is as expected, e.g., [83], even for $1d$ scalar convection diffusion equations and seen clearly in Figures 27 and 28 (the failure when $\mu = 0$) in Section 4.4. Herein, we include two ensemble eddy viscosity (**EEV**) numerical regularizations ($-\nabla \cdot (\nu_T \nabla u_j)$) with parametrizations

$$\textbf{EEV1:}\quad \nu_T = \mu|u'|\triangle x, \quad \textbf{EEV2:}\quad \nu_T = \mu|u'|^2\triangle t.$$

These are based on direct calculation of the kinetic energy in the fluctuations, $\frac{1}{2}|u'|^2$ with no modeling, Section 4.1. Both preserve the structure of the linear system (4.0.1). We note that both give the same parametrization for each ensemble member (necessary to preserve the efficiencies arising from the above block structure). Some favorable aspects of this feature (called universality therein) was pointed out in [15].

EEV2 below arises from *a redefinition of the mixing length* suggested by the stability analysis (Remark 3 in Section 4.2) to

$$l(x,t) = \textit{ distance a fluctuating eddy travels in one time step} = |u'|\triangle t.$$

Theorem 6 and preliminary tests (Section 4.4, Tests 2, 3) show greater stability and reduced over-diffusion. The choice $l(x,t) = |u'|\triangle t$ also enforces $l(x,t) \to 0$ as $x \to walls$ without van Driest damping. It was suggested (but not developed subsequently to our knowledge) by Prandtl:

> ...may be considered as the diameter of the masses of fluid moving as a whole in each individual case; or again, as the distance traversed by a mass of this type before it becomes blended in with neighboring masses..., L. Prandtl in: *Proc. Second Int. Congr. Appl. Mech.*. Zurich, 1926.

4.1 REGULARIZATIONS AND TIME DISCRETIZATIONS

The Euclidean length of a vector and Frobenius norm of an array is $|\cdot|$. The symmetric part of the velocity gradient tensor is denoted ∇^s. The ensemble mean $\langle u \rangle$, fluctuation u'_j, its magnitude $|u'|$ and the induced kinetic energy density k' are

$$\text{mean: } < u >:= \frac{1}{J}\sum_{j=1}^{J} u_j, \text{ fluctuation: } u'_j := u_j - < u > ,$$

$$|u'|^2 := \sum_{j=1}^{J} |u'_j|^2 \text{ and energy density: } \quad k'(x,t) := \frac{1}{2}\,|u'|^2(x,t).$$

To present the method, suppress the secondary spacial discretization and let superscripts denote the timestep number. Thus, for example, $< u >^n, u'^n_j$ denote respectively approximations to $\frac{1}{J}\sum_{j=1}^{J} u_j(\cdot,t_n)$ and $u'_j(\cdot,t_n) = u_j(\cdot,t_n) - \frac{1}{J}\sum_{j=1}^{J} u_j(\cdot,t_n)$ where $t_n := n\triangle t$. This report considers the method: for $\quad j = 1, ..., J,\ \nabla \cdot u_j^{n+1} = 0, \quad$ and

$$\frac{u_j^{n+1} - u_j^n}{\Delta t} + < u >^n \cdot \nabla u_j^{n+1} + (u_j^n - < u >^n) \cdot \nabla u_j^n \tag{4.1.1}$$
$$+\nabla p_j^{n+1} - \nu \Delta u_j^{n+1} - \nabla \cdot (2\nu_T(l^n, k'^n)\nabla^s u_j^{n+1}) = f_j^{n+1}.$$

We consider EEV in the method as a numerical regularization of the type used for simulation of under-resolved, convection dominated flow in $1, 2$ or 3 dimensions. Nevertheless, while it uses ensemble information in a new way, the form of ν_T is consistent with conventional models of turbulence. Since fluctuations' effects on the mean flow are envisioned as a mixing process, $\nu_T(\cdot)$ increases with increasing k', consistent with adding numerical damping for oscillations resulting from under resolution. The Kolmogorov-Prandtl relation gives for $\nu_T(\cdot)$

$$\begin{aligned} \nu_T(\cdot) = \nu_T &= \sqrt{2}\mu l\sqrt{k'}, \\ l = &\text{ mixing length of fluctuations,} \\ k' = &\text{ kinetic energy in fluctuations.} \end{aligned}$$

Often extensive (and optimistic) modeling steps are needed to generate representations of these two quantities, e.g., [85], [68]. The order of calculations in algorithm (4.1.1) allows direct calculation of both:

$$k' = \frac{1}{2}|u'|^2 \quad \text{and} \quad l = \begin{cases} \text{either } \triangle x, \\ \text{or } |u'|\triangle t \end{cases} .$$

The linkage with the discretization parameters ($\triangle x$ or $\triangle t$) shows a connection with ideas in large eddy simulation, e.g., [51], [85], blurring the distinction between numerical regularizations and continuum models. From the latter vantage, Pope, [82], calculates the value $\mu = 0.55$ from the $(3d)$ law of the wall; we shall regard herein μ simply as a tuning parameter.

Analysis of the second mixing length near walls. There is a classical analysis (possibly even due to Prandtl, for background see Pope [82]) of near wall behavior of mixing length suggesting $l(y) \sim O(y)$ as the wall-normal distance $y \to 0$. The analysis is based on the hypothesis that mixing length due to fluctuations is equivalent to the effect of a wall normal displacement of the mean flow. This yields $l(y) \sim |\langle u \rangle (y_1) - \langle u \rangle (y_2)|$. Letting $y_1 \to 0$ this gives $l(y) \sim y|\frac{\partial}{\partial y}\langle u \rangle|$. For the second mixing length herein $l = |u'|\triangle t$ we note that

$$\begin{aligned} l(y) &\sim |u_i(y) - u_j(y)|\triangle t = \text{ (since at the wall } u_i(0) = u_j(0)) \\ &= |u_i(y) - u_i(0) + u_j(0) - u_j(y)|\triangle t \sim y\left(|\frac{\partial}{\partial y}u_i(y)| + |\frac{\partial}{\partial y}u_j(y)|\right)\triangle t \end{aligned}$$

which exhibits the correct asymptotic rate $l(y) \sim O(y)$ as the wall-normal distance $y \to 0$. This suggests no additional damping in the near-wall regions, such as the van Driest damping, is needed.

Remark 1 (**Ensemble average equation**). *Taking the ensemble average of (4.1.1) gives a discretization (consistent since $\nu_T \to 0$ as $\triangle x, \triangle t \to 0$) of the ensemble averaged momentum equation:*

$$\begin{aligned}
&\frac{< u >^{n+1} - < u >^n}{\Delta t} + < u >^n \cdot \nabla < u >^{n+1} \\
&\quad + \left[< u_j^n \cdot \nabla u_j^n > - < u >^n \cdot \nabla < u >^n \right] \\
&+\nabla < p >^{n+1} - \nu \Delta < u >^{n+1} - \nabla \cdot (\nu_T(l^n, k'^n) \nabla < u >^{n+1}) =< f >^{n+1} .
\end{aligned}$$

The term in brackets is the usual Reynolds stress term. Since this contains both the Reynolds stresses and the EEV term, the EEV term herein functions as a regularization in each realization rather than a continuum model (in which eddy viscosity would replace the Reynolds stress terms).

Remark 2 (Bred-Vectors). *The Bred-Vectors algorithm of [89] is non intrusive and generates perturbations with components in the direction of maximal trajectory separation. It proceeds by selecting a time update interval $\triangle T$ and an initial perturbation $\varepsilon(x)$. Solutions $u(x,t), u_\pm(x,t)$ with initial conditions $u_0(x)$ and $u_0(x) \pm \varepsilon(x)$ are calculated. At the next update time (initially $\triangle T$) the perturbed solutions $u_\pm(x, \triangle T)$ are normalized*

$$u_\pm(x, \triangle T) \Leftarrow u(x, \triangle T) \pm [u(x, \triangle T) - u_\pm(x, \triangle T)] \frac{||\varepsilon||}{||u(x, \triangle T) - u_\pm(x, \triangle T)||}.$$

This is repeated a few times. A complete analysis in the nonlinear case seems to be open. However, for the linear evolution equation $u_t + Au = f$ by subtraction this is equivalent to the following algorithm acting on the perturbation ε: given ε_0

$$\varepsilon_0 \to e^{-A\triangle T}\varepsilon_0 \to e^{-A\triangle T}\varepsilon_0 \frac{||\varepsilon_0||}{||e^{-A\triangle T}\varepsilon_0||} = \varepsilon_1 \to \cdots$$

which is exactly the power method for $e^{-A\triangle T}$ converging to the dominant eigenvector of $e^{-A\triangle T}$.

4.2 STABILITY OF THE ALGORITHM WITH REGULARIZATION

Many spacial discretizations are used for flow problems. Thus we shall begin by studying stability of the discrete time, continuous space approximation. Consider (4.1.1) where ν_T is given by

$$\textbf{EEV1:} \quad \nu_T = \mu|u'|\triangle x, \text{ or } \quad \textbf{EEV2:} \quad \nu_T = \mu|u'|^2\triangle t. \tag{4.2.1}$$

The stability analysis of Theorems $6-9$ below is based on energy methods (and without Gronwall's inequality). Thus, "stability" herein means global, nonlinear, long time stability. One striking result (Theorem 6) is unconditional stability for EEV2 when $\mu \geq 1/2$. In the spatially discrete case and with the most common form of the NSE nonlinearity, stability requires control of $\|\nabla \cdot u'^n\|_{L^4}$, Theorem 8. (The conditions on $\|\nabla \cdot u'\|$ are not necessary when the rotational form of the NSE nonlinearity are used in the discrete algorithms.) For EEV1, stability requires more: either an Re dependent global timestep condition or a local timestep condition, Theorems $7, 9$ and 10.

Theorem 6 (Unconditional Stability of **EEV2**). *The method (4.1.1) with **EEV2** $\nu_T = \mu|u'|^2\triangle t$ is unconditionally, nonlinearly, long time stable (even for $\nu = 0$) if*

$$\mu \geq \frac{1}{2}, \tag{4.2.2}$$

or if

$$\frac{\triangle t|u_j'^n|^2}{2\nu} \leq 1, \tag{4.2.3}$$

or if, for some $\theta, 0 \leq \theta \leq 1$, the timestep condition holds:

$$\mu_2 \geq \frac{\theta}{2}, \quad \textit{and} \quad (1-\theta)\frac{\triangle t|u_j'^n|^2}{2\nu} \leq 1. \tag{4.2.4}$$

Proof. Take the inner product of the equation (4.1.1) with u_j^{n+1}. Multiplying by $2\triangle t$, using skew symmetry of the first nonlinear term and the polarization identity in the time difference term yields

$$||u_j^{n+1}||^2 - ||u_j^n||^2 + ||u_j^{n+1} - u_j^n||^2 + 2\triangle t\left((u_j^n - < u >^n) \cdot \nabla u_j^n, u_j^{n+1}\right) +$$
$$+2\triangle t \int_\Omega [\nu + \nu_T(l^n, k'^n)]|\nabla u_j^{n+1}|^2 dx = 2\triangle t\left(f_j^{n+1}, u_j^{n+1}\right).$$

By skew symmetry we have

$$\begin{aligned}\left((u_j^n - < u >^n) \cdot \nabla u_j^n, u_j^{n+1}\right) &= \left((u_j^n - < u >^n) \cdot \nabla u_j^n, u_j^{n+1} - u_j^n\right) = \\ &= \left((u_j^n - < u >^n) \cdot \nabla [u_j^n + u_j^{n+1} - u_j^n], u_j^{n+1} - u_j^n\right) \\ &= \left((u_j^n - < u >^n) \cdot \nabla u_j^{n+1}, u_j^{n+1} - u_j^n\right).\end{aligned}$$

Nonlinear, long time stability thus follows provided

$$\begin{aligned}&||u_j^{n+1} - u_j^n||^2 + 2\triangle t \int_\Omega [\nu + \nu_T(l^n, k'^n)] |\nabla u_j^{n+1}|^2 dx \\ &+2\triangle t \left((u_j^n - < u >^n) \cdot \nabla u_j^{n+1}, u_j^{n+1} - u_j^n\right) \geq 0.\end{aligned}$$

The first two terms are nonnegative and the third can have two signs. We thus consider the third term. We have

$$2\triangle t \left|\left((u_j^n - < u >^n) \cdot \nabla u_j^{n+1}, u_j^{n+1} - u_j^n\right)\right| \leq ||u_j^{n+1} - u_j^n||^2 + \triangle t^2 \int_\Omega |u_j'^n|^2 |\nabla u_j^{n+1}|^2 dx.$$

Using this as a worst case bound for the third term gives the sufficient condition

$$\int_\Omega \left\{2[\nu + \nu_T(l^n, k'^n)] |\nabla u_j^{n+1}|^2 - \triangle t |u_j'^n|^2 |\nabla u_j^{n+1}|^2\right\} dx \geq 0.$$

With the EEV parameterization $\nu_T = \mu |u'|^2 \triangle t$, this becomes

$$\int_\Omega [2\nu + \triangle t \left(2\mu |u'^n|^2 - |u_j'^n|^2\right)] |\nabla u_j^{n+1}|^2 dx \geq 0,$$

from which the first stability result follows when $\mu \geq \frac{1}{2}$, i.e., (4.2.2). For the second condition (4.2.3), noting that it makes no reference to the eddy viscosity term, stability under the second condition follows by absorbing the term $\triangle t |u'|^2 |\nabla u|^2$ in the viscous term $2\nu |\nabla u|^2$ similarly. The third condition (4.2.4) is a combination of the first two. □

We prove stability for EEV1 under the following, pointwise, timestep condition.

Theorem 7 (Conditional stability of **EEV1**). *Consider (4.1.1) with **EEV1**: $\nu_T = \mu|u'|\triangle x$. A sufficient condition for stability is that there holds pointwise*

$$\frac{\triangle t|u'(x,t_n)|}{\triangle x} \leq \frac{1}{2}\mu + \sqrt{\frac{\mu^2}{4} + \frac{\nu\triangle t}{\triangle x^2}}. \tag{4.2.5}$$

This is implied by the two special cases

$$\frac{\triangle t|u'(x,t_n)|}{\triangle x} \leq \mu, \quad or \quad \frac{\triangle t|u'(x,t_n)|^2}{\nu} \leq 1. \tag{4.2.6}$$

Proof. The proof for EEV2 was independent of the particular EEV parameterization until the last step. Inserting EEV1 gives the sufficient condition

$$\int_\Omega [2\nu + \left(2\mu\triangle x|u'| - \triangle t|u_j'^n|^2\right)]|\nabla u_j^{n+1}|^2 dx \geq 0.$$

A sufficient condition for this is that the quadratic form $[2\nu + (2\mu\triangle x|u'^n| - \triangle t|u'^n|^2)] \geq 0$. Let

$$s = \frac{\triangle t|u'^n|}{2\triangle x} \geq 0.$$

By rescaling, the following condition suffices for stability

$$\nu + 2\mu\frac{\triangle x^2}{\triangle t}s - 2\frac{\triangle x^2}{\triangle t}s^2 \geq 0.$$

The first stability condition (4.2.5) follows by solving the quadratic inequality. The second condition (4.2.6) follows by dropping terms in the RHS. □

Remark 3 (The proof strategy). *For each variant we take $\int_\Omega Method \cdot u_j^{n+1} dx$ and arrive at*

$$E^{n+1} - E^n + \triangle t[D^{n+1} - N^{n+1}] = \triangle t P^{n+1},$$

where, at the indicated time, E = system energy, D = rate of viscous, numerical and eddy viscosity dissipation, N = nonlinear term, and P = rate of energy input through body force - flow interactions. Long time, nonlinear stability thus follows provided $D^{n+1} \geq N^{n+1}$. The key step in the proofs is to show the following

$$\int_\Omega \left\{2[\nu + \nu_T(l^n, k'^n)]|\nabla u_j^{n+1}|^2 - \triangle t|u_j'^n|^2|\nabla u_j^{n+1}|^2\right\} dx \geq 0.$$

One consequence. *Stability by energy methods and without Gronwall's inequality can imply equilibrium of important time averaged statistics. For example, for* $\mu > 1/2$, $D^{n+1} - N^{n+1} \geq c||u^{n+1}||^2$. *Using this, if* $||f(t)||$ *is uniformly bounded in time, it follows that* E^n *is also uniformly bounded in time. Summing the energy estimate and dividing gives*

$$\frac{1}{t^m}\left(E^m - E^0\right) + \frac{1}{t^m}\sum_{n=0}^{m-1}[D^{n+1} - N^{n+1}]\triangle t = \frac{1}{t^m}\sum_{n=0}^{m-1}P^{n+1}\triangle t.$$

The first term $\frac{1}{t^m}\left(E^m - E^0\right) \to 0$ *as* $t^m \to \infty$. *Thus, if* LIM *denotes a generalized or Banach limit, it follows that*

$$LIM_{t^m\to\infty}\frac{1}{t^m}\sum_{n=0}^{m-1}[D^{n+1} - N^{n+1}]\triangle t = LIM_{t^m\to\infty}\frac{1}{t^m}\sum_{n=0}^{m-1}P^{n+1}\triangle t$$

which expresses equilibrium between time averaged energy input (the RHS) and dissipation (the LHS).

4.3 STABILITY : DISCRETE SPACE AND TIME

This section analyzes stability under spacial discretization by finite element methods; extension to other methods is both interesting and important. There are two essential deviations from the spatially continuous case. First, new options are available for analysis of stability: since the FEM spaces are finite dimensional, norm equivalence tools can be used and lead to conditions involving the ratio $\triangle t/\triangle x$. Second, since common FEM velocity spaces are not exactly divergence free, new restrictions depending on the size of $||\nabla \cdot u_h'||$ emerge from the nonlinear term. These are not active for Fourier spectral methods or when using divergence free FEM spaces and suggest further study of the methods with grad-div stabilization, e.g., [80], [20], added. Similarly to the analysis in [63], these terms occur here from the nonlinearity rather than from the pressure-incompressibility coupling. The analysis is performed for the most common form of the nonlinear term. If the rotation form of the nonlinearity is used instead, *no condition linking the timestep with* $\nabla \cdot u_j'^n$ *is needed for stability.*

Since all velocities and pressures in this section are discrete we do not include subscripts "h" on discrete velocities and pressures. The usual fully discrete EEV FEM is: *Given* u_j^n, *find* $u_j^{n+1} \in X_h$, $p_j^{n+1} \in Q_h$ *satisfying*

$$\begin{gathered}(\frac{u_j^{n+1}-u_j^n}{\Delta t}, v) + b^*(< u >^n, u_j^{n+1}, v) + b^*(u_j^n - < u >^n, u_j^n, v) \\ -(p_j^{n+1}, \nabla \cdot v) + ([\nu + \nu_T(l^n, k'^n)]\,\nabla u_j^{n+1}, \nabla v) = (f_j^{n+1}, v), \qquad \forall v \in X_h, \\ (\nabla \cdot u_j^{n+1}, q) = 0, \qquad \forall q \in Q_h, \text{ and } u_j(0) \in X_h \text{ given.}\end{gathered} \tag{4.3.1}$$

Theorem 8 (**EEV2** Stability)**.** *The method (4.3.1) with the parameterization* ***EEV2,*** $\nu_T = \mu\triangle t|u'|^2$**,** *is nonlinearly, long time stable if, for some* θ *and* α, $0 \le \theta \le 1$, $0 < \alpha < 1$, *the timestep condition holds,*

$$\theta\nu + 2\Delta t(\mu - \frac{1}{2\alpha})|u_j'^n| \ge 0 \quad \textit{and} \quad (1-\theta)\nu - \frac{C}{4(1-\alpha)}\Delta t\|\nabla \cdot u_j'^n\|_{L^4}^2 \ge 0. \tag{4.3.2}$$

In particular, stability follows if

$$\nabla \cdot u_j'^n = 0 \textit{ and } \mu > \frac{1}{2}.$$

Proof. We follow the proof of Theorem 1 to the divergence point. Set $v = u_j^{n+1}$, $q = p_j^{n+1}$ and multiply by $2\triangle t$. Using skew symmetry of $b^*(< u >^n, u_j^{n+1}, v)$ and the polarization identity in (u_j^n, u_j^{n+1}) in the time difference term gives

$$\begin{gathered}||u_j^{n+1}||^2 - ||u_j^n||^2 + ||u_j^{n+1} - u_j^n||^2 + 2\triangle t b^*\left(u_j'^n, u_j^{n+1}, u_j^{n+1} - u_j^n\right) + \\ +2\triangle t \int_\Omega [\nu + \nu_T(l^n, k'^n)]|\nabla u_j^{n+1}|^2 dx = 2\triangle t\left(f_j^{n+1}, u_j^{n+1}\right).\end{gathered}$$

Applying Young's inequality to the right hand side gives

$$\begin{gathered}||u_j^{n+1}||^2 - ||u_j^n||^2 + ||u_j^{n+1} - u_j^n||^2 + 2\triangle t b^*\left(u_j'^n, u_j^{n+1}, u_j^{n+1} - u_j^n\right) + \\ +\triangle t \int_\Omega [\nu + 2\nu_T(l^n, k'^n)]|\nabla u_j^{n+1}|^2 dx \le \frac{\triangle t}{\nu}\|f_j^{n+1}\|_*^2.\end{gathered}$$

Using Lemma 1,

$$2\triangle t b^*\left(u_j'^n, u_j^{n+1}, u_j^{n+1}-u_j^n\right) =$$
$$2\triangle t\left(u_j'^n\cdot\nabla u_j^{n+1}, u_j^{n+1}-u_j^n\right)+\triangle t\left(\nabla\cdot u_j'^n, u_j^{n+1}\cdot(u_j^{n+1}-u_j^n)\right).$$

For the two terms on the above RHS we have, for any $0<\alpha<1$,

$$\text{(Term 1)}\quad 2\triangle t\left|\left(u_j'^n\cdot\nabla u_j^{n+1}, u_j^{n+1}-u_j^n\right)\right| \le$$
$$\le \alpha\|u_j^{n+1}-u_j^n\|^2+\frac{\triangle t^2}{\alpha}\int_\Omega |u_j'^n|^2|\nabla u_j^{n+1}|^2dx,$$
$$\text{(Term 2)}\quad \triangle t\left|\left(\nabla\cdot u_j'^n, u_j^{n+1}\cdot(u_j^{n+1}-u_j^n)\right)\right| \le$$
$$\le (1-\alpha)\|u_j^{n+1}-u_j^n\|^2+\frac{\triangle t^2}{4(1-\alpha)}\int_\Omega |\nabla\cdot u_j'^n|^2|u_j^{n+1}|^2dx.$$

Inserting these bounds and EEV2 into the energy estimate, nonlinear, long time stability thus follows provided

$$\int_\Omega\{(\nu+2\mu\triangle t|u'^n|^2)|\nabla u_j^{n+1}|^2$$
$$-\triangle t(\frac{1}{\alpha}|u_j'^n|^2|\nabla u_j^{n+1}|^2+\frac{1}{4(1-\alpha)}|\nabla\cdot u_j'^n|^2|u_j^{n+1}|^2)\}dx\ge 0.$$

This follows provided, for some θ, $0\le\theta\le 1$,

$$\int_\Omega\{[\theta\nu+2\triangle t(\mu-\frac{1}{2\alpha})|u'^n|^2]|\nabla u_j^{n+1}|^2 \tag{4.3.3}$$
$$+[(1-\theta)\nu|\nabla u_j^{n+1}|^2-\frac{1}{4(1-\alpha)}\triangle t|\nabla\cdot u_j'^n|^2|u_j^{n+1}|^2]\}dx\ge 0.$$

(4.3.3) holds if

$$\theta\nu+2\triangle t(\mu_2-\frac{1}{2\alpha})|u'^n|^2\ge 0,\qquad\text{and} \tag{4.3.4}$$
$$(1-\theta)\nu\|\nabla u_j^{n+1}\|^2-\frac{1}{4(1-\alpha)}\triangle t\|\nabla\cdot u_j'^n\|_{L^4}^2\|u_j^{n+1}\|_{L^4}^2\ge 0.$$

By Sobolev embedding theorem, a sufficient condition for (4.3.4) is

$$\theta\nu + 2\triangle t(\mu - \frac{1}{2\alpha})|u'^n|^2 \geq 0, \qquad \text{and}$$
$$(1-\theta)\nu\|\nabla u_j^{n+1}\|^2 - \frac{C}{4(1-\alpha)}\triangle t\|\nabla\cdot u_j'^n\|_{L^4}^2\|\nabla u_j^{n+1}\|^2 \geq 0,$$

which, completing the proof, is equivalent to (4.3.2). □

Next EEV1 is considered.

Theorem 9 (**EEV1** Stability). *Consider (4.3.1) with **EEV1** $\nu_T = \mu|u'|\triangle x$. A sufficient condition for stability is that if for some θ, $0 \leq \theta \leq 1$, the two timestep conditions hold,*

$$(1-\theta)\nu - \frac{C}{2}\Delta t\|\nabla\cdot u_j'^n\|_{L^4}^2 \geq 0, \quad \frac{\triangle t|u'(x,t_n)|}{\triangle x} \leq \frac{1}{2}\mu + \frac{1}{2}\sqrt{\mu^2 + \frac{\theta\nu\triangle t}{\triangle x^2}}. \tag{4.3.5}$$

This is implied by the two special cases

$$(1-\theta)\nu - \frac{C}{2}\Delta t\|\nabla\cdot u_j'^n\|_{L^4}^2 \geq 0 \quad \textit{and} \quad \frac{\triangle t|u'(x,t_n)|}{\triangle x} \leq \frac{1}{2}\mu,$$
$$\textit{or} \quad (1-\theta)\nu - \frac{C}{2}\Delta t\|\nabla\cdot u_j'^n\|_{L^4}^2 \geq 0 \quad \textit{and} \quad \frac{\triangle t|u'(x,t_n)|^2}{\theta\nu} \leq \frac{1}{4}.$$

Proof. Following the proof of Theorem 8 with EEV1 gives the sufficient condition

$$\int_\Omega \{[\nu + 2\mu\triangle x|u'^n|]|\nabla u_j^{n+1}|^2$$
$$-\triangle t[2|u_j'^n|^2|\nabla u_j^{n+1}|^2 + \frac{1}{2}|\nabla\cdot u_j'^n|^2|u_j^{n+1}|^2]\}dx \geq 0.$$

This follows provided, for some θ, $0 \leq \theta \leq 1$,

$$\int_\Omega \{[\theta\nu + 2\mu\triangle x|u'^n| - 2\triangle t|u'^n|^2]|\nabla u_j^{n+1}|^2 \tag{4.3.6}$$
$$+[(1-\theta)\nu|\nabla u_j^{n+1}|^2 - \frac{1}{2}\triangle t|\nabla\cdot u_j'^n|^2|u_j^{n+1}|^2]\}dx \geq 0.$$

(4.3.6) holds if

$$\theta\nu + 2\mu\triangle x|u'^n| - 2\triangle t|u'^n|^2 \geq 0, \qquad \text{and}$$
$$(1-\theta)\nu\|\nabla u_j^{n+1}\|^2 - \frac{1}{2}\triangle t\|\nabla\cdot u_j'^n\|_{L^4}^2\|u_j^{n+1}\|_{L^4}^2 \geq 0.$$

Since $\|u\|_{L^4} \leq C(\Omega)\|\nabla u\|$, the stability conditions become

$$\theta\nu + 2\mu\triangle x|u'^n| - 2\triangle t|u'^n|^2 \geq 0, \qquad \text{and}$$
$$(1-\theta)\nu - \frac{C}{2}\triangle t\|\nabla \cdot u_j'^n\|_{L^4}^2 \geq 0.$$

Rescale by $s = \triangle t|u'^n|/\triangle x \geq 0$:

$$\theta\nu + 2\mu\frac{\triangle x^2}{\triangle t}s - 2\frac{\triangle x^2}{\triangle t}s^2 \geq 0.$$

Solving the quadratic inequality, we obtain (4.3.5). □

All the stability conditions can be applied locally when the $\triangle x$ in the model is the local meshwidth h_e, e.g.,

$$\frac{\triangle t|u'(x,t_n)|}{\triangle x} \leq \frac{1}{2}\mu \text{ replaced by} \frac{\triangle t \max_{x\in e}|u'(x,t_n)|}{h_e} \leq \frac{1}{2}\mu.$$

Since both EEV terms are nonnegative, stability follows from any of the conditions derived in [53] for the laminar case. We summarize these without proof.

Theorem 10 (Stability: laminar flow timestep conditions)**.** *Consider the method (4.3.1) with either EEV1 or EEV2. Stability holds under any of the conditions below:*

$$C\frac{\Delta t}{\nu\triangle x}\|\nabla u_j'^n\|^2 \leq 1, \quad \textit{in } 2d \textit{ and } 3d,$$
$$C\frac{|ln(h)|\Delta t}{\nu}\|\nabla u_j'^n\|^2 \leq 1, \textit{ and } C\frac{\Delta t}{\nu\triangle x^2}(\|u_j'^n\|^2 + \|\nabla\cdot u_j'^n\|^2) \leq 1, \quad \textit{in } 2d\ ,$$
$$C\frac{\Delta t}{\nu\triangle x^2}\|u_j'^n\|_{L^3}^2 \leq 1, \textit{ and } C\max_e\frac{\Delta t}{\nu h_e}\|\nabla u_j'^n\|_{L^2(e)}^2 \leq 1, \quad \textit{in } 3d.$$

4.4 NUMERICAL TESTS

The goal herein is to test the EEV term as a *numerical regularization*. Thus, the first inescapable issues for numerical tests are accuracy and stability. These are algorithmic (or numerical) issues, far from the ultimate targeted applications and far from the mysteries arising from adding stochasticity to the Navier-Stokes equations. The tests were performed using the software FreeFEM++, [50].

Test 1: Accuracy. We test the accuracy of the methods for a test problem with closed form solution (so errors are calculable). Since the solution is smooth, the question is simply: *Is reasonable accuracy obtained for smooth solutions on coarse meshes or does the added nonlinearity cause pollution of the error?* The test problem, from [41], has spacial patterns of the Green-Taylor solution, [8], [40], without time decay. For the discrete equations the nonlinearity is active due to the EEV term and discretization effects since $\nabla \cdot u^h \neq 0$.

The analytical solution of the Navier-Stokes equations in the unit square $\Omega = [0,1]^2$ is given by

$$
\begin{aligned}
u_{true} &= (-g(t)\cos x \sin y, +g(t)\sin x \cos y)^T, \\
p_{true} &= -\frac{1}{4}[\cos(2x) + \cos(2y)]g^2(t), \quad \text{where } g(t) = \sin(2t),
\end{aligned}
$$

with source term $f(x,y,t) = [g'(t) + 2\nu g(t)](-\cos x \sin y, \sin x \cos y)^T$. The boundary condition on the problem is taken to be inhomogeneous Dirichlet: $u = u_{true}$ on $\partial\Omega$.

We consider an ensemble of two members $u_{1,2} = (1 \pm \epsilon)u_{true}$, $\epsilon = 10^{-3}$, which are the solutions to NSE corresponding to two different initial conditions $u^0_{1,2} = (1 \pm \epsilon)u^0_{true}$, respectively, with the source term and boundary condition adjusted accordingly. We compute the solutions of EEV1 and EEV2 at $T = 1$ and compute errors.

Tables 1 and 2 show acceptable accuracy (error $\sim 10^{-2}$) even on coarse meshes ($h = \triangle x = 0.1$). This is evidence that the nonlinearity introduced by EEV1&2 is small for smooth functions.

Error	EEV1	EEV2
$\|\nabla u_1 - \nabla u_{1,h}\|_{2,0}$	0.02016440759	0.0162905579
$\|\nabla u_2 - \nabla u_{2,h}\|_{2,0}$	0.02012253135	0.0162294437
$\|\nabla u_{true} - \nabla u_{ave,h}\|_{2,0}$	0.02014346778	0.01625999831
$\|\nabla p_1 - \nabla p_{1,h}\|_{2,0}$	0.03308893594	0.02667901262
$\|\nabla p_2 - \nabla p_{2,h}\|_{2,0}$	0.03258390956	0.02619554571

Table 5: Re=800, $\Delta t = 0.05, h = 0.1$

Test 2: Stability of EEV1&2. The test problem is *flow between offset cylinders*[1] driven by a rotating body force solved on an *under resolved* mesh. Space averaged statistics of interest to rotating flow are tracked in time to evaluate stability. Tests in [53] with $\nu_T = 0$ showed instability for non-adaptive time steps for $Re = 800$. We add an EEV2 ($\mu = 1$) term for $Re = 800, 1200, 2400$. All cases are stable with constant timestep $\Delta t = 0.025$. We also test with EEV1 ($\mu \Delta x = 0.2$) for $Re = 800$ and compare the results with EEV2. While these first tests are $2d$, they reveal interesting differences between EEV1 and EEV2.

The domain is a disk with a smaller, off-center obstacle inside. Let $r_1 = 1$, $r_2 = 0.1$, $c = (c_1, c_2) = (0.5, 0)$. The domain and body force are given by

$$\Omega = \{(x, y) : x^2 + y^2 \leq r_1^2 \text{ and } (x - c_1)^2 + (y - c_2)^2 \geq r_2^2\},$$
$$f(x, y, t) = (-4y * (1 - x^2 - y^2), 4x * (1 - x^2 - y^2))^T,$$

with no-slip boundary conditions on both circles. The flow, driven by a counterclockwise force with $f \equiv 0$ at the outer circle, rotates about $(0, 0)$ and interacts with the immersed circle $(x - c_1)^2 + (y - c_2)^2 \leq r_2^2$. This induces a von Kármán vortex street which re-interacts with the immersed circle creating more complex structures. The (under resolved) mesh has

[1] While we do not herein test predictions of $2d$ turbulence, it is relevant to understanding the test problem. The Kraichnan-Leith-Batchelor dual cascade is valid in an infinite domain without boundaries. In the case of decaying turbulence, the (related) self-organization hypothesis concerning convergence of Dirichlet quotients is only proven for periodic boundary conditions, [45], [90], [74]. Thus, $2d$ flow bounded by no-slip walls with structures generated by flow-wall interactions is not described by either and has interest beyond as a test problem.

Error	EEV1	EEV2
$\|\nabla u_1 - \nabla u_{1,h}\|_{2,0}$	0.02071888682	0.04244542311
$\|\nabla u_2 - \nabla u_{2,h}\|_{2,0}$	0.02067566768	0.04229541702
$\|\nabla u_{true} - \nabla u_{ave,h}\|_{2,0}$	0.02069727546	0.04237040275
$\|\nabla p_1 - \nabla p_{1,h}\|_{2,0}$	0.0330861719	0.0274518365
$\|\nabla p_2 - \nabla p_{2,h}\|_{2,0}$	0.03257960354	0.02697616082

Table 6: Re=10,000, $\Delta t = 0.05, h = 0.1$

$n = 40$ mesh points around the outer circle and $m = 10$ mesh points around the immersed circle, and extended to Ω as a Delaunay mesh, Figure 4.4.

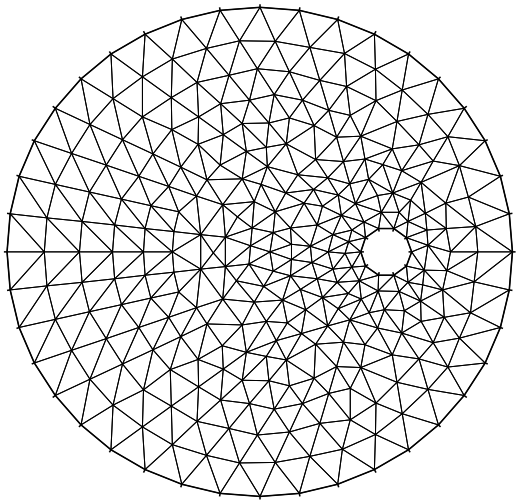

Figure 19: Coarse mesh with 40 mesh points on the outer circle and 10 mesh points on the inner circle.

Generation of the initial conditions. Our goal is to test stability. Thus, we did not test coupling the algorithm plus EEV term to Bred-Vectors initialization procedures. Perturbed Initial conditions $u_j^0, j = 1, 2$ are generated by solving the steady Stokes problem

with perturbed body forces

$$f(x,y,t) \pm \epsilon(sin(3\pi x)sin(3\pi y), cos(3\pi x)cos(3\pi y))^T \text{ with } \epsilon = 10^{-3}.$$

u_0^0 is generated in the same way with $\epsilon \equiv 0$ ('no perturbation'). This gives initial conditions that are divergence free and satisfy the no-slip conditions. From the initial transients in the plotted statistics below, it is clear that the initial conditions are not statistically steady. We compute an ensemble of two ensemble members u_1 (initial condition u_1^0) and u_2 (initial condition u_2^0) using our method and give statistics of these two ensemble members in Figures 2-7. We also give statistices of $u_{ave} = (u_1 + u_2)/2$ (marked as 'average' in Figures 2-7) and u_0 (initial condition u_0^0 - marked as 'no perturbation' in Figures 2-7) for comparison. Here u_0 is solved with the same method with only one ensemble member. In this case there is no fluctuation and thus no EEV regularization. u_0 is computed on the same coarse mesh and thus does not represent the true solution. We emphasize that u_{ave} does not necessarily converge to u_0.

Quantities plotted. We plot over $0 \leq t \leq 10$ *angular momentum*, *enstrophy* and *energy* (integral invariants of the Euler equations of relevance to rotational flows):

$$|\text{Angular Momentum}| = |\int_\Omega \vec{x} \times \vec{u}\, d\vec{x}|, \quad \text{Enstrophy} = \frac{1}{2}\|\nabla \times \vec{u}\|^2,$$
$$\text{Energy} = \frac{1}{2}\|\vec{u}\|^2.$$

Stability of EEV2. EEV2[2] ($\mu = 1$) was stable for timestep $\triangle t = 0.025$, $\nu = 1/800$ as measured by volume-averaged energy, enstrophy and angular velocity statistics, see Figure 20.

Next the Reynolds number was increased to $Re = 1200$ and 2400. EEV2 remained stable, Figures 21, 22.

EEV1 vs. EEV2. EEV1 ($\mu\Delta x = 0.2$) and EEV2 ($\mu = 1$) are compared for the same geometry at $Re = 800$ and constant timestep $\triangle t = 0.025$. *EEV2 gave better solutions than EEV1.* Indeed, *EEV1 dramatically over-diffused the flow,* Figures 23, 24, 25. This over-diffusion is likely because EEV1 has larger estimate of the mixing length near walls.

[2]A stable, time adaptive run *without* EEV required very small timesteps and yielded solutions with the non physical, $O(\triangle x)$ structures typical in underresolved flow simulations.

Streamlines of the EEV1 solution (not given herein) showed that the velocity had incorrectly converged to an over diffused, Stokes flow-like solution.

Test 3: A 3d Test. The well-known 3d Ethier-Steinman analytical solutions to the incompressible Navier-Stokes equations, [27], are commonly used as a 3d benchmark, e.g., [81], [10]. The solutions exhibit complex structures due to their nontrivial helicity. With exact solutions known, we can compare the performances of EEV1 and EEV2.

The exact NSE solution on a $[0,1]^3$ box is given by

$$
\begin{aligned}
u_1 &= -a(e^{ax}sin(ay+dz)+e^{az}cos(ax+dy))e^{-\nu d^2 t}, \\
u_2 &= -a(e^{ay}sin(az+dx)+e^{ax}cos(ay+dz))e^{-\nu d^2 t}, \\
u_3 &= -a(e^{az}sin(ax+dy)+e^{ay}cos(az+dx))e^{-\nu d^2 t}, \\
p &= -\frac{a^2}{2}(e^{2ax}+e^{2ay}+e^{2az}+2sin(ax+dy)cos(az+dx)e^{a(y+z)} \\
&\quad +2sin(ay+dz)cos(ax+dy)e^{a(z+x)} \\
&\quad +2sin(az+dx)cos(ay+dz)e^{a(x+y)})e^{-2\nu d^2 t}.
\end{aligned}
\tag{4.4.1}
$$

To visualize the flow (4.4.1), we plot stream ribbons of the exact velocity in the box, velocity streamlines and speed contours on the sides, Figure 26.

We compute approximations to (4.4.1) with EEV1 and EEV2 respectively with different choices of μ. We take parameters $a = 1.25, d = 2.25$, kinematic viscosity $\nu = 0.001$, mesh size $h\ (= \Delta x) = 0.1$, timestep $\Delta t = 0.05$ and end time $T = 1$. Perturbations are generated in the same way as in Test 1 with the same parameters $\epsilon_1 = 10^{-3}$, $\epsilon_2 = -10^{-3}$. We plot energy of the average velocity $u_{ave} = (u_1 + u_2)/2$ versus time in Figures 27, 28. The method without any regularizations ($\mu = 0$) becomes unstable in the first few time integration steps. EEV2 has an instability excited but successfully controls the instability, Figure 28, and tracks the true solutions kinetic energy accurately thereafter. EEV1 performs better in this test than in test 2 possibly because near wall behavior is unimportant for this flow, Figure 27.

Other tests: A number of other tests were performed including reinitialization of perturbations, flow in a domain with a contraction and two outflows, including grad-div stabilization and tests giving more details. These gave results consistent with those presented herein.

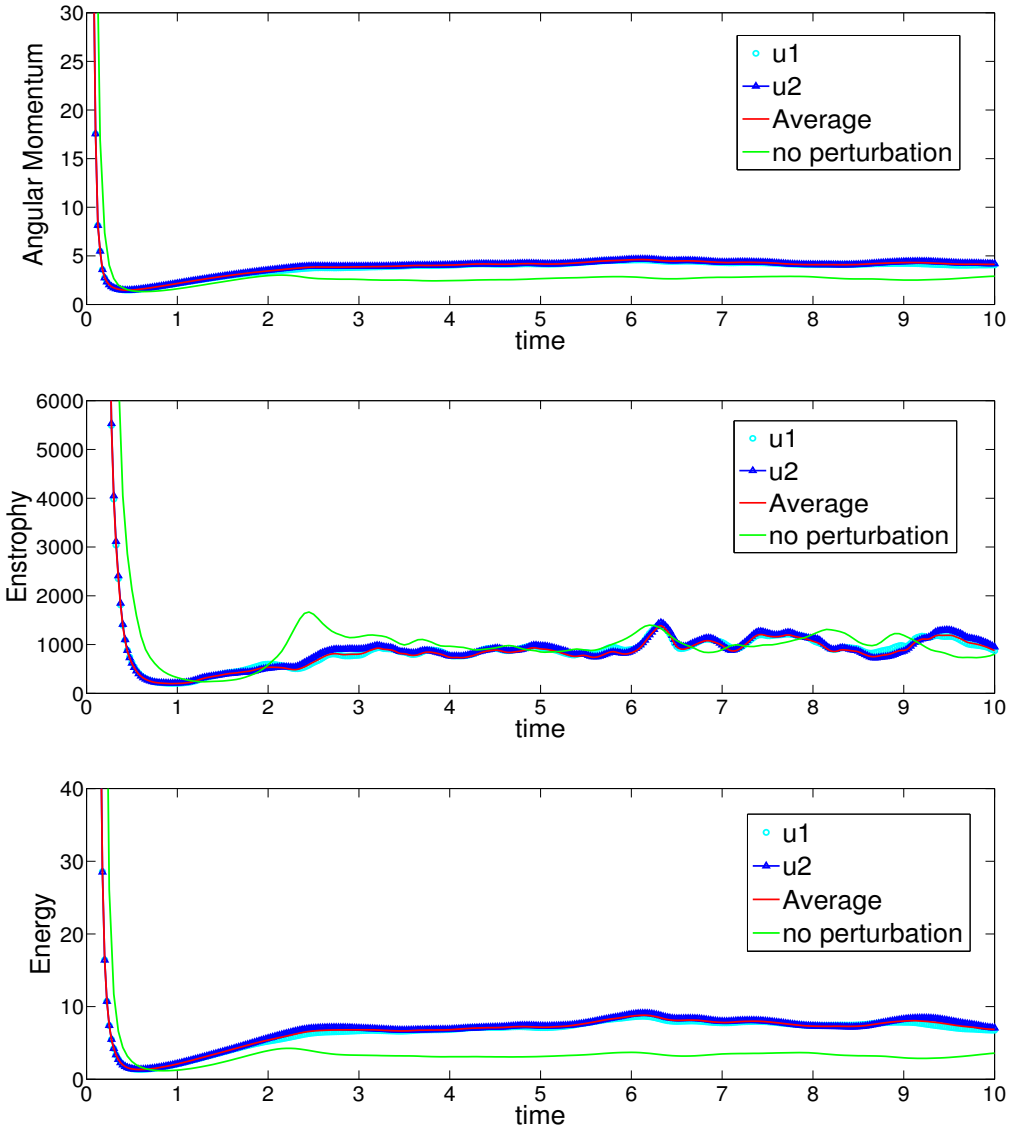

Figure 20: Space averaged statistics of interest obtained by EEV2 with $\mu = 1$, $\nu = 1/800$ and constant timestep $\Delta t = 0.025$ on the coarse mesh. From top to bottom: Angular Momentum; Enstrophy; Energy.

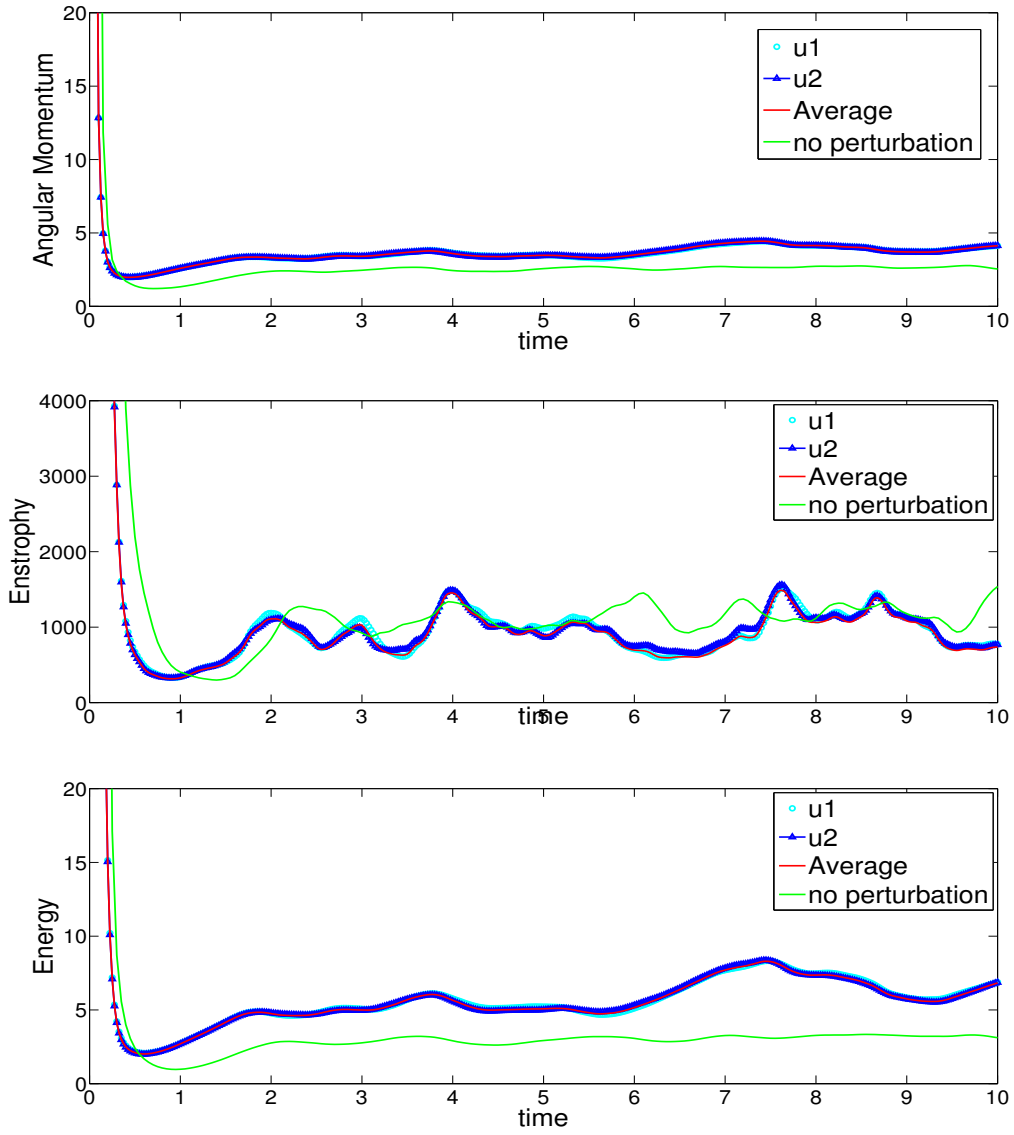

Figure 21: Space averaged statistics of interest obtained by EEV2 with $\mu = 1$, $\nu = 1/1200$ and constant timestep $\Delta t = 0.025$ on the coarse mesh. From top to bottom: Angular Momentum; Enstrophy; Energy.

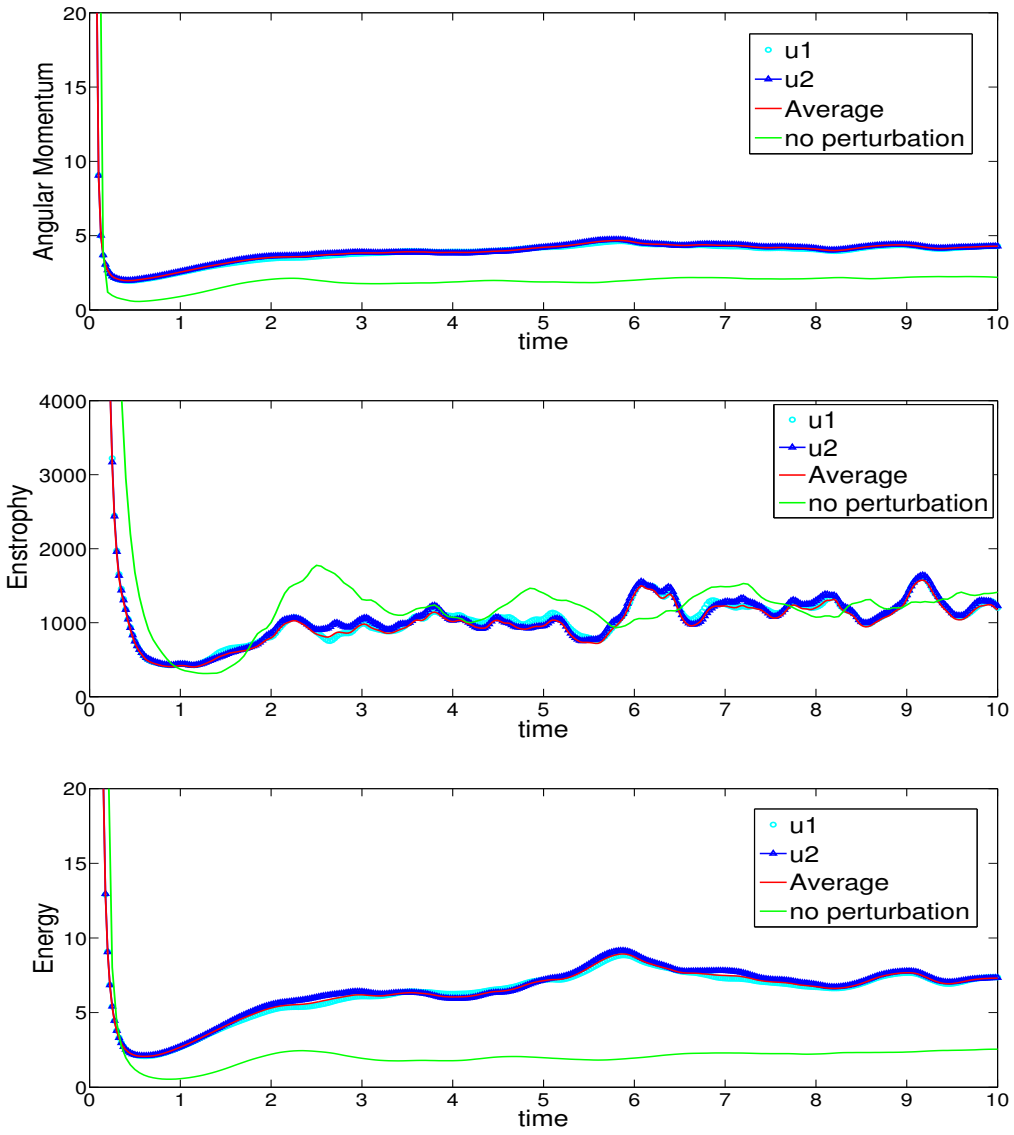

Figure 22: Space averaged statistics of interest obtained by EEV2 with $\mu = 1$, $\nu = 1/2400$ and constant timestep $\Delta t = 0.025$ on the coarse mesh. From top to bottom: Angular Momentum; Enstrophy; Energy.

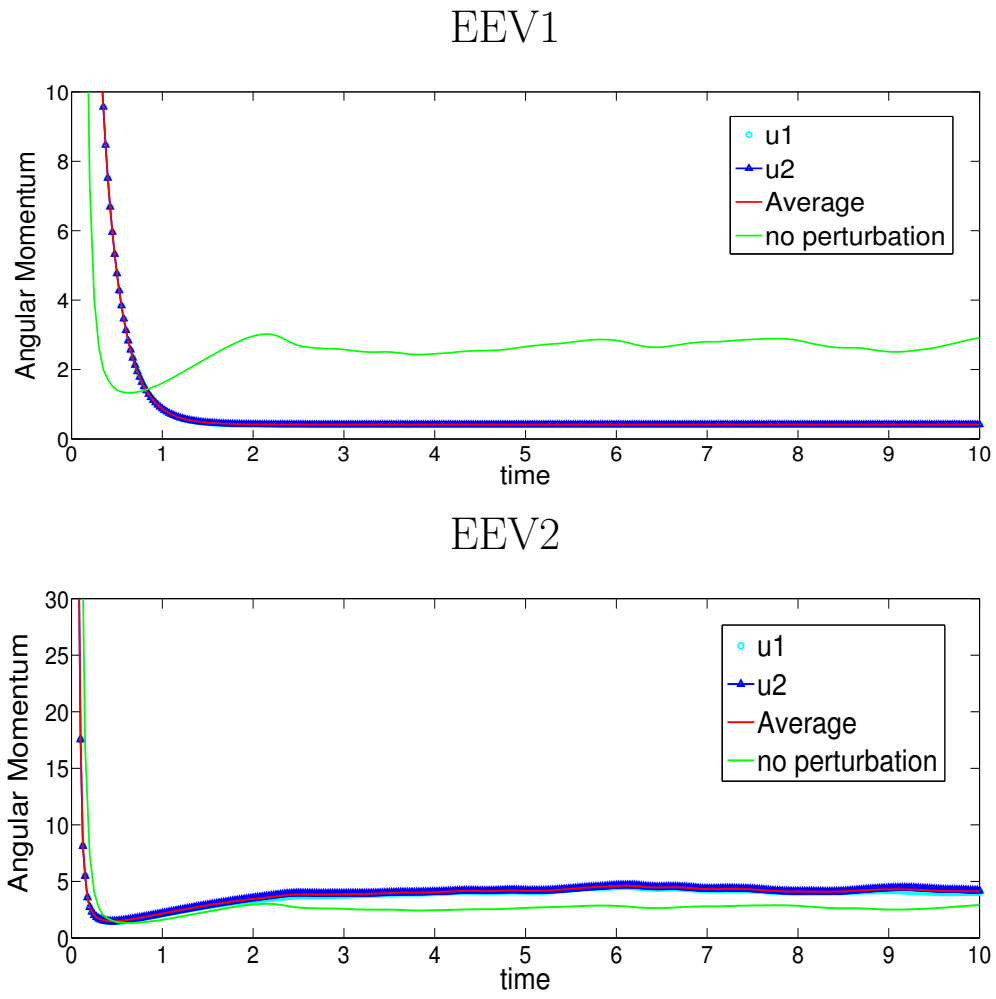

Figure 23: Comparison of Angular Momentum obtained from EEV1 ($\mu\Delta x = 0.2$) and EEV2 ($\mu = 1$) with $\nu = 1/800$ and constant timestep $\Delta t = 0.025$ on the coarse mesh.

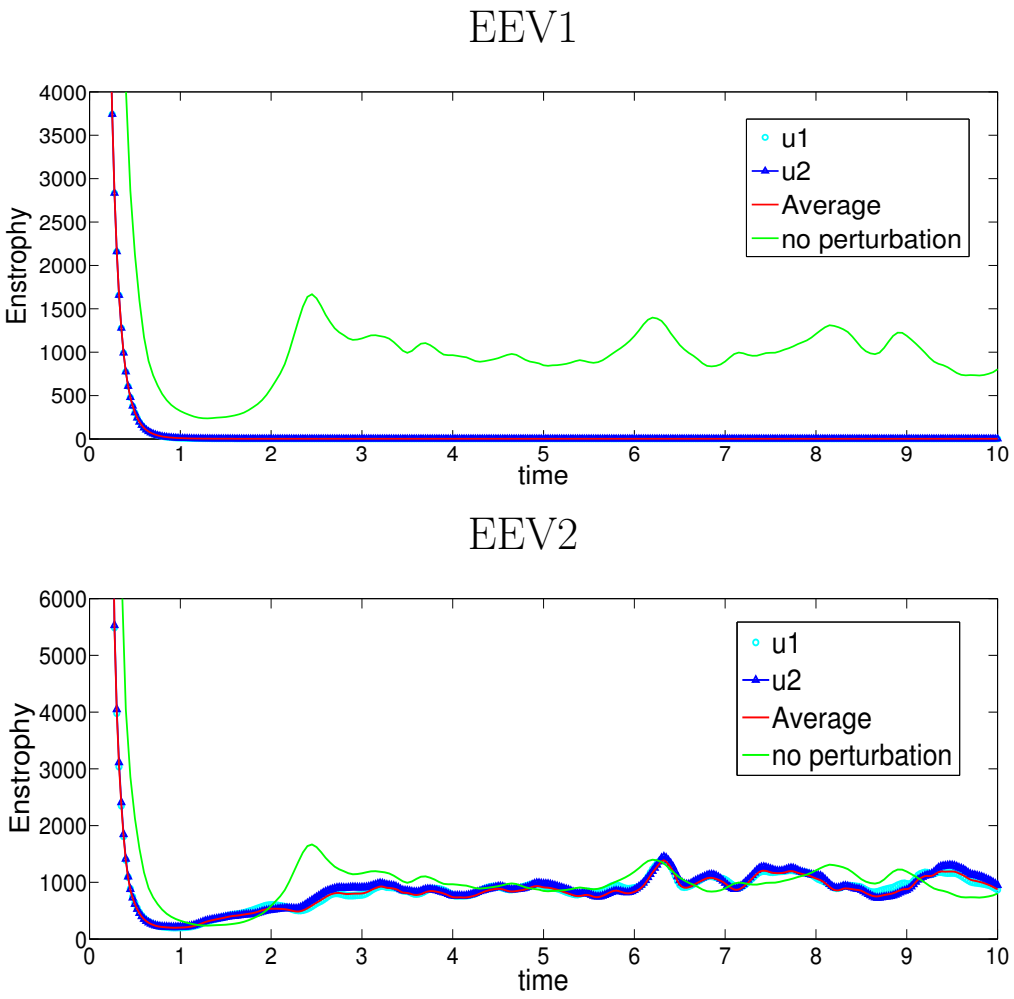

Figure 24: Comparison of Enstrophy obtained from EEV1 ($\mu\Delta x = 0.2$) and EEV2 ($\mu = 1$) with $\nu = 1/800$ and constant timestep $\Delta t = 0.025$ on the coarse mesh.

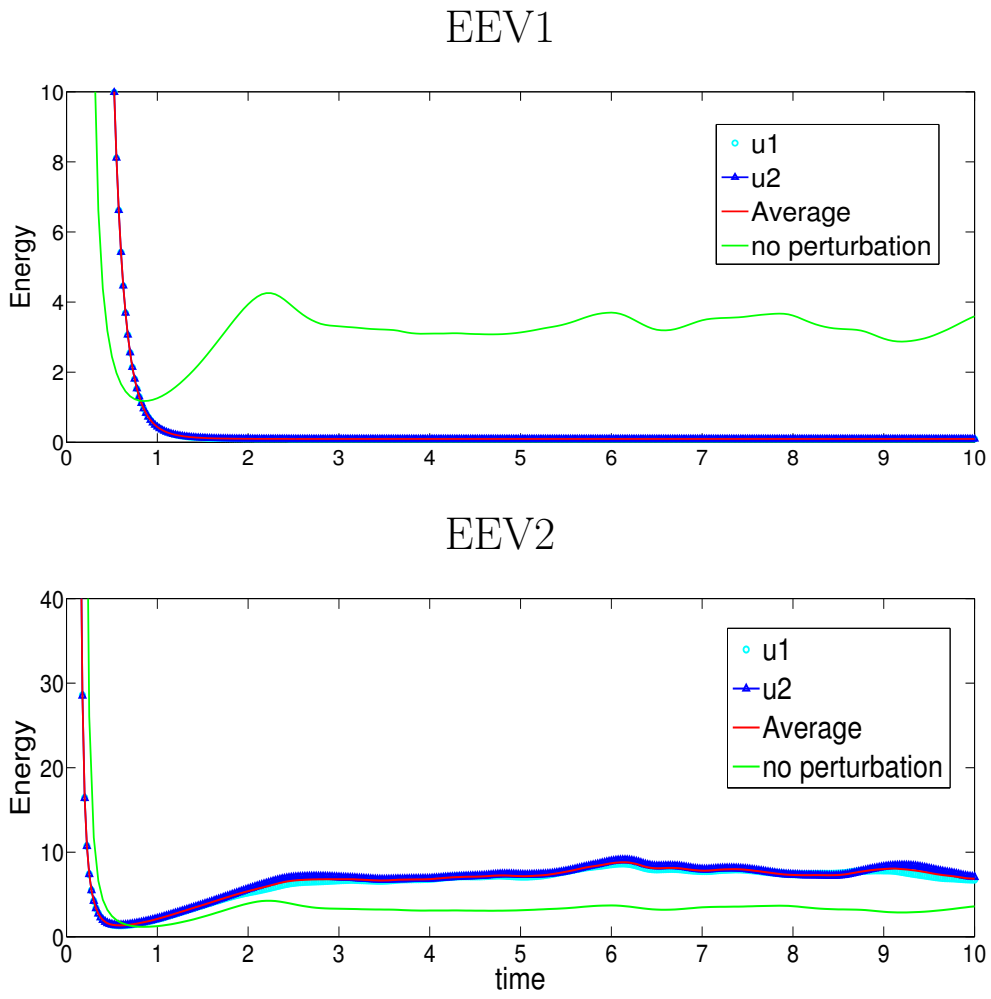

Figure 25: Comparison of Energy obtained from EEV1 ($\mu\Delta x = 0.2$) and EEV2 ($\mu = 1$) with $\nu = 1/800$ and constant timestep $\Delta t = 0.025$ on the coarse mesh.

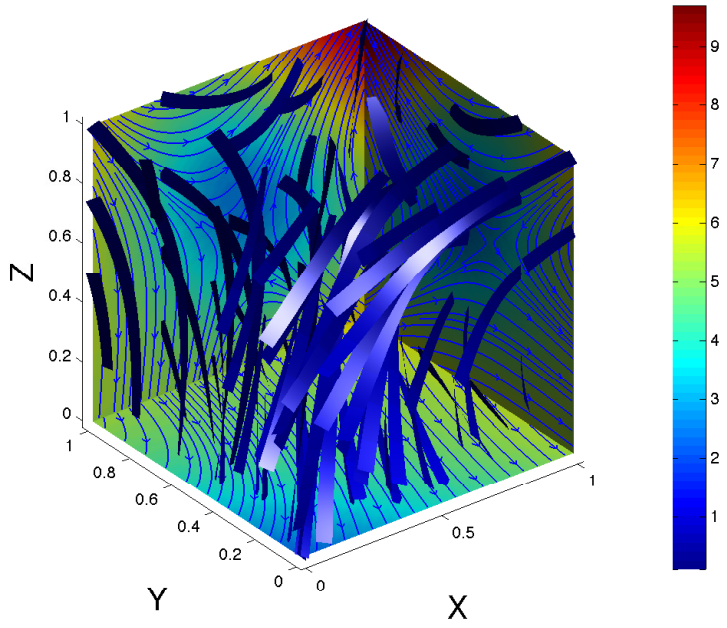

Figure 26: Visualization of the exact solution of Ethier-Steinman problem at time $T = 1$ with parameters $\nu = 0.001$, $a = 1.25, d = 2.25$.

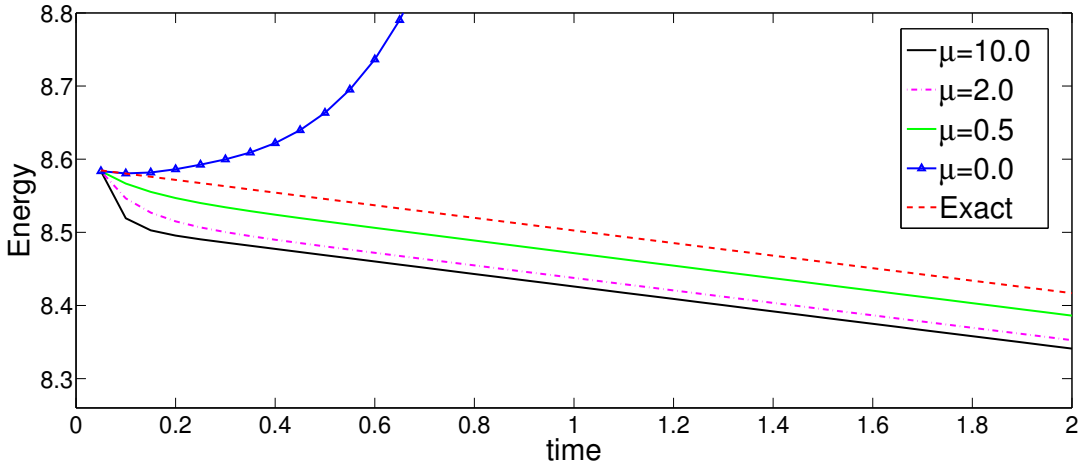

Figure 27: Energy (of the average velocity) vs. time: $\nu = 0.001$, $\Delta t = 0.05$, $h = 0.1$, computed by EEV1 with varying parameter μ.

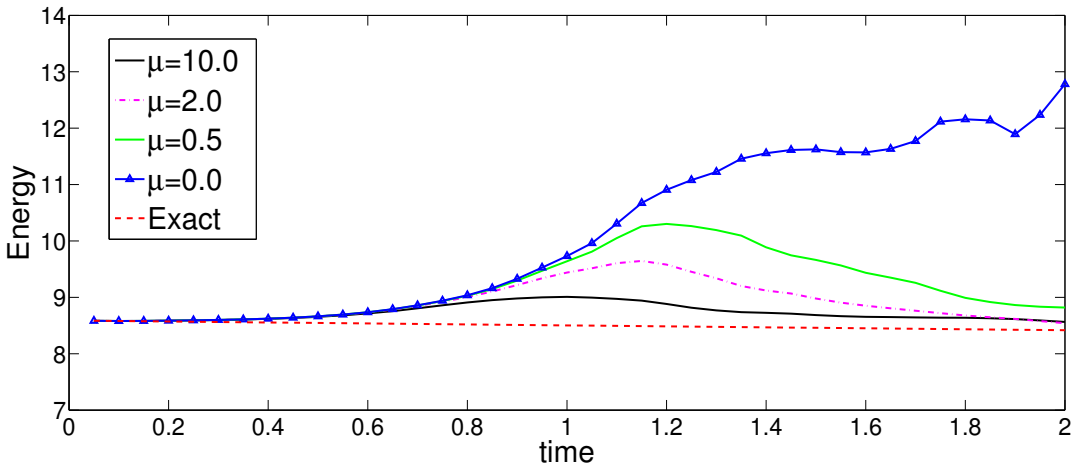

Figure 28: Energy (of the average velocity) vs. time: $\nu = 0.001$, $\Delta t = 0.05$, $h = 0.1$, computed by EEV2 with varying parameter μ.

4.5 CONCLUSIONS AND OPEN QUESTIONS

While the tests were preliminary, EEV2 outperformed EEV1 as a numerical regularization. Strong over-damping of EEV1 was a consistent result for problems with significant wall effects. To improve EEV1 one possibility is a better choice of μ. In other tests (not reported herein), we found the EEV1 solutions to be very sensitive to μ with a narrow range of μ values producing good results.

There are many questions open. Extensions of the Bred-Vectors algorithm are needed when the ensemble is generated by varying body forces or physical parameters. Analytic questions arise on existence of solutions to the NSE+EEV2:

$$u_{j,t} + u_j \cdot \nabla u_j - \nu \triangle u_j + \nabla p_j - \nabla \cdot (\mu \tau |u'|^2 \nabla u_j) = f_j(x,t), \text{ in } \Omega,$$
$$\nabla \cdot u_j = 0, \text{ in } \Omega.$$

The closest analog is the (single realization) existence theory in [70]. The EEV2 regularization is not monotone and does not give control over u but rather over

$$\int_0^T \int_\Omega |u_j - \frac{1}{J} \sum_{j=1}^{J} u_j|^2 |\nabla u_j|^2 dx \leq C(data, T).$$

Thus, existence is not completely transparent and uniqueness is a significant challenge.

Worst case, theoretical error analysis of eddy viscosity approximations has been developed in several papers, e.g., [9], [51], [52], [61]. This error analysis treats the additive EV term as a consistency error perturbation. If extensible to EEV methods, its prediction would be error $\simeq O(\triangle t + h^k + ||EEV1 \text{ or } 2 \text{ } term||)$.

5.0 A HIGHER ORDER ENSEMBLE SIMULATION ALGORITHM FOR FLUID FLOW

While efficient, the methods presented in Chapter 3 is only first order accurate. In applications such as the climate and ocean forecasts, which involve both turbulent flows and long time integration, higher order methods incorporating turbulence models are indispensable.

In this Chapter, we extend the method in Chapter 3 to an efficient, *higher order*, ensemble time discretization and extend the ensemble eddy viscosity model in Chapter 4 to the higher order method. The new higher order method preserves the good algorithmic property while being second order convergent. This advantage makes it a promising tool to increase ensemble size and improve data quality. The time stepping method we used here is a combination of a second order in time Backward-differentiation (BDF) and a special explicit Adams-Bashforth (AB) treatment of the advection term. The base ensemble algorithm naturally induces a new definition of the ensemble mean, compatible to the higher order time discretization, see Section 5.1 below.

We give comprehensive stability analysis and error analysis of the higher order method in Sections 5.2 and 5.4, respectively. This method, without any parametrizations of turbulence, requires a timestep restriction, (5.2.2) below, for stability. This condition degrades as the Reynolds number increases. For high Reynolds number flows, we analyze an ensemble eddy viscosity numerical regularization based on the higher order ensemble method. Computing ensembles allows direct parameterization of the turbulence characteristic velocity $|u'|$. We use the mixing length $l = |u'|\Delta t$ studied in Chapter 4. The stability condition derived from the eddy viscosity model, (5.3.2) below, is far less restrictive than (3.1.3) and in our tests large/moderate timesteps are sufficient for stability. In several important cases (5.3.2) implies unconditional stability.

Three numerical tests are presented in Section 5.5. Convergence of each ensemble member is verified and the convergence rate is calculated. The second numerical experiment tests the timestep conditions for stability and gives some insight into the usefulness of the proposed methods. Several important quantities in turbulence simulations, such as turbulence intensity (e.g., [96]), effective Lyapunov exponent (introduced in [6]) and Dirichlet quotient (e.g., [72]), are computed with our method. Lastly, for 3D Ethier-Steinman flow, stability of the discrete ensemble eddy viscosity numerical regularization method is verified.

5.1 METHODS AND MODELS

In this paper, we consider a second order accurate method for computing an ensemble of J Navier-Stokes equations, $j = 1, ..., J$:

$$\begin{aligned} u_{j,t} + u_j \cdot \nabla u_j - \nu \triangle u_j + \nabla p_j &= f_j(x,t), \text{ in } \Omega, \\ \nabla \cdot u_j &= 0, \text{ in } \Omega, \\ u_j &= 0, \text{ on } \partial\Omega, \\ u_j(x,0) &= u_j^0(x), \text{ in } \Omega. \end{aligned} \tag{5.1.1}$$

The first important subtlety is that a new (but consistent) definition of the mean, (5.1.2) below, is needed to match the numerical method.

Definition 1. *Let* $t^n := n\Delta t, n = 0, 1, 2, ..., N_T$, *and* $T := N_T \Delta t$. *Denote* $u_j^n = u_j(t^n)$, $j = 1, ..., J$. *We define the* **ensemble mean** *and* **fluctuation about the mean** *as follows.*

$$< u >^n := \frac{1}{J} \sum_{j=1}^{J} (2u_j^n - u_j^{n-1}), \tag{5.1.2}$$

$$u_j'^n := 2u_j^n - u_j^{n-1} - < u >^n . \tag{5.1.3}$$

Lemma 3. *The ensemble mean and fluctuation have the following properties.*

$$\begin{aligned} &< u' >= 0, \qquad && << u >>=< u >, \\ &<< u > \cdot v >=< u > \cdot < v >, \qquad && << u > \cdot v' >= 0. \end{aligned}$$

In particular, if $u_j \equiv a$, *then* $< u >= a$.

Suppressing the spacial discretization until Section 5.3 for clarity, for laminar flows/small Re, the method is: for $j = 1, ..., J$, given u_j^0 and u_j^1,

$$\begin{aligned} &\frac{3u_j^{n+1} - 4u_j^n + u_j^{n-1}}{2\Delta t} + < u >^n \cdot \nabla u_j^{n+1} \\ &+ u_j'^n \cdot \nabla \left(2u_j^n - u_j^{n-1}\right) + \nabla p_j^{n+1} - \nu \Delta u_j^{n+1} = f_j^{n+1}, \\ &\nabla \cdot u_j^{n+1} = 0. \end{aligned} \tag{EnB}$$

This method is proven to be second order accurate in Section 5.4.

For high Reynolds number flows, we incorporate an eddy viscosity numerical regularization to the method. Following Prandtl's assumption that the eddy viscosity is proportional to the mixing length multiplied by a turbulence characteristic velocity, the eddy viscosity parameterization has the form

$$\nu_T = C_{\nu_T} \left(l \cdot |u'|\right).$$

Definition 2. *Let $|\cdot|$ denote the usual Euclidean length of a vector and the Frobenius norm of an array. Then the* **magnitude of fluctuation** *(the characteristic velocity) is defined to be*

$$|u'^n| := \left(\sum_{j=1}^{J} |u_j'^n|^2 \right)^{1/2}.$$

The **mixing length** *(from [54]) is defined to be the distance that a fluctuating eddy travels in one timestep*

$$l^n = |u'^n| \Delta t.$$

Thus the eddy viscosity parameterization is

$$\nu_T = C_{\nu_T} |u'^n|^2 \Delta t.$$

Let $\nabla^s u$ denote the strain rate tensor. The ensemble eddy viscosity regularization method is, for $j = 1, ..., J$, given u_j^0 and u_j^1,

$$\begin{aligned} &\frac{3u_j^{n+1} - 4u_j^n + u_j^{n-1}}{2\Delta t} + < u >^n \cdot \nabla u_j^{n+1} + u_j'^n \cdot \nabla \left(2u_j^n - u_j^{n-1}\right) \\ &+ \nabla p_j^{n+1} - \nu \Delta u_j^{n+1} - \nabla \cdot \left(2\nu_T \nabla^s u_j^{n+1}\right) = f_j^{n+1}, \\ &\nabla \cdot u_j^{n+1} = 0. \end{aligned} \tag{EVB}$$

As (EnB) and (EVB) are three-step methods, a second order, two-step method, such as Crank-Nicolson method, is needed to compute velocity at step $n = 1$ for each ensemble member. The initialization of velocity at step $n = 0$ has to be divergence free (weakly) for the methods to be stable.

5.2 STABILITY OF THE METHOD WITHOUT EDDY VISCOSITY

For laminar flows, we prove (EnB) is stable under a timestep restriction, (5.2.2) below, relating the timestep to the size of the fluctuations about the mean. The fully discrete method is: given $u_{j,h}^{n-1}, u_{j,h}^{n}$, find $u_{j,h}^{n+1} \in X_h$, $p_{j,h}^{n+1} \in Q_h$ satisfying

$$\begin{aligned}
&\left(\frac{3u_{j,h}^{n+1} - 4u_{j,h}^{n} + u_{j,h}^{n-1}}{2\Delta t}, v_h\right) + b^*\left(< u_h >^n, u_{j,h}^{n+1}, v_h\right) \\
&+b^*\left(u_{j,h}'^n, 2u_{j,h}^{n} - u_{j,h}^{n-1}, v_h\right) - \left(p_{j,h}^{n+1}, \nabla \cdot v_h\right) \\
&+\nu\left(\nabla u_{j,h}^{n+1}, \nabla v_h\right) = \left(f_j^{n+1}, v_h\right), \qquad \forall v_h \in X_h, \\
&\left(\nabla \cdot u_{j,h}^{n+1}, q_h\right) = 0, \qquad \forall q_h \in Q_h.
\end{aligned} \tag{5.2.1}$$

Timestep condition of (EnB). With a standard spacial discretization with mesh size h, in both 2d and 3d (EnB) is stable under the CFL type condition:

$$C\frac{\Delta t}{\nu h}\|\nabla u_{j,h}'^n\|^2 \leq 1, \qquad j = 1, ..., J. \tag{5.2.2}$$

This is improvable in 2d following estimates in [53]. Note that the condition is explicit (i.e., the required information is available at t^n to determine Δt to compute $u_{j,h}^{n+1}$ stably) and depends on the size of the fluctuation $u_{j,h}'^n$. The constant C is independent of the timestep Δt but depends on the domain and minimum angle of the mesh. Pre-computations were used to determine C in our tests.

Theorem 11 (Stability of (EnB)). *Consider the method (5.2.1). Suppose the condition (5.2.2) holds. Then, for any $N > 1$*

$$\frac{1}{4}\|u_{j,h}^N\|^2 + \frac{1}{4}\|2u_{j,h}^N - u_{j,h}^{N-1}\|^2 + \frac{1}{8}\sum_{n=1}^{N-1}\|u_{j,h}^{n+1} - 2u_{j,h}^n + u_{j,h}^{n-1}\|^2 \tag{5.2.3}$$
$$+\frac{\Delta t}{4}\sum_{n=1}^{N-1}\nu\|\nabla u_{j,h}^{n+1}\|^2 \leq \sum_{n=1}^{N-1}\frac{\Delta t}{\nu}\|f_j^{n+1}\|_{-1}^2 + \frac{1}{4}\|u_{j,h}^1\|^2 + \frac{1}{4}\|2u_{j,h}^1 - u_{j,h}^0\|^2 \ .$$

Proof. Set $v_h = u_{j,h}^{n+1}$ in (5.2.1), multiply through by Δt and apply Young's inequality to the right hand side. This gives

$$\frac{1}{4}\left(\|u_{j,h}^{n+1}\|^2 + \|2u_{j,h}^{n+1} - u_{j,h}^n\|^2\right) - \frac{1}{4}\left(\|u_{j,h}^n\|^2 + \|2u_{j,h}^n - u_{j,h}^{n-1}\|^2\right) \tag{5.2.4}$$
$$+\frac{1}{4}\|u_{j,h}^{n+1} - 2u_{j,h}^n + u_{j,h}^{n-1}\|^2 + \Delta t b^*\left(u_{j,h}'^n, 2u_{j,h}^n - u_{j,h}^{n-1}, u_{j,h}^{n+1}\right)$$
$$+\nu\Delta t\|\nabla u_{j,h}^{n+1}\|^2 \leq \frac{\nu\Delta t}{4}\|\nabla u_{j,h}^{n+1}\|^2 + \frac{\Delta t}{\nu}\|f_j^{n+1}\|_{-1}^2 \ .$$

Next, we bound the trilinear term.

$$\Delta t b^*\left(u_{j,h}'^n, 2u_{j,h}^n - u_{j,h}^{n-1}, u_{j,h}^{n+1}\right) \tag{5.2.5}$$
$$= \Delta t b^*\left(u_{j,h}'^n, u_{j,h}^{n+1}, u_{j,h}^{n+1} - 2u_{j,h}^n + u_{j,h}^{n-1}\right)$$
$$\leq C\Delta t\|\nabla u_{j,h}'^n\|\|\nabla u_{j,h}^{n+1}\|\|\nabla(u_{j,h}^{n+1} - 2u_{j,h}^n + u_{j,h}^{n-1})\|^{1/2}\|u_{j,h}^{n+1} - 2u_{j,h}^n + u_{j,h}^{n-1}\|^{1/2}$$
$$\leq C\Delta t h^{-\frac{1}{2}}\|\nabla u_{j,h}'^n\|\|\nabla u_{j,h}^{n+1}\|\|u_{j,h}^{n+1} - 2u_{j,h}^n + u_{j,h}^{n-1}\|$$
$$\leq C\frac{\Delta t^2}{h}\|\nabla u_{j,h}'^n\|^2\|\nabla u_{j,h}^{n+1}\|^2 + \frac{1}{8}\|u_{j,h}^{n+1} - 2u_{j,h}^n + u_{j,h}^{n-1}\|^2 \ .$$

With this bound, combining like terms, (5.2.4) becomes

$$\frac{1}{4}\left(\|u_{j,h}^{n+1}\|^2 + \|2u_{j,h}^{n+1} - u_{j,h}^n\|^2\right) - \frac{1}{4}\left(\|u_{j,h}^n\|^2 + \|2u_{j,h}^n - u_{j,h}^{n-1}\|^2\right) \tag{5.2.6}$$
$$+\frac{\nu\Delta t}{4}\|\nabla u_{j,h}^{n+1}\|^2 + \frac{\nu\Delta t}{2}\left(1 - C\frac{\Delta t}{\nu h}\|\nabla u_{j,h}'^n\|^2\right)\|\nabla u_{j,h}^{n+1}\|^2$$
$$+\frac{1}{8}\|u_{j,h}^{n+1} - 2u_{j,h}^n + u_{j,h}^{n-1}\|^2 \leq \frac{\Delta t}{\nu}\|f_j^{n+1}\|_{-1}^2 \ .$$

With the restriction (5.2.2) assumed, we have

$$\frac{\nu\Delta t}{2}\left(1 - C\frac{\Delta t}{\nu h}\|\nabla u'^{n}_{j,h}\|^2\right)\|\nabla u^{n+1}_{j,h}\|^2 \geq 0\ .$$

Equation (5.2.6) reduces to

$$\begin{aligned}&\frac{1}{4}\left(\|u^{n+1}_{j,h}\|^2 + \|2u^{n+1}_{j,h} - u^{n}_{j,h}\|^2\right) - \frac{1}{4}\left(\|u^{n}_{j,h}\|^2 + \|2u^{n}_{j,h} - u^{n-1}_{j,h}\|^2\right) \\ &+\frac{\nu\Delta t}{4}\|\nabla u^{n+1}_{j,h}\|^2 + \frac{1}{8}\|u^{n+1}_{j,h} - 2u^{n}_{j,h} + u^{n-1}_{j,h}\|^2 \leq \frac{\Delta t}{\nu}\|f^{n+1}_{j}\|^2_{-1}\ .\end{aligned} \tag{5.2.7}$$

Summing up (5.2.7) from $n = 1$ to $n = N - 1$ results in (5.2.3). □

The necessity of a timestep condition of the form (5.2.2) is shown in Section 6.2. Experiments for a similar lower order accurate method in [53] were consistent with the conclusion that some timestep condition is needed.

5.3 STABILITY OF THE METHOD WITH EDDY VISCOSITY

In this section, we analyze the method (EVB) including eddy viscosity. The approximation we study of NSE is: given $u^{n-1}_{j,h}, u^{n}_{j,h}$, find $u^{n+1}_{j,h} \in X_h$, $p^{n+1}_{j,h} \in Q_h$ satisfying

$$\begin{aligned}&\left(\frac{3u^{n+1}_{j,h} - 4u^{n}_{j,h} + u^{n-1}_{j,h}}{2\Delta t}, v_h\right) + b^*\left(< u_h >^n, u^{n+1}_{j,h}, v_h\right) \\ &+b^*\left(u'^{n}_{j,h}, 2u^{n}_{j,h} - u^{n-1}_{j,h}, v_h\right) - \left(p^{n+1}_{j,h}, \nabla\cdot v_h\right) + \nu\left(\nabla u^{n+1}_{j,h}, \nabla v_h\right) \\ &+\int_\Omega C_{\nu_T}\triangle t|u'^{n}|^2\nabla u^{n+1}_{j,h} : \nabla v_h\, dx = \left(f^{n+1}_{j}, v_h\right), \qquad \forall v_h \in X_h, \\ &\left(\nabla\cdot u^{n+1}_{j,h}, q_h\right) = 0, \qquad \forall q_h \in Q_h.\end{aligned} \tag{5.3.1}$$

Timestep conditions of (EVB). With a standard spacial discretization with mesh size h, in both 2d and 3d (EVB) is stable, if the following condition holds

$$C_{\nu_T} > 1 \qquad \text{and} \qquad \Delta t \|\nabla \cdot u'^n_{j,h}\|^2_{L^4} \leq \frac{(C_{\nu_T} - 1)\,\nu}{2C_s C_{\nu_T}}, \qquad j = 1, ..., J. \tag{5.3.2}$$

If exactly divergence free elements (e.g., [11], [19], [34], [97]) are used, this implies unconditional stability if $C_{\nu_T} > 1$. The constant C_s in the second condition of (5.3.2) comes from the Sobolev embedding inequality and thus only depends on the domain.

Remark 4. (5.3.2) *is only one sufficient condition for stability. Other sufficient conditions can be derived, e.g., for some* θ *and* α, $0 \leq \theta \leq \frac{1}{2}$, $0 < \alpha < 1$,

$$\theta\nu + \Delta t \left(C_{\nu_T} - \frac{1}{\alpha}\right) |u'^n_h|^2 \geq 0 \qquad \textit{and}$$
$$\left(\frac{1}{2} - \theta\right) \nu \|\nabla u^{n+1}_{j,h}\|^2 - \frac{1}{1-\alpha} \Delta t \|\nabla \cdot u'^n_{j,h}\|^2_{L^4} \|u^{n+1}_{j,h}\|^2_{L^4} \geq 0.$$

Theorem 12 (Stability of (EVB))**.** *Consider the method (5.3.1). Suppose the conditions in (5.3.2) hold. Then, for any* $N > 1$

$$\begin{aligned} &\frac{1}{4}\|u^N_{j,h}\|^2 + \frac{1}{4}\|2u^N_{j,h} - u^{N-1}_{j,h}\|^2 + \frac{\Delta t}{4} \sum_{n=1}^{N-1} \nu \|\nabla u^{n+1}_{j,h}\|^2 \\ &\qquad \leq \sum_{n=1}^{N-1} \frac{\Delta t}{\nu} \|f^{n+1}_j\|^2_{-1} + \frac{1}{4}\|u^1_{j,h}\|^2 + \frac{1}{4}\|2u^1_{j,h} - u^0_{j,h}\|^2 \ . \end{aligned} \tag{5.3.3}$$

Proof. Setting $v_h = u^{n+1}_{j,h}$ in (5.3.1), multiplying through by Δt and applying Young's inequality to the right hand side yields

$$\begin{aligned} &\frac{1}{4}\left(\|u^{n+1}_{j,h}\|^2 + \|2u^{n+1}_{j,h} - u^n_{j,h}\|^2\right) - \frac{1}{4}\left(\|u^n_{j,h}\|^2 + \|2u^n_{j,h} - u^{n-1}_{j,h}\|^2\right) \\ &+\frac{1}{4}\|u^{n+1}_{j,h} - 2u^n_{j,h} + u^{n-1}_{j,h}\|^2 + \int_\Omega \Delta t \left(\nu + C_{\nu_T}|u'^n_h|^2 \Delta t\right) |\nabla u^{n+1}_{j,h}|^2 dx \\ &+\Delta t b^*\left(u'^n_{j,h}, 2u^n_{j,h} - u^{n-1}_{j,h}, u^{n+1}_{j,h}\right) \leq \frac{\nu \Delta t}{4}\|\nabla u^{n+1}_{j,h}\|^2 + \frac{\Delta t}{\nu}\|f^{n+1}_j\|^2_{-1} \ . \end{aligned} \tag{5.3.4}$$

Next, using identity Lemma 1, we bound the trilinear term as follows, for any $0 < \alpha < 1$

$$\Delta t b^*\left(u'^n_{j,h}, 2u^n_{j,h} - u^{n-1}_{j,h}, u^{n+1}_{j,h}\right) \tag{5.3.5}$$

$$
\begin{aligned}
&= \Delta t b^* \left(u'^n_{j,h}, u^{n+1}_{j,h}, u^{n+1}_{j,h} - 2u^n_{j,h} + u^{n-1}_{j,h}\right) \\
&= \Delta t \left(u'^n_{j,h} \cdot \nabla u^{n+1}_{j,h}, u^{n+1}_{j,h} - 2u^n_{j,h} + u^{n-1}_{j,h}\right) \\
&+ \frac{1}{2}\triangle t \left(\nabla \cdot u'^n_{j,h}, u^{n+1}_{j,h} \cdot \left(u^{n+1}_{j,h} - 2u^n_{j,h} + u^{n-1}_{j,h}\right)\right) \\
&\leq \frac{\Delta t^2}{\alpha} \int_\Omega |u'^n_{j,h}|^2 |\nabla u^{n+1}_{j,h}|^2 dx + \frac{1}{4}\alpha \|u^{n+1}_{j,h} - 2u^n_{j,h} + u^{n-1}_{j,h}\|^2 \\
&+ \frac{\Delta t^2}{1-\alpha} \int_\Omega |\nabla \cdot u'^n_{j,h}|^2 |u^{n+1}_{j,h}|^2 dx + \frac{1}{4}(1-\alpha) \|u^{n+1}_{j,h} - 2u^n_{j,h} + u^{n-1}_{j,h}\|^2 .
\end{aligned}
$$

The stability follows provided for some α, $0 < \alpha < 1$,

$$
\begin{aligned}
&\int_\Omega \Big\{ \left(\frac{\nu}{2} + C_{\nu_T} |u'^n_h|^2 \Delta t\right) |\nabla u^{n+1}_{j,h}|^2 \\
&-\triangle t \left(\frac{1}{\alpha} |u'^n_{j,h}|^2 |\nabla u^{n+1}_{j,h}|^2 + \frac{1}{1-\alpha} |\nabla \cdot u'^n_{j,h}|^2 |u^{n+1}_{j,h}|^2\right) \Big\} dx \geq 0.
\end{aligned} \tag{5.3.6}
$$

We rewrite above inequality with $0 \leq \theta \leq \frac{1}{2}$ as

$$
\begin{aligned}
&\int_\Omega \Big\{ \left(\theta\nu + \Delta t \left(C_{\nu_T} - \frac{1}{\alpha}\right) |u'^n_h|^2\right) |\nabla u^{n+1}_{j,h}|^2 \\
&+ \left(\left(\frac{1}{2} - \theta\right) \nu |\nabla u^{n+1}_{j,h}|^2 - \frac{1}{1-\alpha} \Delta t |\nabla \cdot u'^n_{j,h}|^2 |u^{n+1}_{j,h}|^2\right) \Big\} dx \geq 0.
\end{aligned} \tag{5.3.7}
$$

A sufficient condition for (5.3.7) is

$$
\begin{aligned}
&\theta\nu + \Delta t \left(C_{\nu_T} - \frac{1}{\alpha}\right) |u'^n_h|^2 \geq 0 \qquad \text{and} \\
&\left(\frac{1}{2} - \theta\right) \nu \|\nabla u^{n+1}_{j,h}\|^2 - \frac{1}{1-\alpha} \Delta t \|\nabla \cdot u'^n_{j,h}\|^2_{L^4} \|u^{n+1}_{j,h}\|^2_{L^4} \geq 0.
\end{aligned} \tag{5.3.8}
$$

By Sobolev embedding theorem, (5.3.8) holds if

$$
\begin{aligned}
&\theta\nu + \Delta t \left(C_{\nu_T} - \frac{1}{\alpha}\right) |u'^n_h|^2 \geq 0 \qquad \text{and} \\
&\left(\frac{1}{2} - \theta\right) \nu \|\nabla u^{n+1}_{j,h}\|^2 - \frac{C_s}{1-\alpha} \Delta t \|\nabla \cdot u'^n_{j,h}\|^2_{L^4} \|\nabla u^{n+1}_{j,h}\|^2 \geq 0.
\end{aligned} \tag{5.3.9}
$$

In particular, let $C_{\nu_T} > 1$, $\alpha = 1/C_{\nu_T}$ and $\theta = 0$, then (5.3.9) reduces to (5.3.2). Assume (5.3.2) holds, then (5.3.4) becomes

$$
\begin{aligned}
&\frac{1}{4}\left(\|u^{n+1}_{j,h}\|^2 + \|2u^{n+1}_{j,h} - u^n_{j,h}\|^2\right) - \frac{1}{4}\left(\|u^n_{j,h}\|^2 + \|2u^n_{j,h} - u^{n-1}_{j,h}\|^2\right) \\
&+ \frac{\nu\Delta t}{4} \|\nabla u^{n+1}_{j,h}\|^2 \leq \frac{\Delta t}{\nu} \|f^{n+1}_j\|^2_{-1} .
\end{aligned} \tag{5.3.10}
$$

Summing up (5.3.10) from $n = 1$ to $N - 1$ completes the proof. □

The question arises: how restrictive is the ν in the RHS of the second condition in (5.3.2) vs $\|\nabla\cdot u_h'\|_{L^4}$ in the LHS since $\nabla\cdot u' = 0$ in the continuous limit? This is explored in numerical tests in Section 6.2, 6.3. In these tests, (5.3.2) did not appear to be restrictive.

5.4 ERROR ANALYSIS

In this section we give error analysis of (EnB). Assume X_h and Q_h satisfy the usual (LBB^h) condition, then the method is equivalent to: *for* $n = 1, ..., N_T - 1$, *find* $u_{j,h}^{n+1} \in V_h$ *such that*

$$\left(\frac{3u_{j,h}^{n+1} - 4u_{j,h}^{n} + u_{j,h}^{n-1}}{2\Delta t}, v_h\right) + b^*\left(< u_h >^n, u_{j,h}^{n+1}, v_h\right) \tag{5.4.1}$$
$$+b^*\left(u_{j,h}'^n, 2u_{j,h}^n - u_{j,h}^{n-1}, v_h\right) + \nu\left(\nabla u_{j,h}^{n+1}, \nabla v_h\right) = \left(f_j^{n+1}, v_h\right) \ , \forall v_h \in V_h.$$

To analyze the rate of convergence of the approximation we assume that the following regularity assumptions on the NSE

$$u_j \in L^\infty\left(0,T;H^1(\Omega)\right) \cap H^1\left(0,T;H^{k+1}(\Omega)\right) \cap H^2\left(0,T;H^1(\Omega)\right),$$
$$p_j \in L^2\left(0,T;H^{s+1}(\Omega)\right), \text{and } f_j \in L^2\left(0,T;L^2(\Omega)\right).$$

Let $e_j^n = u_j^n - u_{j,h}^n$ be the error between the true solution and the approximate solution, then we have the following error estimates.

Theorem 13 (Convergence of (EnB))**.** *Consider the method (EnB). Suppose*

$$C_e\frac{\Delta t}{\nu h}\|\nabla u_{j,h}'^n\|^2 \le 1, \qquad j = 1, ..., J, \tag{5.4.2}$$

where C_e is a constant that depends on the domain and the minimum angle of the mesh, but independent of the timestep. Then there is a positive constant C independent of the mesh

width and timestep such that

$$\begin{aligned}
&\frac{1}{2}\|e_j^N\|^2+\frac{1}{2}\|2e_j^N-e_j^{N-1}\|^2+\frac{1}{4}\sum_{n=1}^{N-1}\|e_j^{n+1}-2e_j^n+e_j^{n-1}\|^2 \\
&\qquad+\frac{\nu\Delta t}{4}\|\nabla e_j^N\|^2+\frac{\nu\Delta t}{8}\|\nabla e_j^{N-1}\|^2 \\
&\leq exp\left(\frac{CT}{\nu^2}\right)\left\{\frac{1}{2}\|e_j^1\|^2+\frac{1}{2}\|2e_j^1-e_j^0\|^2+\frac{\nu\Delta t}{4}\|\nabla e_j^1\|^2+\frac{\nu\Delta t}{8}\|\nabla e_j^0\|^2\right. \\
&\qquad+C\frac{h^{2k}}{\nu}|||\nabla u_j|||_{\infty,0}^2|||u_j|||_{2,k+1}^2+C\frac{\Delta t^4}{\nu}|||\nabla u_{j,tt}|||_{2,0}^2 \\
&\quad+C\frac{h^{2k}}{\nu}|||\nabla u_j|||_{2,k+1}^2+C\Delta t^2h^{2k+1}|||\nabla u_{j,tt}|||_{2,k}^2+C\Delta t^3h|||\nabla u_{j,tt}|||_{2,0}^2 \\
&\qquad+C\frac{h^{2s+2}}{\nu}|||p_j|||_{2,s+1}^2+Ch^{2k+2}\nu^{-1}|||u_{t,j}|||_{2,k+1}^2 \\
&\qquad\left.+C\nu h^{2k}|||\nabla u_j|||_{2,k}^2+\frac{C\Delta t^4}{\nu}|||u_{j,ttt}|||_{2,0}^2\right\}.
\end{aligned} \tag{5.4.3}$$

Remark 5. *The condition* (5.4.2) *is the same type of condition as* (5.2.2) *for (EnB). The constant* C_e *in* (5.4.2) *is possibly different from the one in* (5.2.2).

Corollary 2. *Under the assumptions of Theorem 13, with* (X_h, Q_h) *given by the Taylor-Hood approximation elements* ($k=2, s=1$)*, i.e.,* C^0 *piecewise quadratic velocity space* X_h *and* C^0 *piecewise linear pressure space* Q_h*, we have the following error estimate*

$$\begin{aligned}
&\frac{1}{2}\|e_j^N\|^2+\frac{1}{2}\|2e_j^N-e_j^{N-1}\|^2+\frac{1}{4}\sum_{n=1}^{N-1}\|e_j^{n+1}-2e_j^n+e_j^{n-1}\|^2 \\
&+\frac{\nu\Delta t}{4}\|\nabla e_j^N\|^2+\frac{\nu\Delta t}{8}\|\nabla e_j^{N-1}\|^2\leq C\left(h^4+\Delta t^4+h\Delta t^3+\|\nabla e_j^0\|^2+\|\nabla e_j^1\|^2\right).
\end{aligned} \tag{5.4.4}$$

Proof. The true solution(u_j, p_j) of the NSE satisfies

$$\begin{aligned}
&\left(\frac{3u_j^{n+1}-4u_j^n+u_j^{n-1}}{2\Delta t},v_h\right)+b^*\left(u_j^{n+1},u_j^{n+1},v_h\right)+\nu\left(\nabla u_j^{n+1},\nabla v_h\right) \\
&-\left(p_j^{n+1},\nabla\cdot v_h\right)=\left(f_j^{n+1},v_h\right)+Intp\left(u_j^{n+1};v_h\right),\qquad\text{for all } v_h\in V_h,
\end{aligned} \tag{5.4.5}$$

where $Intp\left(u_j^{n+1};v_h\right)$ is defined as

$$Intp\left(u_j^{n+1};v_h\right)=\left(\frac{3u_j^{n+1}-4u_j^n+u_j^{n-1}}{2\Delta t}-u_{j,t}(t^{n+1}),v_h\right).$$

Let $e_j^n = u_j^n - u_{j,h}^n = \left(u_j^n - I_h u_j^n\right) + \left(I_h u_j^n - u_{j,h}^n\right) = \eta_j^n + \xi_{j,h}^n$, where $I_h u_j^n \in V_h$ is an interpolant of u_j^n in V_h. Subtracting (5.4.1) from (5.4.5) gives

$$\begin{aligned}
&\left(\frac{3\xi_{j,h}^{n+1} - 4\xi_{j,h}^n + \xi_{j,h}^{n-1}}{2\Delta t}, v_h\right) + b^*\left(u_j^{n+1}, u_j^{n+1}, v_h\right) + \nu\left(\nabla\xi_{j,h}^{n+1}, \nabla v_h\right) \qquad (5.4.6)\\
&-b^*\left(2u_{j,h}^n - u_{j,h}^{n-1} - u_{j,h}'^n, u_{j,h}^{n+1}, v_h\right) - b^*\left(u_{j,h}'^n, 2u_{j,h}^n - u_{j,h}^{n-1}, v_h\right) - \left(p_j^{n+1}, \nabla\cdot v_h\right)\\
&= -\left(\frac{3\eta_j^{n+1} - 4\eta_j^n + \eta_j^{n-1}}{2\Delta t}, v_h\right) - \nu\left(\nabla\eta_j^{n+1}, \nabla v_h\right) + Intp\left(u_j^{n+1}; v_h\right) \ .
\end{aligned}$$

Set $v_h = \xi_{j,h}^{n+1} \in V_h$, and rearrange the nonlinear terms, then we have

$$\begin{aligned}
&\frac{1}{4\Delta t}\left(\|\xi_{j,h}^{n+1}\|^2 + \|2\xi_{j,h}^{n+1} - \xi_{j,h}^n\|^2\right) - \frac{1}{4\Delta t}\left(\|\xi_{j,h}^n\|^2 + \|2\xi_{j,h}^n - \xi_{j,h}^{n-1}\|^2\right) \qquad (5.4.7)\\
&\qquad + \frac{1}{4\Delta t}\|\xi_{j,h}^{n+1} - 2\xi_{j,h}^n + \xi_{j,h}^{n-1}\|^2 + \nu\|\nabla\xi_{j,h}^{n+1}\|^2\\
&\qquad = -b^*\left(u_j^{n+1}, u_j^{n+1}, \xi_{j,h}^{n+1}\right) + b^*\left(2u_{j,h}^n - u_{j,h}^{n-1}, u_{j,h}^{n+1}, \xi_{j,h}^{n+1}\right)\\
&\qquad + b^*\left(u_{j,h}'^n, 2u_{j,h}^n - u_{j,h}^{n-1} - u_{j,h}^{n+1}, \xi_{j,h}^{n+1}\right) + \left(p_j^{n+1}, \nabla\cdot\xi_{j,h}^{n+1}\right)\\
&- \left(\frac{3\eta_j^{n+1} - 4\eta_j^n + \eta_j^{n-1}}{2\Delta t}, \xi_{j,h}^{n+1}\right) - \nu\left(\nabla\eta_j^{n+1}, \nabla\xi_{j,h}^{n+1}\right) + Intp\left(u_j^{n+1}; \xi_{j,h}^{n+1}\right) \ .
\end{aligned}$$

Now we bound the right hand side of equation (5.4.7). First, for the nonlinear term, adding and subtracting $b^*(u_j^{n+1}, u_{j,h}^{n+1}, \xi_{j,h}^{n+1})$ (Step 1), $b^*(2u_j^n - u_j^{n-1}, u_{j,h}^{n+1}, \xi_{j,h}^{n+1})$ (Step 2) and $b^*(u_{j,h}'^n, 2u_j^n - u_j^{n-1} - u_j^{n+1}, \xi_{j,h}^{n+1})$ (Step3) respectively, we have

$$\begin{aligned}
&-b^*\left(u_j^{n+1}, u_j^{n+1}, \xi_{j,h}^{n+1}\right) + b^*\left(2u_{j,h}^n - u_{j,h}^{n-1}, u_{j,h}^{n+1}, \xi_{j,h}^{n+1}\right) \qquad (5.4.8)\\
&\qquad + b^*\left(u_{j,h}'^n, 2u_{j,h}^n - u_{j,h}^{n-1} - u_{j,h}^{n+1}, \xi_{j,h}^{n+1}\right)\\
&\qquad = -b^*\left(u_j^{n+1}, e_j^{n+1}, \xi_{j,h}^{n+1}\right) - b^*\left(u_j^{n+1}, u_{j,h}^{n+1}, \xi_{j,h}^{n+1}\right) \qquad \text{(Step 1)}\\
&+ b^*\left(2u_{j,h}^n - u_{j,h}^{n-1}, u_{j,h}^{n+1}, \xi_{j,h}^{n+1}\right) + b^*\left(u_{j,h}'^n, 2u_{j,h}^n - u_{j,h}^{n-1} - u_{j,h}^{n+1}, \xi_{j,h}^{n+1}\right)\\
&= -b^*\left(u_j^{n+1}, e_j^{n+1}, \xi_{j,h}^{n+1}\right) - b^*\left(u_j^{n+1} - (2u_j^n - u_j^{n-1}), u_{j,h}^{n+1}, \xi_{j,h}^{n+1}\right) \qquad \text{(Step 2)}\\
&\quad -b^*\left(2e_j^n - e_j^{n-1}, u_{j,h}^{n+1}, \xi_{j,h}^{n+1}\right) + b^*\left(u_{j,h}'^n, 2u_{j,h}^n - u_{j,h}^{n-1} - u_{j,h}^{n+1}, \xi_{j,h}^{n+1}\right)\\
&= -b^*\left(u_j^{n+1}, e_j^{n+1}, \xi_{j,h}^{n+1}\right) - b^*\left(u_j^{n+1} - \left(2u_j^n - u_j^{n-1}\right), u_{j,h}^{n+1}, \xi_{j,h}^{n+1}\right) \qquad \text{(Step 3)}\\
&\quad -b^*\left(2e_j^n - e_j^{n-1}, u_{j,h}^{n+1}, \xi_{j,h}^{n+1}\right) - b^*\left(u_{j,h}'^n, 2e_j^n - e_j^{n-1} - e_j^{n+1}, \xi_{j,h}^{n+1}\right)\\
&\quad +b^*\left(u_{j,h}'^n, 2u_j^n - u_j^{n-1} - u_j^{n+1}, \xi_{j,h}^{n+1}\right)
\end{aligned}$$

$$= -b^*\left(u_j^{n+1}, \eta_j^{n+1}, \xi_{j,h}^{n+1}\right) - b^*\left(u_j^{n+1} - (2u_j^n - u_j^{n-1}), u_{j,h}^{n+1}, \xi_{j,h}^{n+1}\right)$$
$$-b^*\left(2\eta_j^n - \eta_j^{n-1}, u_{j,h}^{n+1}, \xi_{j,h}^{n+1}\right) - b^*\left(2\xi_{j,h}^n - \xi_{j,h}^{n-1}, u_{j,h}^{n+1}, \xi_{j,h}^{n+1}\right)$$
$$-b^*\left(u_{j,h}'^n, 2\xi_{j,h}^n - \xi_{j,h}^{n-1} - \xi_{j,h}^{n+1}, \xi_{j,h}^{n+1}\right) - b^*\left(u_{j,h}'^n, 2\eta_j^n - \eta_j^{n-1} - \eta_j^{n+1}, \xi_{j,h}^{n+1}\right)$$
$$+b^*\left(u_{j,h}'^n, 2u_j^n - u_j^{n-1} - u_j^{n+1}, \xi_{j,h}^{n+1}\right) \ .$$

We estimate the nonlinear terms using (2.2.1), (2.2.2) and Young's inequality as follows.

$$b^*\left(u_j^{n+1}, \eta_j^{n+1}, \xi_{j,h}^{n+1}\right) \le C\|\nabla u_j^{n+1}\|\|\nabla \eta_j^{n+1}\|\|\nabla \xi_{j,h}^{n+1}\| \tag{5.4.9}$$
$$\le \frac{\nu}{64}\|\nabla \xi_{j,h}^{n+1}\|^2 + C\nu^{-1}\|\nabla u_j^{n+1}\|^2\|\nabla \eta_j^{n+1}\|^2 \ .$$

$$b^*\left(u_j^{n+1} - \left(2u_j^n - u_j^{n-1}\right), u_{j,h}^{n+1}, \xi_{j,h}^{n+1}\right) \tag{5.4.10}$$
$$\le C\|\nabla\left(u_j^{n+1} - 2u_j^n + u_j^{n-1}\right)\|\|\nabla u_{j,h}^{n+1}\|\|\nabla \xi_{j,h}^{n+1}\|$$
$$\le \frac{\nu}{64}\|\nabla \xi_{j,h}^{n+1}\|^2 + C\nu^{-1}\|\nabla\left(u_j^{n+1} - 2u_j^n + u_j^{n-1}\right)\|^2\|\nabla u_{j,h}^{n+1}\|^2$$
$$\le \frac{\nu}{64}\|\nabla \xi_{j,h}^{n+1}\|^2 + C\nu^{-1}\Delta t^3\left(\int_{t^{n-1}}^{t^{n+1}} \|\nabla u_{j,tt}\|^2 dt\right)\|\nabla u_{j,h}^{n+1}\|^2 \ .$$

$$b^*\left(2\eta_j^n - \eta_j^{n-1}, u_{j,h}^{n+1}, \xi_{j,h}^{n+1}\right) \le C\|\nabla\left(2\eta_j^n - \eta_j^{n-1}\right)\|\|\nabla u_{j,h}^{n+1}\|\|\nabla \xi_{j,h}^{n+1}\| \tag{5.4.11}$$
$$\le \frac{\nu}{64}\|\nabla \xi_{j,h}^{n+1}\|^2 + C\nu^{-1}\left(\|\nabla \eta_j^n\|^2 + \|\nabla \eta_j^{n-1}\|^2\right)\|\nabla u_{j,h}^{n+1}\|^2.$$

$$2b^*\left(\xi_{j,h}^n, u_{j,h}^{n+1}, \xi_{j,h}^{n+1}\right) \le C\|\nabla \xi_{j,h}^n\|^{\frac{1}{2}}\|\xi_{j,h}^n\|^{\frac{1}{2}}\|\nabla u_{j,h}^{n+1}\|\|\nabla \xi_{j,h}^{n+1}\| \tag{5.4.12}$$
$$\le C\|\nabla \xi_{j,h}^n\|^{\frac{1}{2}}\|\xi_{j,h}^n\|^{\frac{1}{2}}\|\nabla \xi_{j,h}^{n+1}\|$$
$$\le C\left(\epsilon\|\nabla \xi_{j,h}^{n+1}\|^2 + \frac{1}{\epsilon}\|\nabla \xi_{j,h}^n\|\|\xi_{j,h}^n\|\right)$$
$$\le C\left(\epsilon\|\nabla \xi_{j,h}^{n+1}\|^2 + \frac{1}{\epsilon}\left(\delta\|\nabla \xi_{j,h}^n\|^2 + \frac{1}{\delta}\|\xi_{j,h}^n\|^2\right)\right)$$
$$\le \left(\frac{\nu}{64}\|\nabla \xi_{j,h}^{n+1}\|^2 + \frac{\nu}{16}\|\nabla \xi_{j,h}^n\|^2\right) + C\nu^{-3}\|\xi_{j,h}^n\|^2.$$

Similarly,

$$
\begin{aligned}
b^*\left(\xi_{j,h}^{n-1}, u_{j,h}^{n+1}, \xi_{j,h}^{n+1}\right) &\leq C\|\nabla\xi_{j,h}^{n-1}\|^{\frac{1}{2}}\|\xi_{j,h}^{n-1}\|^{\frac{1}{2}}\|\nabla u_{j,h}^{n+1}\|\|\nabla\xi_{j,h}^{n+1}\| \\
&\leq C\|\nabla\xi_{j,h}^{n-1}\|^{\frac{1}{2}}\|\xi_{j,h}^{n-1}\|^{\frac{1}{2}}\|\nabla\xi_{j,h}^{n+1}\| \\
&\leq C\left(\epsilon\|\nabla\xi_{j,h}^{n+1}\|^2 + \frac{1}{\epsilon}\|\nabla\xi_{j,h}^{n-1}\|\|\xi_{j,h}^{n-1}\|\right) \\
&\leq C\left(\epsilon\|\nabla\xi_{j,h}^{n+1}\|^2 + \frac{1}{\epsilon}\left(\delta\|\nabla\xi_{j,h}^{n-1}\|^2 + \frac{1}{\delta}\|\xi_{j,h}^{n-1}\|^2\right)\right) \\
&\leq \left(\frac{\nu}{64}\|\nabla\xi_{j,h}^{n+1}\|^2 + \frac{\nu}{16}\|\nabla\xi_{j,h}^{n-1}\|^2\right) + C\nu^{-3}\|\xi_{j,h}^{n-1}\|^2.
\end{aligned} \tag{5.4.13}
$$

By skew symmetry

$$
\begin{aligned}
b^*\left(u_{j,h}'^n, 2\xi_{j,h}^n - \xi_{j,h}^{n-1} - \xi_{j,h}^{n+1}, \xi_{j,h}^{n+1}\right) &= -b^*\left(u_{j,h}'^n, \xi_{j,h}^{n+1} - 2\xi_{j,h}^n + \xi_{j,h}^{n-1}, \xi_{j,h}^{n+1}\right) \\
&= b^*\left(u_{j,h}'^n, \xi_{j,h}^{n+1}, \xi_{j,h}^{n+1} - 2\xi_{j,h}^n + \xi_{j,h}^{n-1}\right).
\end{aligned}
$$

Using (2.2.3) and inverse inequality gives

$$
\begin{aligned}
&b^*\left(u_{j,h}'^n, 2\xi_{j,h}^n - \xi_{j,h}^{n-1} - \xi_{j,h}^{n+1}, \xi_{j,h}^{n+1}\right) \\
&\leq C\|\nabla u_{j,h}'^n\|\|\nabla\xi_{j,h}^{n+1}\|\|\nabla(\xi_{j,h}^{n+1} - 2\xi_{j,h}^n + \xi_{j,h}^{n-1})\|^{1/2}\|\xi_{j,h}^{n+1} - 2\xi_{j,h}^n + \xi_{j,h}^{n-1}\|^{1/2} \\
&\leq C\|\nabla u_{j,h}'^n\|\|\nabla\xi_{j,h}^{n+1}\|\left(h^{-1/2}\right)\|\xi_{j,h}^{n+1} - 2\xi_{j,h}^n + \xi_{j,h}^{n-1}\| \\
&\leq \frac{1}{8\Delta t}\|\xi_{j,h}^{n+1} - 2\xi_{j,h}^n + \xi_{j,h}^{n-1}\|^2 + \frac{C_e}{16}\frac{\Delta t}{h}\|\nabla u_{j,h}'^n\|^2\|\nabla\xi_{j,h}^{n+1}\|^2.
\end{aligned} \tag{5.4.14}
$$

$$
\begin{aligned}
&b^*\left(u_{j,h}'^n, \eta_j^{n+1} - 2\eta_j^n + \eta_j^{n-1}, \xi_{j,h}^{n+1}\right) \\
&\leq C\|\nabla u_{j,h}'^n\|\|\nabla\left(\eta_j^{n+1} - 2\eta_j^n + \eta_j^{n-1}\right)\|\|\nabla\xi_{j,h}^{n+1}\| \\
&\leq \frac{\nu}{64}\|\nabla\xi_{j,h}^{n+1}\|^2 + C\nu^{-1}\|\nabla u_{j,h}'^n\|^2\|\nabla\left(\eta_j^{n+1} - 2\eta_j^n + \eta_j^{n-1}\right)\|^2 \\
&\leq \frac{\nu}{64}\|\nabla\xi_{j,h}^{n+1}\|^2 + \frac{C\Delta t^3}{\nu}\|\nabla u_{j,h}'^n\|^2\left(\int_{t^{n-1}}^{t^{n+1}}\|\nabla\eta_{j,tt}\|^2\,dt\right).
\end{aligned} \tag{5.4.15}
$$

$$
\begin{aligned}
&b^*\left(u_{j,h}'^n, u_j^{n+1} - 2u_j^n + u_j^{n-1}, \xi_{j,h}^{n+1}\right) \\
&\leq C\|\nabla u_{j,h}'^n\|\|\nabla\left(u_j^{n+1} - 2u_j^n + u_j^{n-1}\right)\|\|\nabla\xi_{j,h}^{n+1}\|
\end{aligned} \tag{5.4.16}
$$

$$\leq \frac{\nu}{64}\|\nabla\xi_{j,h}^{n+1}\|^2 + C\nu^{-1}\|\nabla u_{j,h}'^{n}\|^2\|\nabla\left(u_j^{n+1} - 2u_j^n + u_j^{n-1}\right)\|^2$$
$$\leq \frac{\nu}{64}\|\nabla\xi_{j,h}^{n+1}\|^2 + C\nu^{-1}\Delta t^3\|\nabla u_{j,h}'^{n}\|^2\left(\int_{t^{n-1}}^{t^{n+1}} \|\nabla u_{j,tt}\|^2\ dt\right)\ .$$

Next, consider the pressure term. Since $\xi_{j,h}^{n+1} \in V_h$ we have

$$\begin{aligned}\left(p_j^{n+1}, \nabla\cdot\xi_{j,h}^{n+1}\right) &= \left(p_j^{n+1} - q_{j,h}^{n+1}, \nabla\cdot\xi_{j,h}^{n+1}\right) \\ &\leq \|p_j^{n+1} - q_{j,h}^{n+1}\|\|\nabla\cdot\xi_{j,h}^{n+1}\| \\ \leq \frac{\nu}{64}\|\nabla\xi_{j,h}^{n+1}\|^2 + C\nu^{-1}\|p_j^{n+1} - q_{j,h}^{n+1}\|^2, &\qquad \forall q_{j,h}^{n+1} \in Q_h\ .\end{aligned} \tag{5.4.17}$$

The other terms, are bounded as

$$\begin{aligned}\left(\frac{3\eta_j^{n+1} - 4\eta_j^n + \eta_j^{n-1}}{2\Delta t}, \xi_{j,h}^{n+1}\right) &\leq C\|\frac{3\eta_j^{n+1} - 4\eta_j^n + \eta_j^{n-1}}{2\Delta t}\|\|\nabla\xi_{j,h}^{n+1}\| \\ &\leq C\nu^{-1}\|\frac{3\eta_j^{n+1} - 4\eta_j^n + \eta_j^{n-1}}{2\Delta t}\|^2 + \frac{\nu}{64}\|\nabla\xi_{j,h}^{n+1}\|^2 \\ &\leq C\nu^{-1}\|\frac{1}{\Delta t}\int_{t^{n-1}}^{t^{n+1}} \eta_{j,t}\ dt\| + \frac{\nu}{64}\|\nabla\xi_{j,h}^{n+1}\|^2 \\ &\leq \frac{C}{\nu\Delta t}\int_{t^{n-1}}^{t^{n+1}} \|\eta_{j,t}\|^2\ dt + \frac{\nu}{64}\|\nabla\xi_{j,h}^{n+1}\|^2\ .\end{aligned} \tag{5.4.18}$$

$$\begin{aligned}\nu\left(\nabla\eta_j^{n+1}, \nabla\xi_{j,h}^{n+1}\right) &\leq \nu\|\nabla\eta_j^{n+1}\|\|\nabla\xi_{j,h}^{n+1}\| \\ &\leq C\nu\|\nabla\eta_j^{n+1}\|^2 + \frac{\nu}{64}\|\nabla\xi_{j,h}^{n+1}\|^2\ .\end{aligned} \tag{5.4.19}$$

Finally,

$$\begin{aligned}Intp\left(u_j^{n+1}; \xi_{j,h}^{n+1}\right) &= \left(\frac{3u_j^{n+1} - 4u_j^n + u_j^{n-1}}{2\Delta t} - u_{j,t}(t^{n+1}), \xi_{j,h}^{n+1}\right) \\ &\leq C\|\frac{3u_j^{n+1} - 4u_j^n + u_j^{n-1}}{2\Delta t} - u_{j,t}(t^{n+1})\|\|\nabla\xi_{j,h}^{n+1}\| \\ &\leq \frac{\nu}{64}\|\nabla\xi_{j,h}^{n+1}\|^2 + \frac{C}{\nu}\|\frac{3u_j^{n+1} - 4u_j^n + u_j^{n-1}}{2\Delta t} - u_{j,t}(t^{n+1})\|^2\end{aligned} \tag{5.4.20}$$

$$\leq \frac{\nu}{64}\|\nabla\xi_{j,h}^{n+1}\|^2 + \frac{C\Delta t^3}{\nu}\int_{t^{n-1}}^{t^{n+1}} \|u_{j,ttt}\|^2 dt \ .$$

Combining, we now have the following inequality

$$\begin{aligned}
&\frac{1}{4\Delta t}\left(\|\xi_{j,h}^{n+1}\|^2 + \|2\xi_{j,h}^{n+1} - \xi_{j,h}^{n}\|^2\right) - \frac{1}{4\Delta t}\left(\|\xi_{j,h}^{n}\|^2 + \|2\xi_{j,h}^{n} - \xi_{j,h}^{n-1}\|^2\right) \\
&\quad + \frac{1}{8\Delta t}\|\xi_{j,h}^{n+1} - 2\xi_{j,h}^{n} + \xi_{j,h}^{n-1}\|^2 + \frac{\nu}{16}\left(\|\nabla\xi_{j,h}^{n+1}\|^2 - \|\nabla\xi_{j,h}^{n}\|^2\right) \\
&\quad + \frac{\nu}{16}\left(\left(\|\nabla\xi_{j,h}^{n+1}\|^2 + \|\nabla\xi_{j,h}^{n}\|^2\right) - \left(\|\nabla\xi_{j,h}^{n}\|^2 + \|\nabla\xi_{j,h}^{n-1}\|^2\right)\right) \\
&\quad + \left(\frac{\nu}{16} - \frac{C_e}{16}\frac{\Delta t}{h}\|\nabla u_{j,h}'^{n}\|^2\right)\|\nabla\xi_{j,h}^{n+1}\|^2 \leq C\nu^{-3}\left(\|\xi_{j,h}^{n}\|^2 + \|\xi_{j,h}^{n-1}\|^2\right) \\
&\quad + C\nu^{-1}\|\nabla u_j^{n+1}\|^2\|\nabla\eta_j^{n+1}\|^2 + \frac{C\Delta t^3}{\nu}\left(\int_{t^{n-1}}^{t^{n+1}} \|\nabla u_{j,tt}\|^2 dt\right)\|\nabla u_{j,h}^{n+1}\|^2 \\
&\quad + C\nu^{-1}\left(\|\nabla\eta_j^{n}\|^2 + \|\nabla\eta_j^{n-1}\|^2\right)\|\nabla u_{j,h}^{n+1}\|^2 + \frac{C\Delta t^3}{\nu}\|\nabla u_{j,h}'^{n}\|^2\left(\int_{t^{n-1}}^{t^{n+1}} \|\nabla\eta_{j,tt}\|^2 \ dt\right) \\
&\quad + \frac{C\Delta t^3}{\nu}\|\nabla u_{j,h}'^{n}\|^2\left(\int_{t^{n-1}}^{t^{n+1}} \|\nabla u_{j,tt}\|^2 \ dt\right) + C\nu^{-1}\|p_j^{n+1} - q_{j,h}^{n+1}\|^2 \\
&\quad + \frac{C}{\nu\Delta t}\int_{t^{n-1}}^{t^{n+1}} \|\eta_{j,t}\|^2 \ dt + C\nu\|\nabla\eta_j^{n+1}\|^2 + \frac{C\Delta t^3}{\nu}\int_{t^{n-1}}^{t^{n+1}} \|u_{j,ttt}\|^2 dt.
\end{aligned} \tag{5.4.21}$$

Under the assumption of (5.4.2), $(\frac{\nu}{16} - \frac{C_e}{16}\frac{\Delta t}{h}\|\nabla u_{j,h}'^{n}\|^2)$ is nonnegative and thus can be eliminated from the LHS of (5.4.21). We then take the sum of (5.4.21) from $n = 1$ to $n = N-1$ and multiply through by $2\Delta t$. This yields

$$\begin{aligned}
&\frac{1}{2}\|\xi_{j,h}^{N}\|^2 + \frac{1}{2}\|2\xi_{j,h}^{N} - \xi_{j,h}^{N-1}\|^2 + \frac{1}{4}\sum_{n=1}^{N-1}\|\xi_{j,h}^{n+1} - 2\xi_{j,h}^{n} + \xi_{j,h}^{n-1}\|^2 \\
&\quad + \frac{\nu\Delta t}{8}\|\nabla\xi_{j,h}^{N}\|^2 + \frac{\nu\Delta t}{8}\left(\|\nabla\xi_{j,h}^{N}\|^2 + \|\nabla\xi_{j,h}^{N-1}\|^2\right) \\
&\leq \frac{1}{2}\|\xi_{j,h}^{1}\|^2 + \frac{1}{2}\|2\xi_{j,h}^{1} - \xi_{j,h}^{0}\|^2 + \frac{\nu\Delta t}{8}\|\nabla\xi_{j,h}^{1}\|^2 + \frac{\nu\Delta t}{8}\left(\|\nabla\xi_{j,h}^{1}\|^2 + \|\nabla\xi_{j,h}^{0}\|^2\right) \\
&\quad + \Delta t\sum_{n=0}^{N-1} C\nu^{-3}\|\xi_{j,h}^{n}\|^2 + \Delta t\sum_{n=0}^{N-1}\Big\{C\nu^{-1}\|\nabla u_j^{n+1}\|^2\|\nabla\eta_j^{n+1}\|^2 \\
&\quad + \frac{C\Delta t^3}{\nu}\left(\int_{t^{n-1}}^{t^{n+1}} \|\nabla u_{j,tt}\|^2 \ dt\right) + C\nu^{-1}\|\nabla\eta_j^{n}\|^2
\end{aligned} \tag{5.4.22}$$

$$+C\Delta t^2 h\left(\int_{t^{n-1}}^{t^{n+1}}\|\nabla\eta_{j,tt}\|^2dt\right)+C\Delta t^2 h\left(\int_{t^{n-1}}^{t^{n+1}}\|\nabla u_{j,tt}\|^2dt\right)$$
$$+C\nu^{-1}\|p_j^{n+1}-q_{j,h}^{n+1}\|^2+\frac{C}{\nu\Delta t}\int_{t^{n-1}}^{t^{n+1}}\|\eta_{j,t}\|^2dt$$
$$+C\nu\|\nabla\eta_j^{n+1}\|^2+\frac{C\Delta t^3}{\nu}\int_{t^{n-1}}^{t^{n+1}}\|u_{j,ttt}\|^2\ dt\Big\}.$$

Applying interpolation inequalities gives

$$\frac{1}{2}\|\xi_{j,h}^N\|^2+\frac{1}{2}\|2\xi_{j,h}^N-\xi_{j,h}^{N-1}\|^2+\frac{1}{4}\sum_{n=1}^{N-1}\|\xi_{j,h}^{n+1}-2\xi_{j,h}^n+\xi_{j,h}^{n-1}\|^2 \tag{5.4.23}$$
$$+\frac{\nu\Delta t}{4}\|\nabla\xi_{j,h}^N\|^2+\frac{\nu\Delta t}{8}\|\nabla\xi_{j,h}^{N-1}\|^2$$
$$\leq\frac{1}{2}\|\xi_{j,h}^1\|^2+\frac{1}{2}\|2\xi_{j,h}^1-\xi_{j,h}^0\|^2+\frac{\nu\Delta t}{4}\|\nabla\xi_{j,h}^1\|^2+\frac{\nu\Delta t}{8}\|\nabla\xi_{j,h}^0\|^2+\Delta t\sum_{n=0}^{N-1}C\nu^{-3}\|\xi_{j,h}^n\|^2$$
$$+C\frac{h^{2k}}{\nu}|||\nabla u_j|||_{\infty,0}^2|||u_j|||_{2,k+1}^2+C\frac{\Delta t^4}{\nu}|||\nabla u_{j,tt}|||_{2,0}^2$$
$$+C\frac{h^{2k}}{\nu}|||\nabla u_j|||_{2,k+1}^2+C\Delta t^2h^{2k+1}|||\nabla u_{j,tt}|||_{2,k}^2+C\Delta t^3h|||\nabla u_{j,tt}|||_{2,0}^2$$
$$+C\frac{h^{2s+2}}{\nu}|||p_j|||_{2,s+1}^2+Ch^{2k+2}\nu^{-1}|||u_{t,j}|||_{2,k+1}^2$$
$$+C\nu h^{2k}|||\nabla u_j|||_{2,k}^2+\frac{C\Delta t^4}{\nu}|||u_{j,ttt}|||_{2,0}^2.$$

The next step will be the application of the discrete Gronwall inequality (Girault and Raviart [37], p. 176).

$$\frac{1}{2}\|\xi_{j,h}^N\|^2+\frac{1}{2}\|2\xi_{j,h}^N-\xi_{j,h}^{N-1}\|^2+\frac{1}{4}\sum_{n=1}^{N-1}\|\xi_{j,h}^{n+1}-2\xi_{j,h}^n+\xi_{j,h}^{n-1}\|^2 \tag{5.4.24}$$
$$+\frac{\nu\Delta t}{4}\|\nabla\xi_{j,h}^N\|^2+\frac{\nu\Delta t}{8}\|\nabla\xi_{j,h}^{N-1}\|^2$$
$$\leq exp\left(\frac{CN\Delta t}{\nu^2}\right)\left\{\frac{1}{2}\|\xi_{j,h}^1\|^2+\frac{1}{2}\|2\xi_{j,h}^1-\xi_{j,h}^0\|^2+\frac{\nu\Delta t}{4}\|\nabla\xi_{j,h}^1\|^2+\frac{\nu\Delta t}{8}\|\nabla\xi_{j,h}^0\|^2\right.$$
$$+C\frac{h^{2k}}{\nu}|||\nabla u_j|||_{\infty,0}^2|||u_j|||_{2,k+1}^2+C\frac{\Delta t^4}{\nu}|||\nabla u_{j,tt}|||_{2,0}^2$$
$$+C\frac{h^{2k}}{\nu}|||\nabla u_j|||_{2,k+1}^2+C\Delta t^2h^{2k+1}|||\nabla u_{j,tt}|||_{2,k}^2+C\Delta t^3h|||\nabla u_{j,tt}|||_{2,0}^2$$
$$+C\frac{h^{2s+2}}{\nu}|||p_j|||_{2,s+1}^2+Ch^{2k+2}\nu^{-1}|||u_{t,j}|||_{2,k+1}^2$$

$$+C\nu h^{2k}|||\nabla u_j|||^2_{2,k} + \frac{C\Delta t^4}{\nu}|||u_{j,ttt}|||^2_{2,0}\Big\} .$$

Using triangle inequality on the error and absorbing constants into a new constant C, we obtain (5.4.3). □

5.5 NUMERICAL EXPERIMENTS

In this section, we test the ensemble simulation methods. The first experiment verifies the convergence rate predicted by our analysis. Next, we test the severity of the timestep conditions and explore the use of ensemble methods to interrogate flows on a 2D flow between two offset cylinders. In the third experiment, we test the effect of the EV term on 3D Ethier-Steinman flow.

5.5.1 Convergence

We check the convergence rate on a simple test problem from [41], with known exact solution. This problem preserves spacial patterns of the Green-Taylor solution, [8], [40], but the vortices do not decay as $t \to \infty$. The analytical solution of the Navier-Stokes equations in the unit square $\Omega = [0,1]^2$ is given by

$$u_{true} = (-g(t)\cos x \sin y, +g(t)\sin x \cos y)^T,$$
$$p_{true} = -\frac{1}{4}[\cos(2x) + \cos(2y)]g^2(t), \quad \text{where } g(t) = \sin(2t),$$

with source term $f(x,y,t) = [g'(t) + 2\nu g(t)](-\cos x \sin y, \sin x \cos y)^T$. The boundary condition is taken to be inhomogeneous Dirichlet: $u = u_{true}$ on $\partial\Omega$.

The generation of perturbations to initial conditions and source terms is application dependable. In this simple test, we generate perturbations to initial conditions in the same way as in Chapter 4. Consider an ensemble of two members $u_{1,2} = (1 \pm \epsilon)u_{true}$, $\epsilon = 10^{-3}$, which are the solutions to NSE corresponding to two different initial conditions $u^0_{1,2} = (1 \pm \epsilon)u^0_{true}$, respectively. Note the source term and boundary condition are adjusted accordingly.

Δt	$\|u_1 - u_{1,h}\|_{\infty,0}$	rate	$\|\nabla u_1 - \nabla u_{1,h}\|_{2,0}$	rate
0.05	$4.85642 \cdot 10^{-4}$	–	$5.11092 \cdot 10^{-3}$	–
0.025	$1.26128 \cdot 10^{-4}$	1.9450	$1.18810 \cdot 10^{-3}$	2.1049
0.0125	$3.21716 \cdot 10^{-5}$	1.9710	$2.92502 \cdot 10^{-4}$	2.0221
0.00625	$8.12342 \cdot 10^{-6}$	1.9856	$7.31031 \cdot 10^{-5}$	2.0004
0.003125	$2.04078 \cdot 10^{-6}$	1.9930	$1.83094 \cdot 10^{-5}$	1.9974

Table 7: (EnB): Errors and convergence rates for the first ensemble member

Taking $\nu = 0.01$, $T = 1$, $h = 2\Delta t$, we compute approximations to the test problem with both (EnB) and (EVB) on 5 successive mesh refinements and corresponding timestep reductions. From Table 7 and Table 8 we can see u_1 and u_2 computed with (EnB) are second order convergent as predicted. The eddy viscosity term in (EVB) results in extra errors that depend on the magnitude of the fluctuations. A comparison of data from Table 7, 8, 9 and 10 shows that the errors from (EVB) are comparable to although slightly greater than errors from (EnB).

5.5.2 Flow between two offset cylinders

We test the stability of our methods on a 2D flow between two offset cylinders. The domain is a disk with a smaller off center obstacle inside. Let $r_1 = 1$, $r_2 = 0.1$, $c = (c_1, c_2) = (\frac{1}{2}, 0)$. The domain is given by

$$\Omega = \{(x, y) : x^2 + y^2 \leq r_1^2 \text{ and } (x - c_1)^2 + (y - c_2)^2 \geq r_2^2\}.$$

We enforce no-slip boundary conditions on the both circles. The flow is driven by a counterclockwise rotational body force

$$f(x, y, t) = (-4y * (1 - x^2 - y^2), 4x * (1 - x^2 - y^2))^T.$$

Δt	$\|u_2 - u_{2,h}\|_{\infty,0}$	rate	$\|\nabla u_2 - \nabla u_{2,h}\|_{2,0}$	rate
0.05	$4.84794 \cdot 10^{-4}$	–	$5.09708 \cdot 10^{-3}$	–
0.025	$1.25913 \cdot 10^{-4}$	1.9449	$1.18528 \cdot 10^{-3}$	2.1044
0.0125	$3.21161 \cdot 10^{-5}$	1.9711	$2.91837 \cdot 10^{-4}$	2.0220
0.00625	$8.10943 \cdot 10^{-6}$	1.9856	$7.29391 \cdot 10^{-5}$	2.0004
0.003125	$2.03726 \cdot 10^{-6}$	1.9930	$1.82684 \cdot 10^{-5}$	1.9973

Table 8: (EnB): Errors and convergence rates for the second ensemble member

The flow interacts with the inner circle generating complex flow structures including the forming of a Von Kármán vortex street that reinteracts with the inner circle. Extensive experiments on this flow of a first order ensemble method can be found in [53].

Perturbations of the initial conditions are generated in the same way as given in [53] for the same test problem. We first solve steady Stokes problem with two perturbed body forces given by

$$f_1(x,y,t) = f(x,y,t) + \epsilon_1 * (sin(3\pi x)sin(3\pi y), cos(3\pi x)cos(3\pi y))^T,$$

$$f_2(x,y,t) = f(x,y,t) + \epsilon_2 * (sin(3\pi x)sin(3\pi y), cos(3\pi x)cos(3\pi y))^T.$$

This gives us two discretely divergence free initial perturbations. To compute velocity at step $n = 1$, we use one Crank-Nicolson step. Given the initializations, we compute approximations to the test problem with both (EnB) and (EVB), with perturbation parameters $\epsilon_1 = 10^{-3}$, $\epsilon_2 = -10^{-3}$. The mesh is generated by Delaunay triangulation with 40 mesh points on the outer circle and 10 mesh points on the inner circle.

For (EnB), we cut Δt according to the following specific timestep condition

$$\Delta t \|\nabla u_{j,h}'^n\|^2 \leq 80000\nu h, \qquad (j = 1, 2). \tag{5.5.1}$$

For (EVB), we cut Δt according to the following specific timestep condition

$$\Delta t \|\nabla \cdot u_{j,h}'^n\|_{L^4}^2 \leq 40000\nu, \qquad (j = 1, 2). \tag{5.5.2}$$

Δt	$\|u_1 - u_{1,h}\|_{\infty,0}$	rate	$\|\nabla u_1 - \nabla u_{1,h}\|_{2,0}$	rate
0.05	$4.85644 \cdot 10^{-4}$	–	$5.11094 \cdot 10^{-3}$	–
0.025	$1.26129 \cdot 10^{-4}$	1.9450	$1.18812 \cdot 10^{-3}$	2.1049
0.0125	$3.21721 \cdot 10^{-5}$	1.9710	$2.92508 \cdot 10^{-4}$	2.0221
0.00625	$8.12367 \cdot 10^{-6}$	1.9856	$7.31064 \cdot 10^{-5}$	2.0004
0.003125	$2.0409 \cdot 10^{-6}$	1.9929	$1.83110 \cdot 10^{-5}$	1.9973

Table 9: (EVB): Errors and convergence rates for the first ensemble member

Pre-computations were used to determine the coefficients ($80,000$ and $40,000$) in the conditions. The timestep is cut in half if the condition is violated and doubled if the magnitude of the fluctuations gets small enough (specifically, $\Delta t\|\nabla u'^n_{j,h}\|^2 \leq 40000\nu h$ for (EnB); $\Delta t\|\nabla \cdot u'^n_{j,h}\|^2_{L^4} \leq 20000\nu$ for (EVB)). In all cases, Δt is enforced to not exceed 0.05.

Figure 29 shows the kinetic energy of the average velocity from different methods. The curve marked with 'no perturbation' is computed using the linearly implicit Backward Euler method with no perturbation on the initial condition. The other two curves are computed by (EnB) (marked with 'noEV') and (EVB) (marked with 'EV', with eddy viscosity coefficient $C_{\nu_T} = 1$) respectively. *Figure 29 shows that the choice $C_{\nu_T} = 1.0$ results in too much damping. EV models share this sensitivity to the precise values of the EV coefficients.*

There is a significant difference between the simulations with the averaged initial conditions and the averaged simulations with 10^{-3} perturbation of the initial conditions. We can see from Figure 1 that the (EnB) gives a better approximation for $\nu = 0.02$ than (EVB) which is somewhat over-diffused. For $\nu = 0.02$, both (EnB) and (EVB) are stable under the timestep conditions given above with timestep reduced to 0.00625 for (EnB) while timestep kept to be 0.05 all the time for (EVB).

Figure 30 shows a comparison of kinetic energy of the average velocity approximated by (EVB) with different eddy viscosity parameters. For $\nu = 0.001$, (EnB) fails with timestep cut to $< 10^{-7}$, while (EVB) stays stable with large/moderate timesteps. The upper picture in Figure 30 is obtained by adapting timestep according to the timestep restriction (5.5.2) and the statistics in the lower picture are obtained by computing with constant timestep

Δt	$\|u_2 - u_{2,h}\|_{\infty,0}$	rate	$\|\nabla u_2 - \nabla u_{2,h}\|_{2,0}$	rate
0.05	$4.84796 \cdot 10^{-4}$	–	$5.09709 \cdot 10^{-3}$	–
0.025	$1.25915 \cdot 10^{-4}$	1.9449	$1.185291 \cdot 10^{-3}$	2.1044
0.0125	$3.21166 \cdot 10^{-5}$	1.9711	$2.91844 \cdot 10^{-4}$	2.0220
0.00625	$8.10968 \cdot 10^{-6}$	1.9856	$7.29423 \cdot 10^{-5}$	2.0004
0.003125	$2.03738 \cdot 10^{-6}$	1.9929	$1.82701 \cdot 10^{-5}$	1.9973

Table 10: (EVB): Errors and convergence rates for the second ensemble member

$\Delta t = 0.0125$. The approximations are sensitive to the choice of the eddy viscosity parameter C_{ν_T}, consistent with [2].

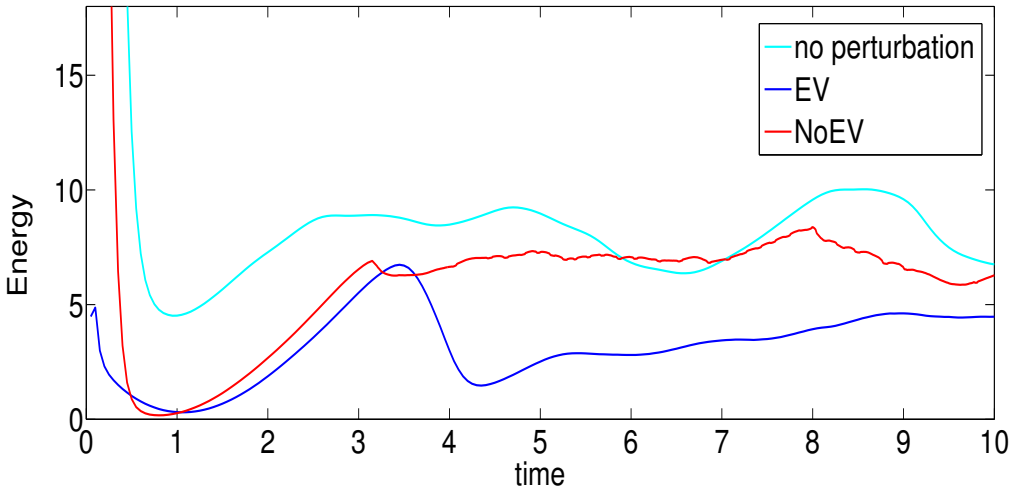

Figure 29: Kinetic Energy for $\nu = 0.02$.

It is believed that 2D (unforced) turbulent flow has a larger window of predictability than similar 3D flows due to lack of vortex stretching in 2D and to the trend for energy to cascade to large, coherent structures, [42], [59]. This trend may be connected to the selective decay principle and convergence of Dirichlet quotients; see Majda and Wang [72], Ghil et al. [42] for elaborations. We test this for the above 2D flow between offset circles as follows. We solve the problem with the same initial conditions generated by the above perturbed body forces until complex, small scale structures appear at time T^* using (EVB) with eddy

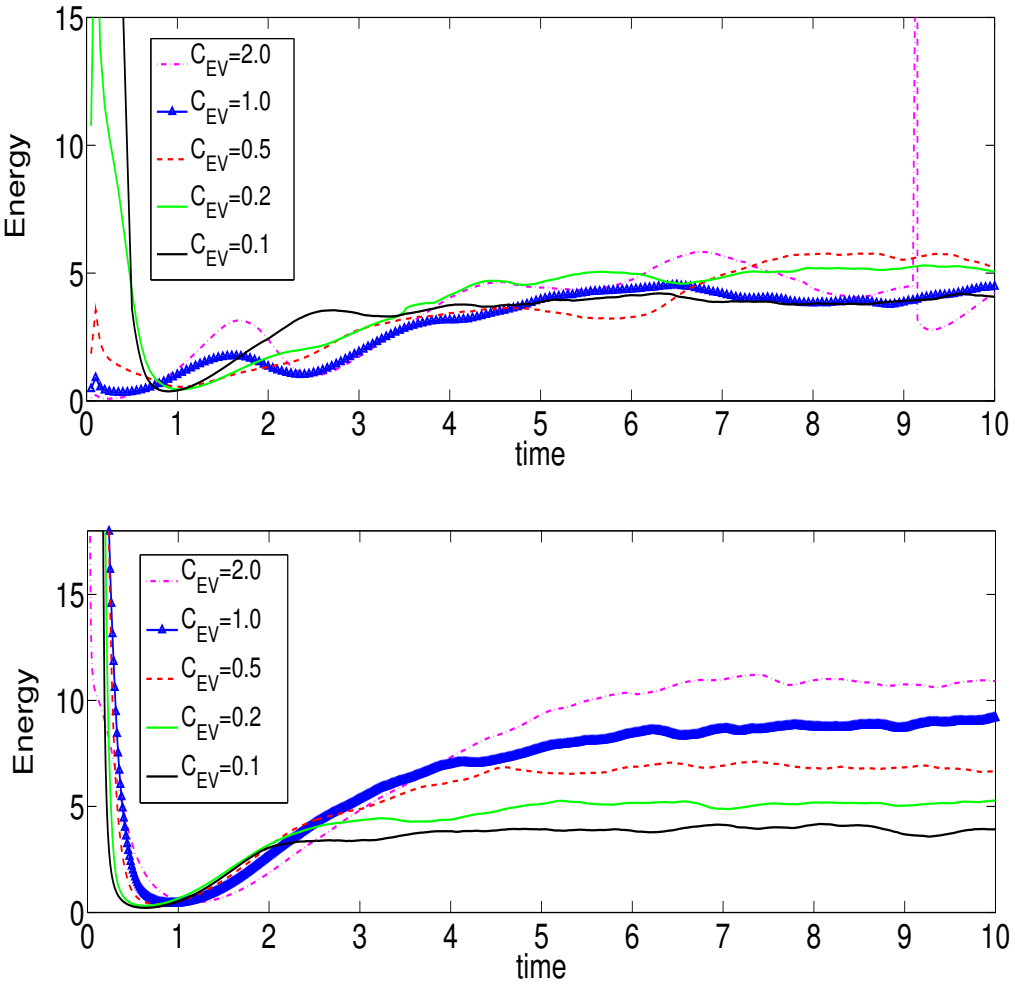

Figure 30: Kinetic Energy for $\nu = 0.001$. UPPER: adapted timestep; LOWER: constant timestep $\Delta t = 0.0125$.

viscosity parameter $C_{EV} = 1.0$. The time T^* is selected to be $T^* = 9.6$, a time of (near) maximal enstrophy from Figure 31. Thereafter (for $t > T^*$) we set $f(x,t) \equiv 0$ and study the decay of the flow thereafter. We compute the following statistics.

Definition 3. *The* **turbulence intensity** $I(t)$ *is*

$$I(t) := \frac{\left\langle \|u_j'\|^2 \right\rangle^{1/2}}{\| \langle u \rangle \|},$$

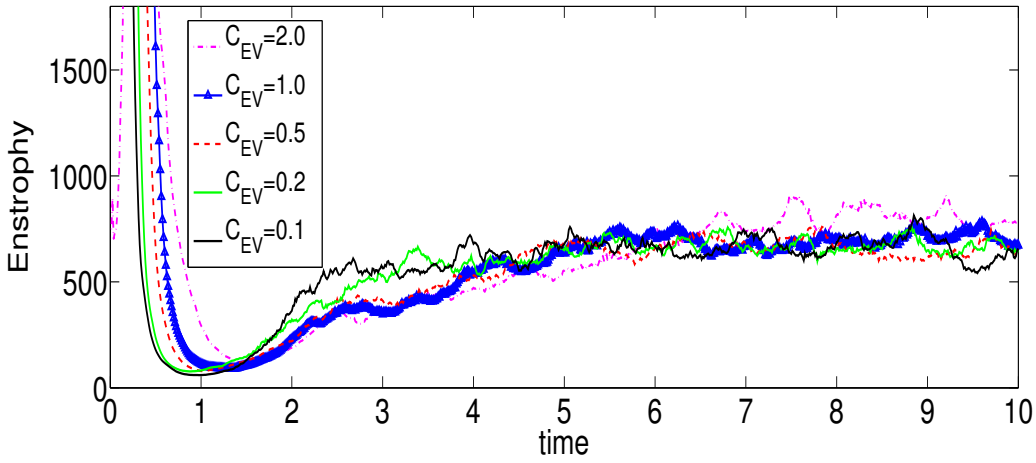

Figure 31: Enstrophy for $\nu = 0.001$ with constant timestep $\Delta t = 0.0125$.

and the **Dirichlet quotients** *are*

$$D(t) := \frac{\|\nabla \times \langle u \rangle\|^2}{\|\langle u \rangle\|^2}, \text{ and } \langle D \rangle (t) := \left\langle \frac{\|\nabla \times u_j\|^2}{\|u_j\|^2} \right\rangle.$$

The **relative energy fluctuation** *is*

$$r(t) := \frac{\|u_1 - u_2\|^2}{\|u_1\|\|u_2\|},$$

and the **average, effective Lyapunov exponent** *over* $0 \leq t \leq T$ *is*

$$\gamma_T(t) := \frac{1}{2T} log \left(\frac{r(t+T)}{r(t)} \right).$$

Remark 6. *The definition of* $\gamma_T(t)$*, where* T *is the simulation time, is from [6].*

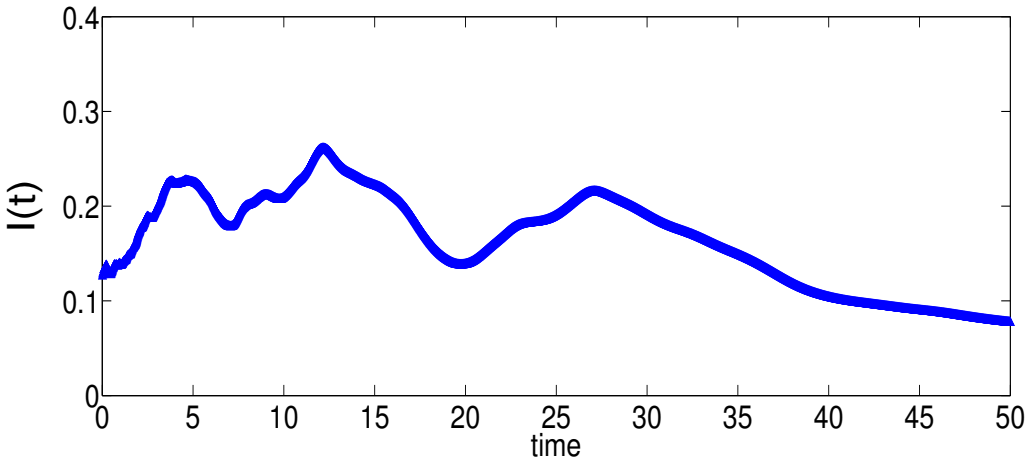

Figure 32: Turbulence Intensity, $\nu = 0.001$, $\Delta t = 0.0125$.

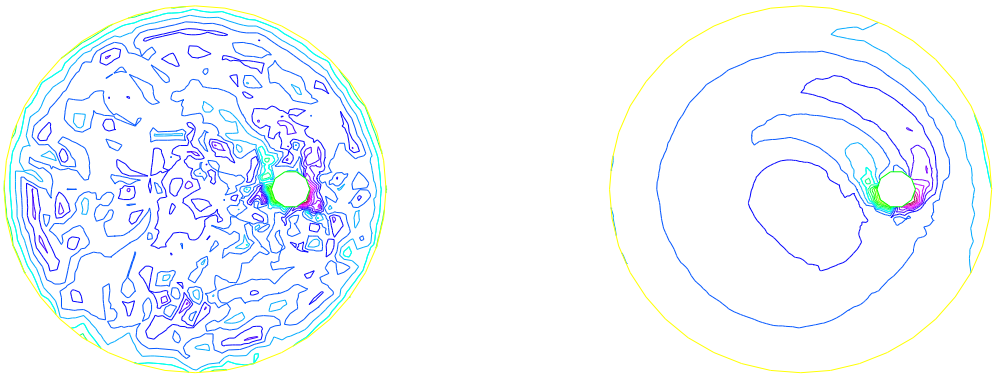

Figure 33: Vorticity, $\nu = 0.001$, $\Delta t = 0.0125$. LEFT: t=0; RIGHT: t=50.

We solve the problem as described and give plots of $I(t), D(t), \langle D \rangle (t)$, $r(t)$ and $\gamma_t(0)$ versus time in Figure 32, 34, 35, 36. The turbulence intensity is above 5% during the entire simulation time, see Figure 32, which is normally associated with significant turbulent fluctuations. Figure 5 shows vorticity contours of the freely evolving turbulent flows at $t = 0$ (reinitiation) and $t = 50$ respectively. At $t = 0$, the domain is filled with vortices of a wide range of scales. As time evolves, the size of eddies continually grows, associated with the

cascade of energy from small scales to large scales, and then a large scale, coherent structure starts to show up. We can see clearly from Figure 5 a large scale, coherent structure formed at $t = 50$. Figure 34 shows that the Dirichlet quotients approach a constant around 32, consistent with the selective decay theorem for freely decaying 2D Navier-Stokes flows in [72]. The relative energy fluctuation is plotted in Figure 35. For only a short time $r(t)$ is above 0.25, which is the threshold used in [6] to define the predictability time. The difference here is that $r(t)$ grows exponentially for only a short time period ($t = 0 \sim 5$, approximately) and after which $r(t)$ fluctuates with time and is actually decreasing to small values after time $t = 30$. Our conjecture is that dissipation is already active after $t = 5$ and the separation of the two trajectories is slowed down due to lost of energy. The approximated Lyapunov exponent corresponding to different simulation times is plotted in Fig. 36. It is positive until around $t = 44$. After this point (until $t = 50$), the two trajectories are actually closer than they initially were.

5.5.3 3D Ethier-Steinman Flow

We give a 3D test to confirm the positive effect of the eddy viscosity model for high Reynolds number flows compared to the laminar flow model.

The well-known 3D Ethier-Steinman analytical solutions to the incompressible Navier-Stokes euqations are studied in [27] to provide benchmarks for testing Navier-Stokes solvers. The solutions are valid for all Reynolds numbers and complex structures may also be expected due to the nontrivial helicity, see [71], [81]. The exact 3D NSE solutions on a $[0, 1]^3$ box are given by

$$
\begin{aligned}
u_1 &= -a(e^{ax}sin(ay + dz) + e^{az}cos(ax + dy))e^{-\nu d^2 t} \ , \\
u_2 &= -a(e^{ay}sin(az + dx) + e^{ax}cos(ay + dz))e^{-\nu d^2 t} \ , \\
u_3 &= -a(e^{az}sin(ax + dy) + e^{ay}cos(az + dx))e^{-\nu d^2 t} \ , \\
p &= -\frac{a^2}{2}(e^{2ax} + e^{2ay} + e^{2az} + 2sin(ax + dy)cos(az + dx)e^{a(y+z)} \\
&+2sin(ay + dz)cos(ax + dy)e^{a(z+x)} + 2sin(az + dx)cos(ay + dz)e^{a(x+y)})e^{-2\nu d^2 t}.
\end{aligned}
\tag{5.5.3}
$$

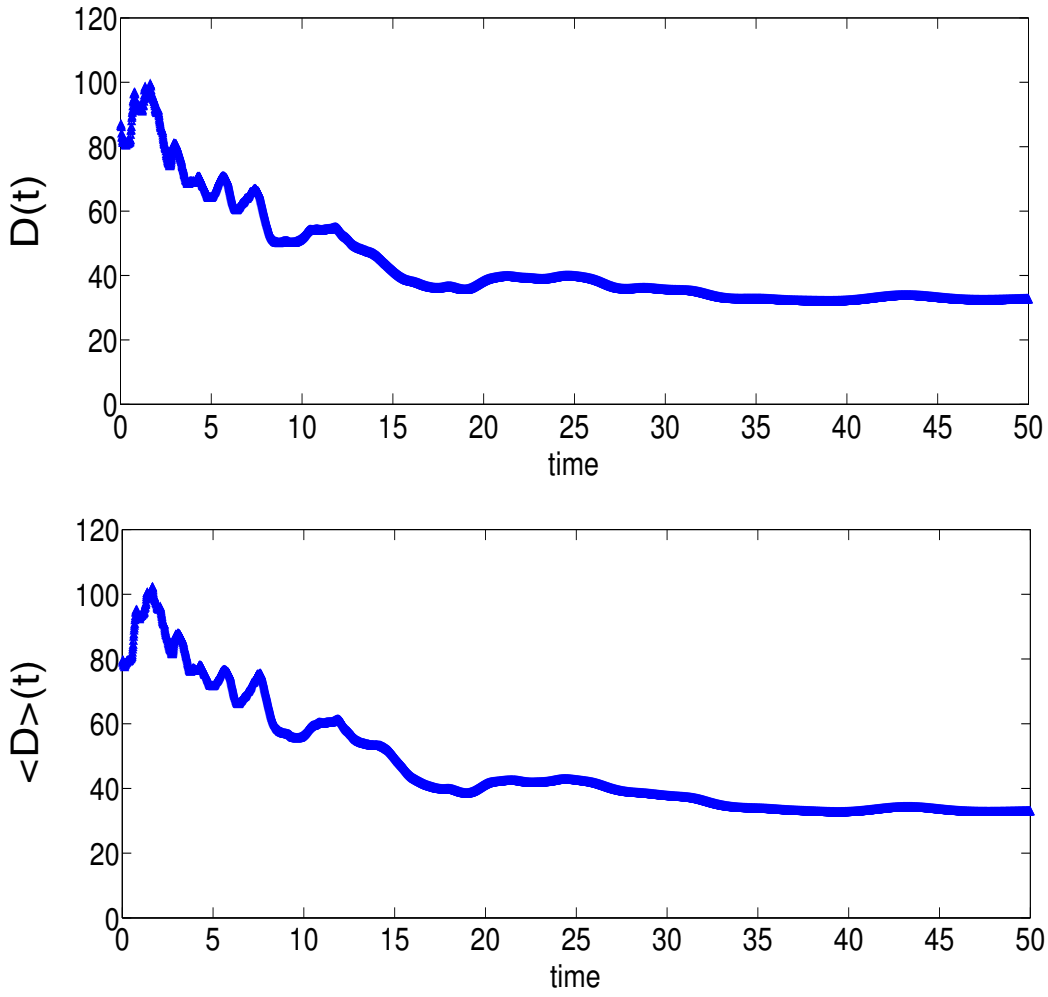

Figure 34: Dirichlet Quotients, $\nu = 0.001$, $\Delta t = 0.0125$.

We compute approximations to (5.5.3) with parameters $a = 1.25, d = 2.25$, kinematic viscosity $\nu = 0.001$, mesh size $h = 0.1$ and end time $T = 1$. Two ensemble members are considered in this test. The perturbations are generated in the same way as in Section 6.1 with the same parameters $\epsilon_1 = 10^{-3}$, $\epsilon_2 = -10^{-3}$. (EnB) fails for all timesteps $\Delta t = 0.05, \Delta t = 0.02$ and $\Delta t = 0.01$, while (EVB) gives acceptable approximations. To visualize the flow structure of the test problem, we plot streamribbons in the box, velocity streamlines and speed contours on the sides for the exact velocity field, the average velocity field calculated from (EVB) with $C_{\nu_T} = 1.0$, and the difference between these two in Figure

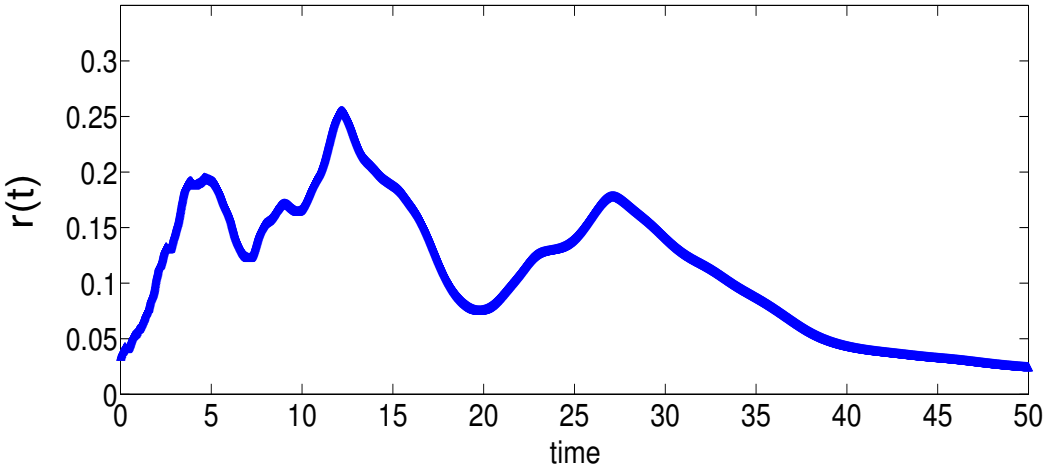

Figure 35: Relative Energy Fluctuation, $\nu = 0.001$, $\Delta t = 0.0125$.

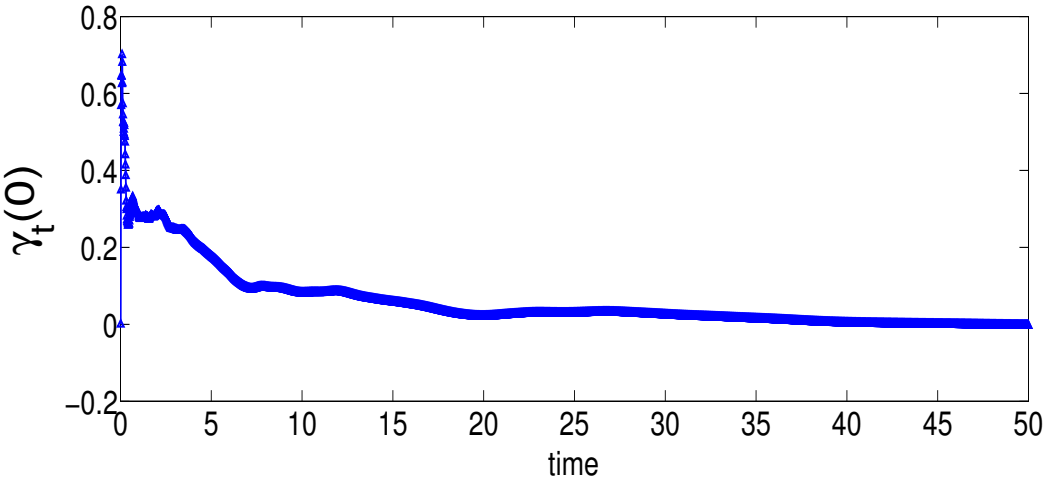

Figure 36: Effective Lyapunov Exponent, $\nu = 0.001$, $\Delta t = 0.0125$.

37. No pattern of the errors is apparent in Figure 37.

Plots of kinetic energy versus time are shown in Figure 38 for $\Delta t = 0.05, \Delta t = 0.02$ and $\Delta t = 0.01$. It can be seen that (EnB) becomes unstable at time around $t = 0.5$ for all cases, while (EVB) stays stable giving better approximations to the exact solutions as timestep

decreased.

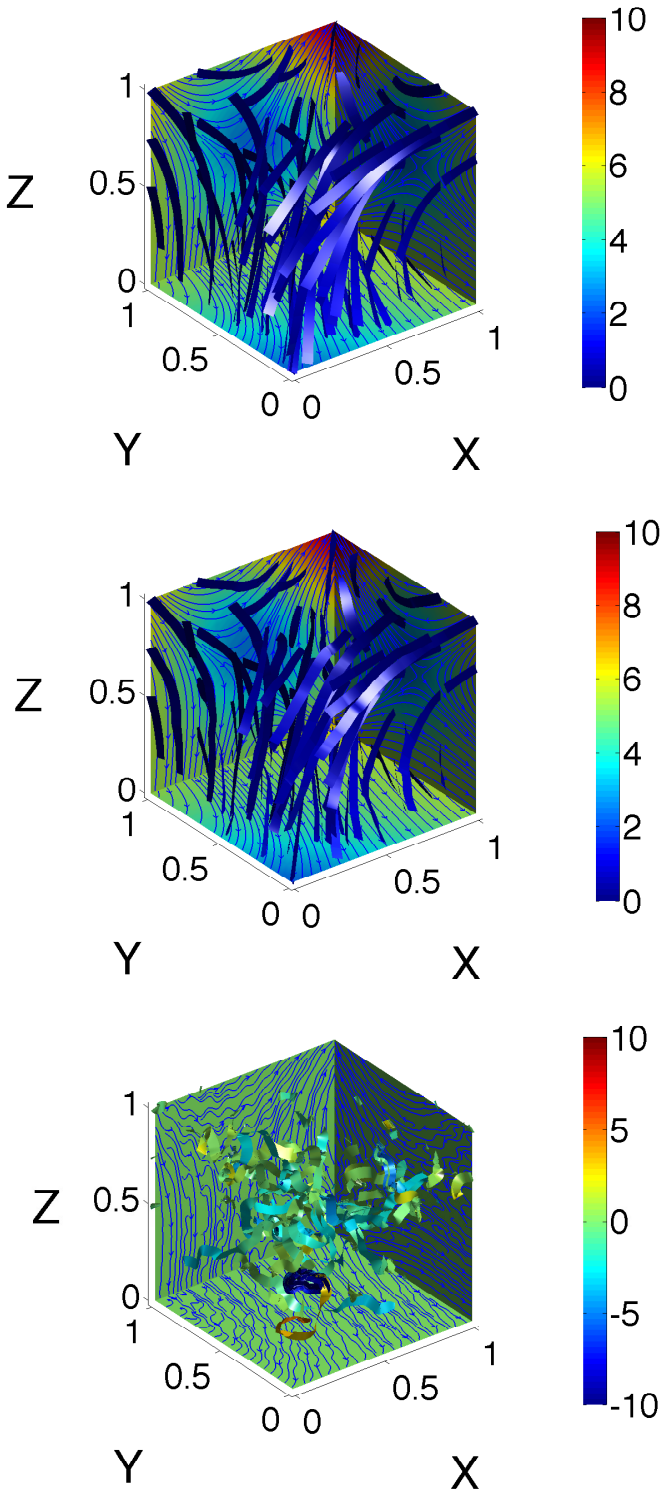

Figure 37: Flow structure for $\nu = 0.001$, $\Delta t = 0.02$. FIRST: Exact solution; SECOND: EV model average velocity; THIRD: Difference between the exact solution and EV model average velocity.

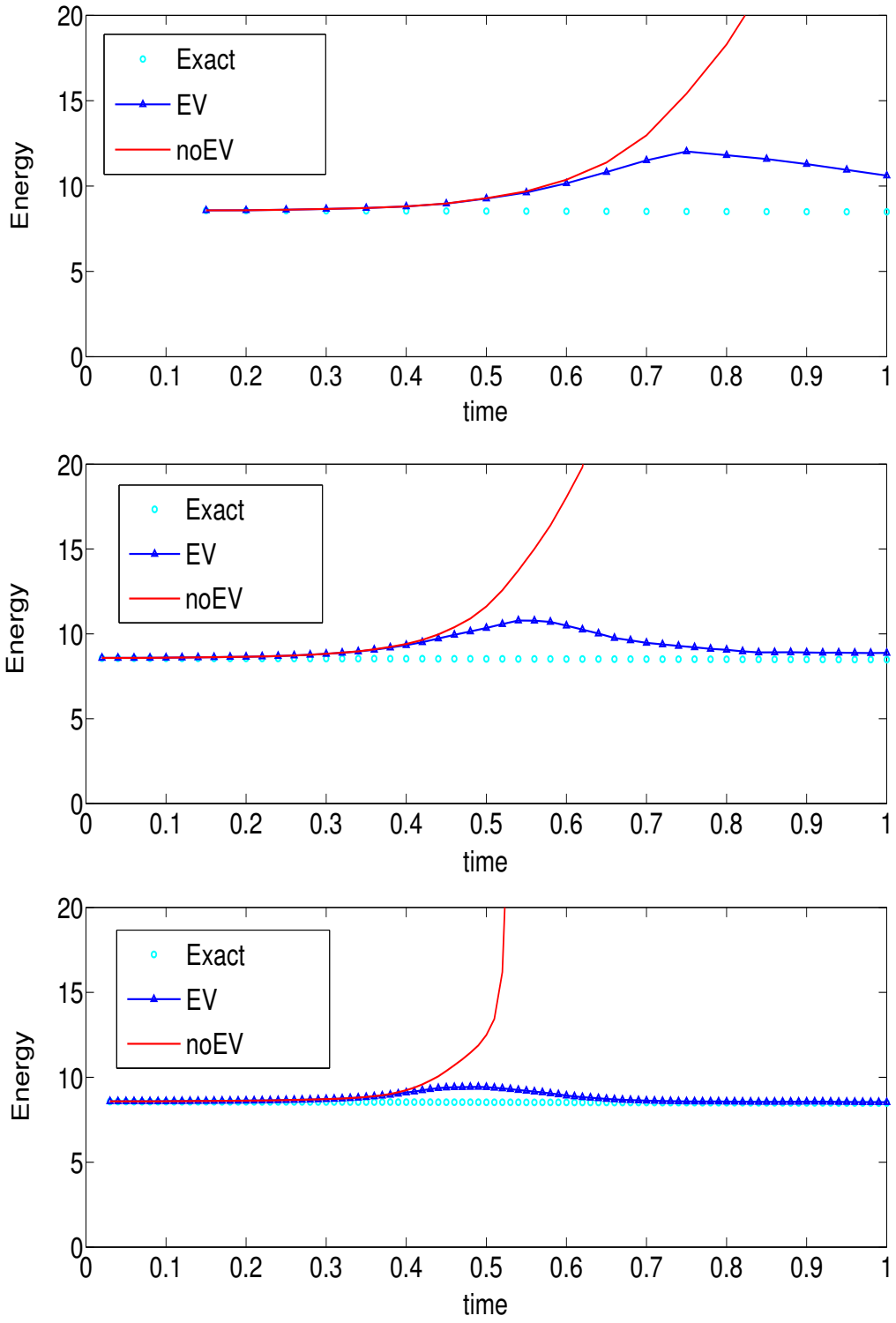

Figure 38: Kinetic Energy for $\nu = 0.001$. FIRST: $\Delta t = 0.05$; SECOND: $\Delta t = 0.02$; THIRD: $\Delta t = 0.01$

5.6 CONCLUSIONS

Computing ensembles of solutions is known to increase reliability and cost. We present a second order method to compute flow ensembles at less cost. Computing an ensemble of solutions opens interesting possibilities for modeling turbulence, also explored. We believe ensemble methods have potential for many important applications, in which the size of the ensemble used has a significant impact on the reliability of prediction but is limited by computer resources. The ensemble mean must be adapted to be compatible with the time discretization. Numerical tests indicate its potential use in exploring various aspects of turbulent flows such as turbulence intensity, Dirichlet quotients and effective Lyapunov exponents.

6.0 ENSEMBLE BASED TURBULENCE MODELING

The fundamental approach in the simulation of turbulence is to seek to approximate suitable averages of velocity instead of pointwise fluid velocity itself. Based on different averaging operators (ensemble, time or spacial), there are various approaches to turbulence modeling (Reynolds Averaged Navier-Stokes equations (RANS), turbulent viscosity models (e.g. $k-\epsilon$ model), large eddy simulation, e.g.,[57, 3, 76, 85, 47]).

The goal of conventional turbulence models (CTMs) (such as RANS and $k-\epsilon$) is to produce a model that accurately predicts time or ensemble averaged flow statistics, [12]. Thus a CTM should quickly converge (in time) to statistical equilibrium that captures averaged flow behavior. This differs from large eddy simulation models that seek to represent the essentially dynamic behavior of local spacial averages. The latter contains more information but also requires many more degrees of freedom. We develop a new family of turbulence models and algorithms for their solution herein and study their convergence to statistical equilibrium by analyzing the evolution of model variance.

Consider J Navier-Stokes equations with J slightly different initial conditions u_j^0 and body forces f_j on a bounded domain in R^d, $d=(2,3)$ subject to no-slip boundary conditions. Let u_j, p_j be solutions of the (NSE):

$$\begin{aligned} &u_{j,t}+u_j\cdot\nabla u_j-\nu\triangle u_j+\nabla p_j=f_j(x,t), \text{ in } \Omega,\ j=1,...,J, \qquad \text{(ENSE)}\\ &\nabla\cdot u_j=0, \text{ and } u_j(x,0)=u_j^0(x), \text{ in } \Omega \text{ and } u_j=0, \text{ on } \partial\Omega. \end{aligned}$$

Define the ensemble average of u by $\langle u\rangle := \frac{1}{J}\sum_{j=1}^{J} u_j$. Taking ensemble of (ENSE) and replacing the trace-free part of the resulting (non-closed) Reynolds stresses by an eddy

viscosity term gives the conventional/RANS turbulence model for $\langle u \rangle$ (see [76], [21], [12] for a detailed derivation)

$$\langle u \rangle_t + \langle u \rangle \cdot \nabla \langle u \rangle - \nabla \cdot ([\nu + \nu_T(l, k')] \nabla \langle u \rangle) + \nabla \langle q \rangle = \langle f \rangle \text{ , in } \Omega, \tag{6.0.1}$$
$$\nabla \cdot \langle u \rangle = 0, \langle u \rangle (x, 0) = \langle u_j^0 \rangle (x) \text{ in } \Omega \text{ and } \langle u \rangle = 0 \text{ on } \partial\Omega.$$

In (6.0.1), the eddy viscosity (EV) term $\nabla \cdot (\nu_T(l, k') \nabla \langle u \rangle)$ replaces the divergence of the Reynolds stresses

$$\text{Reynolds stress: } R(u, u) := \langle u \rangle \langle u \rangle - \langle uu \rangle ,$$
$$-\nabla \cdot R(u, u) \quad \text{replaced by } \; - \nabla \cdot (\nu_T(l, k') \nabla \langle u \rangle) .$$

Since (6.0.1) is a model, its solution is no longer the exact ensemble average. The turbulent viscosity coefficient is given by the Kolmogorov-Prandtl relation

$$\nu_T(l, k') = \sqrt{2} \mu l \sqrt{k'},$$
$$k' = \text{ kinetic energy in fluctuations, and } l \text{ = mixing length.}$$

The unknowns k', l are often modeled by solving additional systems of nonlinear PDEs. On the other hand, if eddy viscosity models are fundamentally sound and if k' can be directly calculated, without modeling, then using an exact value for k' must increase the physical fidelity of (6.0.1). The value of μ herein is taken as a tuning parameter. From the $(3d)$ law of the wall, Pope [82] calculates the value $\mu = 0.55$.

Calculating k' requires solving an ensemble of NSE realizations. New algorithms for ensemble simulation put this within reach (and possibly at lower cost than modeling k'). When k' can be directly calculated, ν_T can be directly calculated giving an ensemble eddy viscosity model. Simply adding an ensemble eddy viscosity term to each realization acts as only a numerical regularization and does not yield a turbulence model for $< u >$. It gives the wrong system for $\langle u \rangle$ (not (6.0.1)). In this Chapter we show that ensemble simulation of (6.0.1) (i.e., its use as a turbulence model) requires new realization equations including

$$u_{j,t} + \langle u \rangle \cdot \nabla u_j - \nabla \cdot ([\nu + \nu_T(l, k')] \nabla u_j) + \nabla p_j = f_j(x, t) \text{ and } \nabla \cdot u_j = 0, \tag{6.0.2}$$

derived in Section 6.4. (6.0.2) contains sufficient regularizations to make its solution plausibly less expensive than a full DNS (Direct Numerical Simulation) for each realization. Further, time discretizations of (6.5.1), (6.5.6) are unconditionally stable. In the methods (6.5.1), (6.5.6) below, each time step requires the solutions of J linear systems with a shared coefficient matrix reducing both storage and work by use of direct methods, projective, [30], or block iterative methods, e.g., [79], [31], [4], [32], [39].

The number of ensemble members J can often be taken moderate. The "bred vectors" algorithm of Toth and Kalnay [89] gives a small set of perturbations of initial conditions that capture maximal ensemble spread. [15] found that 16 realizations suffice to provide reliable statistics and the results change little for more realizations.

Section 6.5 proves that the two numerical methods for (6.0.2) are unconditionally, nonlinearly, long time stable. We prove that the variance of (6.5.1) converges to zero as $t^n \to \infty$. In other words, the solution of (6.5.1) converges to statistical equilibrium as $t^n \to \infty$. This is the first result of this kind we are aware of.

Section 6.3 introduces the definition of variance and its evolution equation. An important consequence (a proof of the Boussinesq assumption) is discussed. Section 6.4 gives the derivation of (6.0.2) and three other models. Section 6.6 gives a few numerical tests for $2d$ forced turbulence. These quantify the difference between the solution of the model herein and the method studied in Chapter 4. The averaged, effective Lyapunov exponent is also calculated to verify that ensemble Leray regularization is effective to squeeze two trajectories together.

6.1 PREVIOUS WORK

The difficulty of accurate prediction of turbulent flows is reflected by the many approaches and multitude of models within each approach. The statistical theory of turbulence (well summarized in [25] and the comprehensive volumes of Monin and Yaglom [77]) seeks to predict ensemble averages of flows at statistical equilibrium through (typically) eddy viscosity models. Often $\nu_T(\cdot)$ is calculated by solving additional nonlinear PDEs such as in the $k-\epsilon$

model [76]. Means can be defined by long time averaging, e.g., [21]. In this case a steady state EV model is often derived. The present approach does not require ad hoc modeling of k' (as k' is calculated directly) or the further assumptions that ensemble averages coincide with time averages and are at steady state. In LES averages are defined by a local spacial filter (related to an underlying mesh). LES models are not addressed herein. The model herein is development of the work in [53], [54], [55]. In contrast, it is the first to address using ensembles for conventional turbulence modeling. For this, (surprisingly) new realization equations (not the NSE) are required and these, when discretized, have better stability properties than the ensemble NSE (studied in [53], [54], [55]). We also prove discrete model convergence to statistical equilibrium, a significant new result.

Incomplete data, quantification of uncertainty and sensitivities and other issues, e.g., [17], [35], [62], [67], [75], [89], require simulation of flow ensembles. This leads to the competition between ensembles vs. high resolution [49].

This approach to ensemble parametrization was begun in [54] where the mixing length $l = |u'|\triangle t$ was investigated. However in [54], EV is a numerical regularization and not a true turbulence model. The ensemble based parametrization (herein) connects the method to ideas and diagnostics from the statistical theory of turbulence, [5], [23], [24], [25].

The readers are referred to [48], [33], for the parallel theory of statistical solution and ensemble average associated with statically equilibrium to [84].

6.2 WHAT IS NOT KNOWN

The entire field of turbulence is beset with difficulties, mathematical gaps and physical mysteries. While we are able to provide some rigorous analysis herein, more is unknown than known. To begin a partial list, existence theory for the model (6.0.2) is an open question. The analysis of variance evolution in Section 6.3 for strong solutions of the NSE is extensible to suitable weak solutions following [64]. Section 6.3 shows that at time average u' has a dissipation effect in $< u >$, i.e., the Boussinesq assumption holds. However, the eddy viscosity hypothesis is simply a convenient engineering simplification known to fail for

some flows. It is believed (e.g., [28] wrote "$\cdots$ very small ensembles may be reasonably assumed to produce adequate estimates of mean quantities $\cdots$") but unproved that only a few realizations suffice to calculate k' well enough to approximate $< u >$. The stability theory of the method is independent of J but efficiency requires a small to moderate J. The statistical theory of turbulence in e.g. [77], is different from the theory fo statistical solutions of the NSE. It is widely believed and supported by both the needs and expects of practice, but also unproved, that many turbulent flows approach statistical equilibrium. Since statistical equilibrium is impossible to assess (without an ensemble of solutions), model developers often appeal to an ergodicity assumption (with many open questions, see [46]) and replace ensemble with time averaging and statistical equilibrium with steady state. It is also believed that some flows do not approach statistical equilibrium, [25]

6.3 VARIANCE EVOLUTION IN THE NAVIER-STOKES EQUATIONS

One goal in a CTM is to achieve a statistically steady solution, i.e., one with variance = 0. Before analyzing model variance, we present the behavior of the Reynolds stresses and the evolution of variance for the Navier-Stokes equations. Consider the $2d$ or $3d$ NSE where the ensemble is generated by a distribution of initial conditions

$$\begin{aligned} &u_{j,t} + u_j \cdot \nabla u_j - \nu \triangle u_j + \nabla p_j = f(x,t), \text{ in } \Omega,\ j = 1, ..., J, \\ &\nabla \cdot u_j = 0, \text{ and } u_j(x,0) = u_j^0(x), \text{ in } \Omega \text{ and } u_j = 0, \text{ on } \partial\Omega. \end{aligned} \tag{6.3.1}$$

We assume that all solutions are strong solutions,.

Definition 4 (Variance)**.** *The variance of u and ∇u are*

$$V(u) := \left\langle ||u_j||^2 \right\rangle - || \left\langle u \right\rangle ||^2 \text{ and } V(\nabla u) := \left\langle ||\nabla u_j||^2 \right\rangle - ||\nabla \left\langle u \right\rangle ||^2.$$

Recall the (standard) result that variance measures fluctuations.

Lemma 4. *We have*

$$V(u) = \left\langle ||u_j'||^2 \right\rangle \geq 0 \text{ and } V(\nabla u) = \left\langle ||\nabla u_j'||^2 \right\rangle \geq 0.$$

Proof. This is a standard calculation. Insert $u_j = \langle u \rangle + u_j'$ and expand each term. □

Averaging the ensemble NSE gives the equation for ensemble averages, $\nabla \cdot \langle u \rangle = 0$ and

$$\langle u \rangle_t + \langle u \rangle \cdot \nabla \langle u \rangle - \nu \triangle \langle u \rangle + \nabla \langle p \rangle - \nabla \cdot R(u,u) = f(x,t),$$
$$\text{where } R(u,u) := \langle u \rangle \langle u \rangle - \langle uu \rangle .$$

Since all solutions are strong solutions we may calculate the kinetic energy in the mean flow by taking the inner product with $\langle u \rangle$. This gives

$$\frac{1}{2}\frac{d}{dt}|| \langle u \rangle ||^2 + \nu ||\nabla \langle u \rangle ||^2 + \int_\Omega R(u,u) : \langle u \rangle \, dx = \int_\Omega f(x,t) \cdot \langle u \rangle \, dx. \tag{6.3.2}$$

From this it is clear that the effect of the fluctuations on the mean flow is contained in $\int R(u,u) : \langle u \rangle \, dx$. When this term is positive, the effect is dissipative and when negative the effect is to increase energy in the mean flow.

Theorem 14 (Variance Evolution)**.** *The variance of strong solutions of the NSE evolves according to*

$$\frac{1}{2}V(u(T)) + \int_0^T \nu V(\nabla u(t)) dt = \frac{1}{2}V(u(0)) + \int_0^T \left(\int_\Omega R(u,u) : \langle u \rangle \, dx \right) dt. \tag{6.3.3}$$

Proof. The energy equality for strong solutions of each realization of the NSE is

$$\frac{1}{2}||u_j(T)||^2 + \int_0^T \nu ||\nabla u_j||^2 dt = \frac{1}{2}||u_j(0)||^2 + \int_0^T (f(x,t), u_j) \, dt.$$

Taking the ensemble average of this gives

$$\frac{1}{2}\left\langle ||u_j(T)||^2 \right\rangle + \int_0^T \nu \left\langle ||\nabla u_j||^2 \right\rangle dt = \frac{1}{2}\left\langle ||u_j(0)||^2 \right\rangle + \int_0^T (f(x,t), \langle u_j \rangle) \, dt.$$

Subtract from this the time integral of the equation (6.3.2). This yields the claimed equation for evolution of variance. □

One consequence of the variance evolution equation is a simple proof of the Boussinesq assumption that turbulent fluctuations (defined by ensemble averaging) are dissipative on the mean flow in a mean sense. See [64] for connections to phenomenology. When the means (and thus fluctuations) are defined by long time averaging, a proof of the Boussinesq assumption has been given by Chacon-Rebollo and Lewandowski [21].

Corollary 3 (Boussinesq assumption in both $2d$ and $3d$)**.** *Assume* $f(x,t) \in L^\infty(0,\infty; L^2(\Omega))$. *For strong solutions of the NSE, we have*

$$\liminf_{T\to\infty} \frac{1}{T}\int_0^T \left(\int_\Omega R(u,u) : \langle u\rangle \, dx\right) dt = \liminf_{T\to\infty} \frac{1}{T}\int_0^T \nu \left\langle ||\nabla u_j'||^2 \right\rangle \geq 0.$$

Proof. For the proof we note that a standard estimate shows that each solution is uniformly bounded $u_j \in L^\infty(0,\infty; L^2(\Omega))$. Thus, $V(u) \in L^\infty(0,\infty)$. Dividing (6.3.3) by T we have

$$\frac{1}{2}\frac{1}{T}V(u(T)) + \frac{1}{T}\int_0^T \nu V(\nabla u(t))dt = \frac{1}{2}\frac{1}{T}V(u(0)) + \frac{1}{T}\int_0^T \left(\int_\Omega R(u,u) : \langle u\rangle \, dx\right) dt.$$

As $T \to \infty$ this is

$$\mathcal{O}\left(\frac{1}{T}\right) + \frac{1}{T}\int_0^T \nu \left\langle ||\nabla u_j'||^2 \right\rangle dt = \mathcal{O}\left(\frac{1}{T}\right) + \frac{1}{T}\int_0^T \left(\int_\Omega R(u,u) : \langle u\rangle \, dx\right) dt.$$

The claimed result now follows. □

This shows that on (time) average, the action of the Reynolds stresses / fluctuations in the NSE in both $2d$ and $3d$ (in bounded domains) is

- To dissipate energy in the mean flow $\langle u\rangle$.
- To act as an energy source to the variance evolution equation (6.3.3) and thus increase variance.

From this analysis, we also see that in a conventional turbulence model the fluctuations should damp both the mean flow and its variance evolution (to approach statistical equilibrium). (In contrast, in a large eddy simulation model, not considered herein, it should on average damp the mean flow but act as a diminished energy source to the model variance equation.)

Remark 7. *There are still important open questions concerning the generality of the Boussinesq assumption. In case where means are defined by time averages (see [21]), it is an open question when* $f = f(x,t)$ *and there are questions about whether some version of the result could hold independent of choice of subsequences. When averages are defined by ensemble averaging, [64], the above proof holds when* $f = f(x,t)$ *but not when* $f = f_j(x,t)$. *Extending the above results to weak solutions is also an open problem.*

6.4 DERIVATION OF THE REALIZATION EQUATION

If a direct numerical simulation of the NSE were possible, (ENSE) could be solved then averaged to obtain k' for (1.1). Naturally, this is infeasible in many cases. We thus seek stabilized realization equations with the correct ensemble average (6.0.1) . Define the ensemble mean $\langle u \rangle$, fluctuation u'_j, its magnitude $|u'|$ and the induced kinetic energy density k' by

$$\langle u \rangle := \frac{1}{J} \sum_{j=1}^{J} u_j, \quad u'_j := u_j - \langle u \rangle ,$$

$$|u'|^2 := \sum_{j=1}^{J} |u'_j|^2 \text{ and } k'(x,t) = \frac{1}{2} |u'|^2(x,t).$$

There are a number of ways to choose the mixing length l including the common choice $l = \triangle x$, the mesh width. In [54], an alternative mixing length

$$l = \textit{ distance a fluctuating eddy travels in one time step} = |u'| \triangle t,$$

yielded better flow predictions, better stability and $l(x) \to 0$ correctly as $x \to$ walls. Thus, take

$$l = |u'| \triangle t.$$

Due to the pioneering work of Reynolds, taking the ensemble average of (ENSE) gives

$$\langle u \rangle_t + \langle u \rangle \cdot \nabla \langle u \rangle - \nu \triangle \langle u \rangle + \nabla \cdot R(u,u) + \nabla \langle p \rangle = \langle f \rangle . \tag{6.4.1}$$

To get a closed system, the EV models result from *replacing the Reynolds stress term by the eddy viscosity term.*

Thus, we solve *a feasible variation on (ENSE) which, upon ensemble averaging, yields the correct EV model (1.1) above.* Adding, a yet to be determined, $\nabla \cdot Q_j$ to (ENSE) gives

$$u_{j,t} + u_j \cdot \nabla u_j - \nu \triangle u_j + \nabla \cdot Q_j + \nabla p_j = f_j(x,t). \tag{6.4.2}$$

Taking the ensemble average of the perturbed equation and rearranging gives

$$\langle u \rangle_t + \langle u \rangle \cdot \nabla \langle u \rangle - \nu \triangle \langle u \rangle + \nabla \cdot \langle Q \rangle - \nabla \cdot R(u,u) + \nabla \langle q \rangle = \langle f(x,t) \rangle . \tag{6.4.3}$$

Comparing (6.4.3) and (1.1), we must have (model terms incorporated in the pressure)

$$\begin{aligned} \langle Q \rangle &= \langle u \rangle \langle u \rangle - \langle uu \rangle - \nu_T(l,k')\nabla \langle u \rangle \text{ , or} \\ Q_j &= T - u_j u_j - \nu_T(l,k')\nabla u_j \text{ where } < T >= \langle u \rangle \langle u \rangle . \end{aligned}$$

The three natural choices for T (all worthy of study) that satisfy $< T > = \langle u \rangle \langle u \rangle$ are T=$\langle u \rangle \langle u \rangle$, $u_j \langle u \rangle$ and $\langle u \rangle u_j$. These yield

$$\begin{aligned} Q_j &= \langle u \rangle \langle u \rangle - u_j u_j - \nu_T(l,k')\nabla u_j, \\ Q_j &= u_j \langle u \rangle - u_j u_j - \nu_T(l,k')\nabla u_j, \text{ and} \\ Q_j &= \langle u \rangle u_j - u_j u_j - \nu_T(l,k')\nabla u_j \ . \end{aligned}$$

Combinations of these three possibilities also satisfy $< T > =\langle u \rangle \langle u \rangle$. We select the third, Leray inspired, [65], [66], for testing the realization equation

$$u_{j,t} + \langle u \rangle \cdot \nabla u_j - \nabla \cdot ([\nu + \nu_T(l,k')]\nabla u_j) + \nabla p_j = f_j(x,t). \tag{6.4.4}$$

The motivation for this selection is that we may also interpret (6.4.4) as an ensemble-Leray regularization with an eddy viscosity term. Experience with both Leray regularizations (proven robust in computations when the average is smoothing, e.g., [36]) and eddy viscosity models suggests that this realization equation is computationally feasible. The analysis in Section 4 supports this conclusion.

Remark 8. *Leray type of regularization arises by modifying the nonlinear term* $\langle u \rangle \cdot \nabla u_j$ *instead of* $u_j \cdot \nabla u_j$ *. Without EV term, Leray proposed a regularization of the NSE with spatial average whose limits were weak solutions of the NSE. Because of low accuracy of Leray's model, to increase accuracy large eddy simulation based models have been proposed (see,e.g., [43],[22],[44],[69]).*

Remark 9. *Adding eddy viscosity to all equations, studied in [54], leads to the realization equation*

$$u_{j,t} + u_j \cdot \nabla u_j - \nabla \cdot ([\nu + \nu_T(l, k')]\nabla u_j) + \nabla p_j = f_j(x, t). \tag{6.4.5}$$

Taking the ensemble average of the (6.4.5) gives

$$\begin{aligned} &\langle u \rangle_t + \langle u \rangle \cdot \nabla \langle u \rangle - \nu \triangle \langle u \rangle + \nabla \langle q \rangle \\ &+\nabla \cdot R(u, u) - \nabla \cdot (\nu_T(l, k') \nabla \langle u \rangle) = \langle f(x, t) \rangle , \end{aligned}$$

containing both the Reynolds stresses and the EV term. Thus, in (6.4.5), EV is a numerical regularization and not a closure model since it does not replace the Reynolds stresses.

Analysis. The realization equation (6.4.4) contains two new effects: the eddy viscosity term and the advection with correlated advecting velocity (i.e., replacing $u_j \cdot \nabla u_j$ by $\langle u \rangle \cdot \nabla u_j$). Before studying their combination we analyze the effect of the latter alone.

Therefore let u_i, u_j be two solutions of

$$u_t + \langle u \rangle \cdot \nabla u - \nu \triangle u + \nabla p = f, \quad \nabla \cdot u = 0. \tag{6.4.6}$$

subject to the boundary and initial conditions of (ENSE). We prove that the above ensemble Leray regularization suffices to squeeze trajectories together and accelerate convergence to statistical equilibrium.

Proposition 1. *Let u_i, u_j be weak solutions to (6.4.6). If $f_i = f_j$ then*

$$\|u_i(t) - u_j(t)\|^2 \leq e^{-\nu t} \|u_i(0) - u_j(0)\|^2.$$

If $\|f_i - f_j\|^2_{-1}(t) \to 0$ as $t \to \infty$ then $\|u_i - u_j\| \to 0$ as $t \to \infty$.

Proof. $\phi = u_i - u_j$ satisfies $\phi_t + \langle u \rangle \cdot \nabla \phi - \nu \triangle \phi + q = f_i - f_j$, $q = p_i - p_j$. Taking the L^2 inner product with ϕ yields

$$\frac{d}{dt}\frac{1}{2}\|\phi\|^2 + \nu\|\nabla\phi\|^2 \leq (f_i - f_j, \phi) \leq \frac{\nu}{2}\|\nabla\phi\|^2 + \frac{1}{2\nu}\|f_i - f_j\|_{-1}^2.$$

By the Poincaré-Friedrichs inequality and using an integrating factor we obtain:

$$\|\phi(t)\|^2 \leq e^{-\nu t}\|\phi(0)\|^2 + \nu^{-1}\int_0^t e^{-\nu(t-s)}\|f_i - f_j\|_{-1}^2(s)ds.$$

If $f_i - f_j \equiv 0$, the first claim follows immediately. For the second, let $\epsilon > 0$ be given. For $\delta > 0$ let τ be large enough that $\|f_i(t) - f_j(t)\|_{-1}^2 < \delta$ for $t \geq \tau$. Then

$$\|\phi(t)\|^2 \leq e^{-\nu t}\|\phi(0)\|^2 + \nu^{-1}\int_0^\tau e^{\nu(s-t)}\|f_i - f_j\|_{-1}^2 ds + \nu^{-1}\int_\tau^t e^{\nu(s-t)}\delta ds.$$

The first term is $< \epsilon/3$ for t large enough as is the second term. The third term is bounded by $\delta\frac{2}{\nu^2}$, which is also $< \epsilon/3$ for δ small enough. Thus $\|\phi(t)\|^2 \to 0$, as claimed. □

6.5 METHODS AND STABILITY

In this section, we study first and second order method for the realization equation (6.0.2) and prove their unconditional, long-time, nonlinear stability. The proof of stability is independent of any special techniques for spacial discretization. Specifically, the Galerkin method, finite dimensional conforming velocity and pressure subspaces are used. The spacial discretization will be suppressed and the methods and analysis given for the continuous space, discrete time context. Extension to discrete space adds only notational complexity.

We use standard notation for Lebesgue and Sobolev spaces and their norms. Let $\|\cdot\|$ and $(\cdot,\cdot)$ be the $L^2(\Omega)$ norm and the inner product, respectively. The $L^p(\Omega)$ norm and the Sobolev $W_p^k(\Omega)$ norm are represented by $\|\cdot\|_{L^p}$ and $\|\cdot\|_{W_p^k}$. $H^k(\Omega)$ is the Sobolev space $W_2^k(\Omega)$, with norm $\|\cdot\|_k$.

6.5.1 The First Order Method

Let $t^n := n\Delta t$, $n = 0, 1, 2, ..., N$, and $T := N\Delta t$. Denote $u_j^n = u_j(t^n)$, $j = 1, ..., J$. The first order time accurate method is: *Given* u_j^n, *find* u_j^{n+1}, p_j^{n+1} *satisfying*

$$\begin{gathered}\frac{u_j^{n+1} - u_j^n}{\Delta t} + \langle u \rangle^n \cdot \nabla u_j^{n+1} + \nabla p_j^{n+1} \\ -\nu\Delta u_j^{n+1} - \nabla \cdot (2\nu_T(l^n, k'^n)\nabla^s u_j^{n+1}) = f_j^{n+1} \text{ in } \Omega, \\ \text{where } \nu_T(l^n, k'^n) = \mu|u'^n|l^n \text{ and } l^n = |u'^n|\Delta t, \\ \nabla \cdot u_j^{n+1} = 0, \text{ and } u_j^0(x) = u_j^0 \text{ in } \Omega, \ u_j^{n+1} = 0, \text{ on } \partial\Omega\end{gathered} \tag{6.5.1}$$

After spacial discretization, every time step of (6.5.1) requires the solution of a block linear system like (4.0.1) with shared coefficient matrix.

We prove unconditional stability of (6.5.1).

Theorem 15 (Stability of the first order method)**.** *The first order method* (6.5.1) *is unconditionally stable*

$$\begin{aligned}||u_j^N||^2 + \sum_{n=0}^{N-1} \left(||u_j^{n+1} - u_j^n||^2 + \triangle t \int_\Omega [\nu + \nu_T(l^n, k'^n)]|\nabla u_j^{n+1}|^2 dx \right) \\ \leq ||u_j^0||^2 + \frac{\triangle t}{\nu} \sum_{n=0}^{N-1} \|f_j^{n+1}\|_{-1}^2.\end{aligned} \tag{6.5.2}$$

The ensemble average is also similarly stable:

$$\begin{aligned}|| \langle u \rangle^N ||^2 + \sum_{n=0}^{N-1} \left(|| \langle u \rangle^{n+1} - \langle u \rangle^n ||^2 + \triangle t \int_\Omega [\nu + \nu_T(l^n, k'^n)]|\nabla \langle u \rangle^{n+1}|^2 dx \right) \\ \leq || \langle u \rangle^0 ||^2 + \frac{\triangle t}{\nu} \sum_{n=0}^{N-1} \| \langle f \rangle^{n+1} \|_{-1}^2.\end{aligned} \tag{6.5.3}$$

Proof. We take the L^2 inner product of the first equation of (6.5.1) with u_j^{n+1}, the second equation with p_j^{n+1}, add and multiply by $2\triangle t$. Using skew symmetry $\int_\Omega \langle u\rangle^n \cdot \nabla u_j^{n+1}.u_j^{n+1}\, dx = 0$, the polarization identity for (u_j^n, u_j^{n+1}) in the time difference term and integrating by parts the two viscosity terms gives

$$||u_j^{n+1}||^2 - ||u_j^n||^2 + ||u_j^{n+1} - u_j^n||^2 + 2\triangle t \int_\Omega [\nu + \nu_T(l^n, k'^n)]|\nabla u_j^{n+1}|^2 dx \tag{6.5.4}$$
$$= 2\triangle t \left(f_j^{n+1}, u_j^{n+1}\right).$$

Applying Young's inequality to the right hand side

$$||u_j^{n+1}||^2 - ||u_j^n||^2 + ||u_j^{n+1} - u_j^n||^2$$
$$+\triangle t \int_\Omega [\nu + 2\nu_T(l^n, k'^n)]|\nabla u_j^{n+1}|^2 dx \leq \frac{\triangle t}{\nu}\|f_j^{n+1}\|_{-1}^2.$$

Long-time stability of the realization thus follows. For (6.5.3), ensemble average (6.5.1) (giving (6.0.1)), then, repeat the proof. □

The two energy inequalities (6.5.2), (6.5.3) are key steps for establishing convergence to statistical equilibrium.

Proposition 2 (Variance Evolution of the First Order Method)**.** *Suppose in* (6.5.1) $f_j \equiv f$. *The variance of solutions to* (6.5.1) *evolves according to*

$$V(u^N) + \sum_{n=0}^{N-1} \Big\{ V(u^{n+1} - u^n) \tag{6.5.5}$$
$$+\Delta t \int_\Omega [\nu + \nu_T(l^n, k'^n)] \left\langle |\nabla u_j'^{n+1}|^2 \right\rangle dx \Big\} = V(u^0).$$

Proof. Take the ensemble average of (6.5.4) and of the analogous step in the energy estimate for $\| < u >^N \|$ then subtract to obtain variance evolution. Note that since $f_j \equiv f$, the RHS cancel:

$$\left\langle 2\Delta t(f^{n+1}, u_j^{n+1}) \right\rangle - 2\Delta t(f^{n+1}, \left\langle u_j^{n+1} \right\rangle) \equiv 0.$$

We then have

$$V(u^{n+1}) - V(u^n) + V(u^{n+1} - u^n)$$
$$+\Delta t \int_\Omega [\nu + \nu_T(l^n, k'^n)] \left\langle |\nabla u_j'^{n+1}|^2 \right\rangle dx = 0.$$

Summing from $n = 0$ to $N - 1$ gives the result. □

This proposition has several important consequences. In particular, we conclude that when $f_j \equiv f \in L^\infty(0,\infty;L^2(\Omega))$, $V(u^N) \to 0$ as $t^N \to \infty$.

Proposition 3. *In (6.5.1) let $f_j \equiv f \in L^\infty(0,\infty;L^2(\Omega))$. Then, as $t^N \to \infty$*

$$V(u^{N+1}-u^N) \to 0,$$
$$V(\nabla u^N) \to 0,$$
$$\int_\Omega \nu_T(l^N,k'^N)\left\langle |\nabla u_j'^{N+1}|^2\right\rangle dx \to 0.$$

Proof. Each term in (6.5.5) is nonnegative and the RHS is independent of N. Letting $N \to \infty$ we conclude that the infinite series (with nonnegative terms) below converges

$$\sum_{n=0}^{\infty}\left\{V(u^{n+1}-u^n)+\Delta t\nu V(\nabla u^{n+1})+\Delta t\int_\Omega \nu_T(l^n,k'^n)\left\langle|\nabla u_j'^{n+1}|^2\right\rangle dx\right\}<\infty.$$

Thus, the N^{th} term must $\to 0$ as $N \to \infty$ and the proposition follows. □

Remark 10. *For the proofs to hold in the discrete space case requires the two viscosity terms to yield symmetric positive definite matrices (i.e., be dissipative under discretization) and the discrete nonlinear term to be skew symmetric (i.e., conservative) or nonnegative (i.e., add numerical dissipation via some upwinding). The tests in Section 6.6 used the FEM with explicitly skew symmetrized (the exactly conservative) nonlinearity, satisfying both conditions.*

6.5.2 The Second Order Method

The second order time accurate method for (1.2) is a combination of $BDF2$ and an interpretation of $AB2$ for the nonlinear term. The second order accurate method is as follows: *Given u_j^{n-1}, u_j^n, find u_j^{n+1}, p_j^{n+1} satisfying*

$$\frac{3u_j^{n+1}-4u_j^n+u_j^{n-1}}{2\Delta t}+\left(2\langle u\rangle^n-\langle u\rangle^{n-1}\right)\cdot\nabla u_j^{n+1}+\nabla p_j^{n+1} \tag{6.5.6}$$
$$-\nu\triangle u_j^{n+1}-\nabla\cdot\left(\tilde\nu_T(l^n,k'^n)\nabla^s u_j^{n+1}\right)=f_j^{n+1}\text{ in }\Omega,$$
$$\text{where }\tilde\nu_T(l^n,k'^n)=\mu|2u'^n-u'^{n-1}|l^n \text{ and } l^n=|2u'^n-u'^{n-1}|\Delta t,$$
$$\nabla\cdot u_j^{n+1}=0,\text{ and } u_j^0(x)=u_j^0 \text{ in }\Omega, u_j^{n+1}=0,\text{ on }\partial\Omega.$$

This is a 3 level/2 step method. Thus an approximation to u_j^1, p_j^1 must be computed by some other method, such as the first order method (6.5.1) above. Like the first order method, it is unconditionally stable.

Theorem 16 (Stability of the second order method)**.** *The second order method (6.5.6) is unconditionally, long-time, nonlinear stable: For any $N > 1$,*

$$\begin{aligned}
&\frac{1}{4}\|u_j^N\|^2 + \frac{1}{4}\|2u_j^N - u_j^{N-1}\|^2 + \sum_{n=1}^{N-1}\frac{1}{4}\|u_j^{n+1} - 2u_j^n + u_j^{n-1}\|^2 \\
&+\Delta t\sum_{n=1}^{N-1}\int_\Omega \tilde{\nu}_T(l^n, k'^n)|\nabla u_j^{n+1}|^2 dx + \frac{\Delta t}{2}\sum_{n=1}^{N-1}\nu\|\nabla u_j^{n+1}\|^2 \\
&\leq \sum_{n=1}^{N-1}\frac{\Delta t}{2\nu}\|f_j^{n+1}\|_{-1}^2 + \frac{1}{4}\|u_j^1\|^2 + \frac{1}{4}\|2u_j^1 - u_j^0\|^2 \ .
\end{aligned}$$

Proof. Take the L^2 inner product of (6.5.6) with u_j^{n+1}, p_j^{n+1} and add. Using skew-symmetry of the nonlinear term, integrating by parts the two viscous terms, canceling the pressure and incompressibility terms and multiplying through by Δt yields:

$$\begin{aligned}
&\frac{1}{4}\left(\|u_j^{n+1}\|^2 + \|2u_j^{n+1} - u_j^n\|^2\right) - \frac{1}{4}\left(\|u_j^n\|^2 + \|2u_j^n - u_j^{n-1}\|^2\right) \\
&+\frac{1}{4}\|u_j^{n+1} - 2u_j^n + u_j^{n-1}\|^2 + \int_\Omega \Delta t\left(\nu + \tilde{\nu}_T(l^n, k'^n)\right)|\nabla u_j^{n+1}|^2 dx \\
&= \Delta t\left(f_j^{n+1}, u_j^{n+1}\right) \ .
\end{aligned} \tag{6.5.7}$$

Applying Young's inequality to the right hand side gives

$$\begin{aligned}
&\frac{1}{4}\left(\|u_j^{n+1}\|^2 + \|2u_j^{n+1} - u_j^n\|^2\right) - \frac{1}{4}\left(\|u_j^n\|^2 + \|2u_j^n - u_j^{n-1}\|^2\right) \\
&+\frac{1}{4}\|u_j^{n+1} - 2u_j^n + u_j^{n-1}\|^2 + \int_\Omega \Delta t\left(\nu + \tilde{\nu}_T(l^n, k'^n)\right)|\nabla u_j^{n+1}|^2 dx \\
&\leq \frac{\nu\Delta t}{2}\|\nabla u_j^{n+1}\|^2 + \frac{\Delta t}{2\nu}\|f_j^{n+1}\|_{-1}^2 \ .
\end{aligned}$$

Combining like terms yields

$$\begin{aligned}
&\frac{1}{4}\left(\|u_j^{n+1}\|^2 + \|2u_j^{n+1} - u_j^n\|^2\right) - \frac{1}{4}\left(\|u_j^n\|^2 + \|2u_j^n - u_j^{n-1}\|^2\right) \\
&+\frac{1}{4}\|u_j^{n+1} - 2u_j^n + u_j^{n-1}\|^2 + \int_\Omega \Delta t\left(\frac{\nu}{2} + \tilde{\nu}_T(l^n, k'^n)\right)|\nabla u_j^{n+1}|^2 dx \leq \frac{\Delta t}{2\nu}\|f_j^{n+1}\|_{-1}^2 \ .
\end{aligned} \tag{6.5.8}$$

Summing up (6.5.8) from $n = 1$ to $N - 1$ completes the proof. □

The second order method also produces approximations that approach statistical equilibrium (by Variance $\to 0$) in the same sense as for the first order method.

Proposition 4 (Variance Evolution of Second Order Method)**.** *Suppose in* (6.5.6) $f_j \equiv f$. *The variance of solutions to* (6.5.6) *satisfies*

$$V(u^N) + V(2u^N - u^{N-1}) + \sum_{n=1}^{N-1} \Big\{ V(u^{n+1} - 2u^n + u^{n-1}) \tag{6.5.9}$$
$$+4\Delta t \int_\Omega (\nu + \tilde{\nu}_T(l^n, k'^n)) \left\langle |\nabla u_j'^{n+1}|^2 \right\rangle dx \Big\} = V(u^1) + V(2u^1 - u^0).$$

Proof. The ensemble average of (6.5.7) and of the analogous step in the energy estimate for $\| \langle u \rangle^N \|$ yields

$$V(u^{n+1}) + V(2u^{n+1} - u^n) - V(u^n) - V(2u^n - u^{n-1})$$
$$+V(u^{n+1} - 2u^n - u^{n-1}) + 4\Delta t \int_\Omega (\nu + \tilde{\nu}_T(l^n, k'^n)) \left\langle |\nabla u_j'^{n+1}|^2 \right\rangle dx = 0.$$

Summing from $n = 1$ to $N - 1$ gives the result. □

Proposition 5. *In* (6.5.6) *let* $f_j \equiv f \in L^\infty(0, \infty; L^2(\Omega))$. *Then, as* $t^N \to \infty$

$$V(u^{N+1} - 2u^N + u^{N-1}) \to 0,$$
$$V(\nabla u^N) \to 0,$$
$$\int_\Omega \tilde{\nu}_T^n \left\langle |\nabla u_j'^{N+1}|^2 \right\rangle dx \to 0.$$

Proof. Note that each term in (6.5.9) is nonnegative and the RHS is independent of N. Letting $N \to \infty$ we conclude that the infinite series (with nonnegative terms) below converges

$$\sum_{n=1}^{\infty} \Big\{ V(u^{n+1} - 2u^n + u^{n-1}) + \Delta t \nu V(\nabla u^{n+1}) + \Delta t \int_\Omega \tilde{\nu}_T(l^n, k'^n) \left\langle |\nabla u_j'^n|^2 \right\rangle dx \Big\} < \infty.$$

Thus, the N^{th} term must $\to 0$ as $N \to \infty$ and the proposition follows. □

6.6 NUMERICAL EXPERIMENTS

6.6.1 Comparing two realization equations

In this section, we investigate the difference between retaining and not retaining the fluctuating term $u_j' \cdot \nabla u_j$ (equivalently, retaining in the ensemble averaged equation both the Reynolds stresses and the eddy viscosity or just the eddy viscosity). We compare ensemble eddy viscosity as a numerical regularization (the approach studied in [JL14b]) and as used herein to generate a conventional turbulence model. Specifically, we discretize in space by a usual velocity-pressure FEM abd solve the two problems:

$$\frac{u_j^{n+1}-u_j^n}{\Delta t} + \langle u\rangle^n \cdot \nabla u_j^{n+1} + \left\{\mathbf{u_j'^n \cdot \nabla u_j^n}\right\} + \nabla p_j^{n+1} \qquad \text{(Refularization)}$$
$$-\nu\Delta u_j^{n+1} - \nabla\cdot(2\nu_T(l^n,k'^n)\nabla^s u_j^{n+1}) = f^{n+1}$$

$$\frac{u_j^{n+1}-u_j^n}{\Delta t} + \langle u\rangle^n \cdot \nabla u_j^{n+1} + \nabla p_j^{n+1} \qquad \text{(CTM)}$$
$$-\nu\Delta u_j^{n+1} - \nabla\cdot(2\nu_T(l^n,k'^n)\nabla^s u_j^{n+1}) = f^{n+1}$$

The difference in the models is the term $u' \cdot \nabla u$ (bold and in brackets) in the first and absent in the second. We compare the predictions especially with respect to convergence to statistical equilibrium. While these first tests are $2d$[1], they reveal differences between ensemble numerical regularizations (retaining $u_j' \cdot \nabla u_j$) and turbulence models (not retaining $u_j' \cdot \nabla u_j$).

Test Problem: flow between offset circles. Pick

$$\Omega = \{(x,y) : x^2+y^2 \le r_1^2 \text{ and } (x-c_1)^2+(y-c_2)^2 \ge r_2^2\},$$
$$r_1 = 1, r_2 = 0.1, c = (c_1,c_2) = (\frac{1}{2},0),$$
$$f(x,y,t) = (-4y(1-x^2-y^2), 4x(1-x^2-y^2))^T,$$

[1]Bounded domains are not covered by the Batchelor-Leith-Kraichnan inverse cascade. On bounded 2d domains under no-slip boundary conditions fluctuations have a dissipative effect on the mean flow (consistent with an eddy viscosity model), Section 2 above, [26], [64], see also [14]. Thus, this test is sensible.

with no-slip boundary conditions on both circles. The flow, driven by a counterclockwise force (with $f \equiv 0$ at the outer circle), rotates about $(0,0)$ and interacts with the immersed circle. This induces a von Kármán vortex street which interacts with the near wall streaks common in turbulent flow and a central ("polar") vortex. All three effects interact in a pulsating fashion. We discretize in space using the usual finite element method with Taylor-Hood elements, [38]. These choices satisfy the requirements for the stability theorems to apply. The tests were performed using FreeFEM++, [50]. The mesh has $n = 40$ mesh points around the outer circle and $m = 10$ mesh points around the immersed circle, and extended to Ω as a Delaunay mesh.

Generation of the initial conditions. Initial conditions $u_j^0, j = 1, 2$, and u_0^0, are generated by solving the steady Stokes problem with body forces

$$f(x, y, 0) + \epsilon(sin(3\pi x)sin(3\pi y), cos(3\pi x)cos(3\pi y))^T,$$

taking $\epsilon = 10^{-3}, -10^{-3}$ and 0. These initial conditions give u_1, u_2, $u_{ave} = (u_1 + u_2)/2$ and u_0 (initial condition u_0^0 -'no perturbation'). Thus we perturb the small scales rather than generate bred vectors herein.

Comparing realization equations (6.4.4) **vs** (6.4.5)

We compare the stability of the two choices and test the relative size (residual) of the extra term $u_j' \cdot \nabla u_j$. For stability, we choose a large time step and compute the kinetic energy vs time and enstrophy vs time t over $0 \leq t \leq 10$

$$\text{Energy} = \frac{1}{2}\|u\|^2, \quad \text{Enstrophy} = \frac{1}{2}\nu\|\nabla \times u\|^2.$$

The plots are given in Figures 39 and 40 below.

Comparing the cases in Figure 39 (energy) and 40 (enstrophy) we see that EV as a turbulence model (the lower figure) produces fewer transient effects than adding EV as a numerical regularization (the top figure). This is consistent with considering the methods studied as conventional turbulence models.

The realization equation (6.0.2) (with nonlinear term $\langle u \rangle \cdot \nabla u_j$) is consistent with the desired statistical turbulence model (6.0.1). However, as $u_j \cdot \nabla u_j =< u > \cdot \nabla u_j + u_j' \cdot \nabla u_j$, it is not a consistent approximation to the NSE as it omits $u_j' \cdot \nabla u_j$. We test the magnitude of

$u_j' \cdot \nabla u_j$. Next, the test investigates the relative size of the extra term $u_j' \cdot \nabla u_j$. We measure the relative significance of both terms by computing over $0 \leq t \leq 10$

$$Q_1 = \left\langle || \langle u \rangle^n \cdot \nabla u_j^{n+1} ||^2 \right\rangle, \quad Q_2 = \left\langle ||(u_j^n - \langle u \rangle^n) \cdot \nabla u_j^n ||^2 \right\rangle,$$
$$Q_3 = \frac{\left\langle ||(u_j^n - \langle u \rangle^n) \cdot \nabla u_j^n ||^2 \right\rangle}{\left\langle || \langle u \rangle^n \cdot \nabla u_j^{n+1} ||^2 \right\rangle}.$$

Figure 41 plots the three vs time.

We compare (Regularization) and (CTM) two ways: testing the differences between their predicted velocities and the relative magnitude of the term $\{u' \cdot \nabla u\}$ present in the first and not the second. Figure 41 shows that this relative difference (between (6.4.4) and (6.4.5)) is smaller than 10^{-10}. Nevertheless, the impact of the extra term on the kinetic energy is $\mathcal{O}(1)$, Figure 39. Excluding $u' \cdot \nabla u$, i.e. solving the (CTM), the energy and enstrophy closely track the unperturbed flow (bottom Figure 39, 40).

We concluded from this first test that the term is small in magnitude but non-negligible as its effects on the transient evolution of the flow.

6.6.2 Interrogation of Convergence to Statistical Equilibrium

One goal of a conventional turbulence model is for its time evolution to very quickly converge to the statistical equilibrium of the flow. This is desired for many reasons including extensive experience that averages at statistical equilibrium can be resolved with many fewer degrees of freedom than the fluctuating velocity. We test this convergence by computing the averaged, effective Lyapunov exponents (introduced by [6]) of the first order method. Negative exponents imply exponential convergence to equilibrium.

Following [6], we define the **relative energy fluctuation** $r(t)$ by

$$r(t) := \frac{\|u_1 - u_2\|^2}{\|u_1\| \|u_2\|}(t),$$

and the **averaged, effective Lyapunov exponent** $\gamma_T(t)$ over $0 \leq t \leq T$ by

$$\gamma_T(t) := \frac{1}{2T} log \left(\frac{r(t+T)}{r(t)} \right).$$

Here T is chosen to be the simulation time.

From figure 42 we see that around $t = 2$ the Lyapunov exponent became negative (and stay negative thereafter), indicating squeezing of the trajectories, as predicted by the theory.

If the solution converges to steady state (physical equilibrium) then as $\frac{d}{dt}\langle u\rangle = 0$ it must be a solution of the steady NSE. At $t^{n+1} = 10$, we compute $\| \langle u\rangle^{n+1} - \langle u\rangle^{n} \| = 0.24256$. This shows the model is not at steady state. On the other hand, $V(\nabla u^{n+1}) = 2.72848^{-12}$ at $t^{n+1} = 10$, which is a clear evidence that the model has reached its statistical equilibrium. This is consistent with the fact the statistically averaged mean flow can be unsteady, clearly illustrated in Figure 5.12, page 102 in [25].

In order to visualize the evolution of the flow we plot vorticity contours of $\langle u\rangle^{n}$ in Figure 43. To resolve the vortices around the inner circle, we compute on a finer mesh (still relatively coarse) with 150 mesh points on the outer circle and with 75 mesh points on the inner circle. Two apparent oppositely-rotating vortices shedding from the inner circle are observed at very early time (clear at $t = 1$, Figure 43). An animation of the flow also shows many interesting features. The two oppositely-rotating vortices are shed and detach from the inner circle periodically. On the other hand, the near wall streaks appear and disappear in a pulsating fashion and also a central ("polar") vortex appear and disappear. The eddies are shed by the inner circle sometimes break up into streaks and sometimes are captured by a large central vortex.

With $u_j' \cdot \nabla u_j$

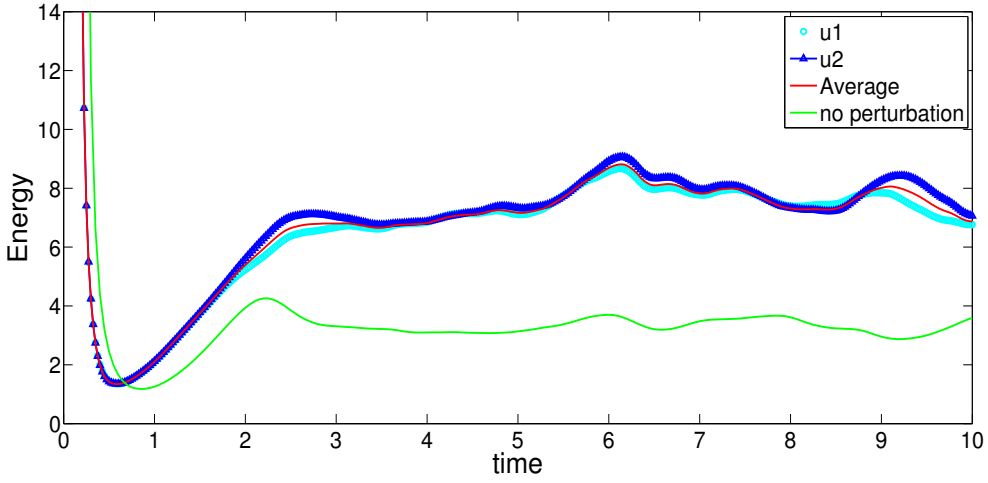

Without $u_j' \cdot \nabla u_j$

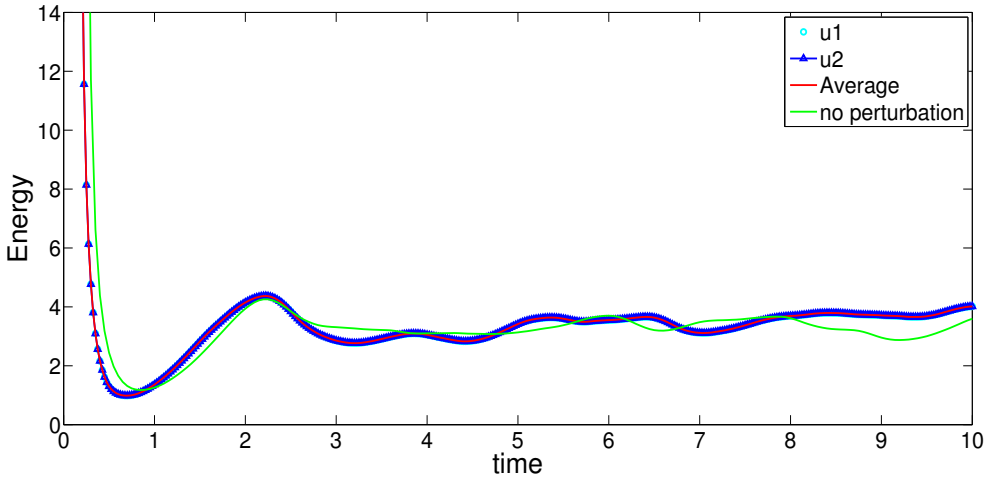

Figure 39: Energy, $\nu = 1/800$, $\Delta t = 0.025$.

With $u_j' \cdot \nabla u_j$

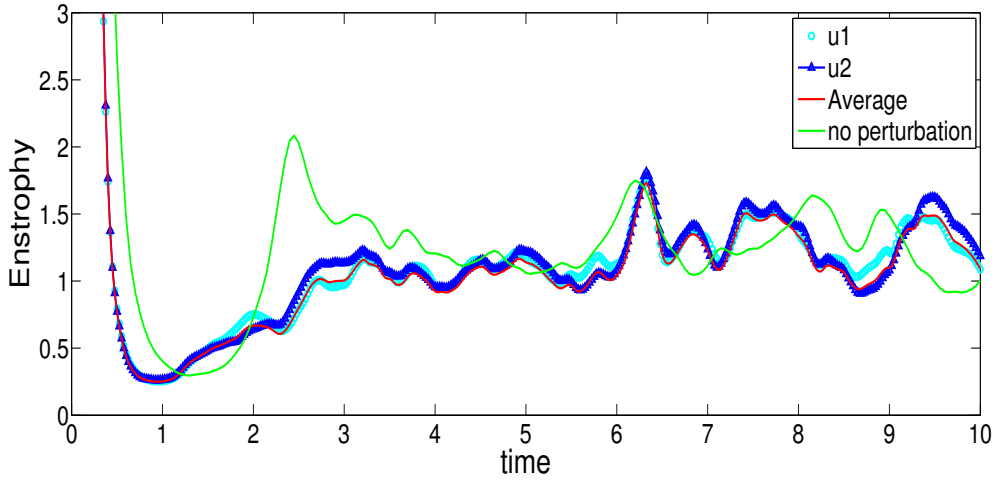

Without $u_j' \cdot \nabla u_j$

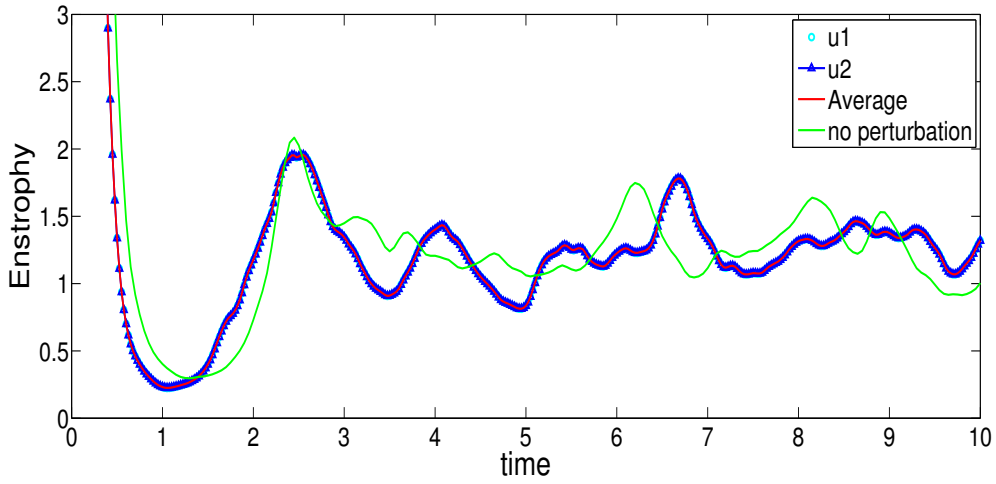

Figure 40: Enstrophy, $\nu = 1/800$, $\Delta t = 0.025$.

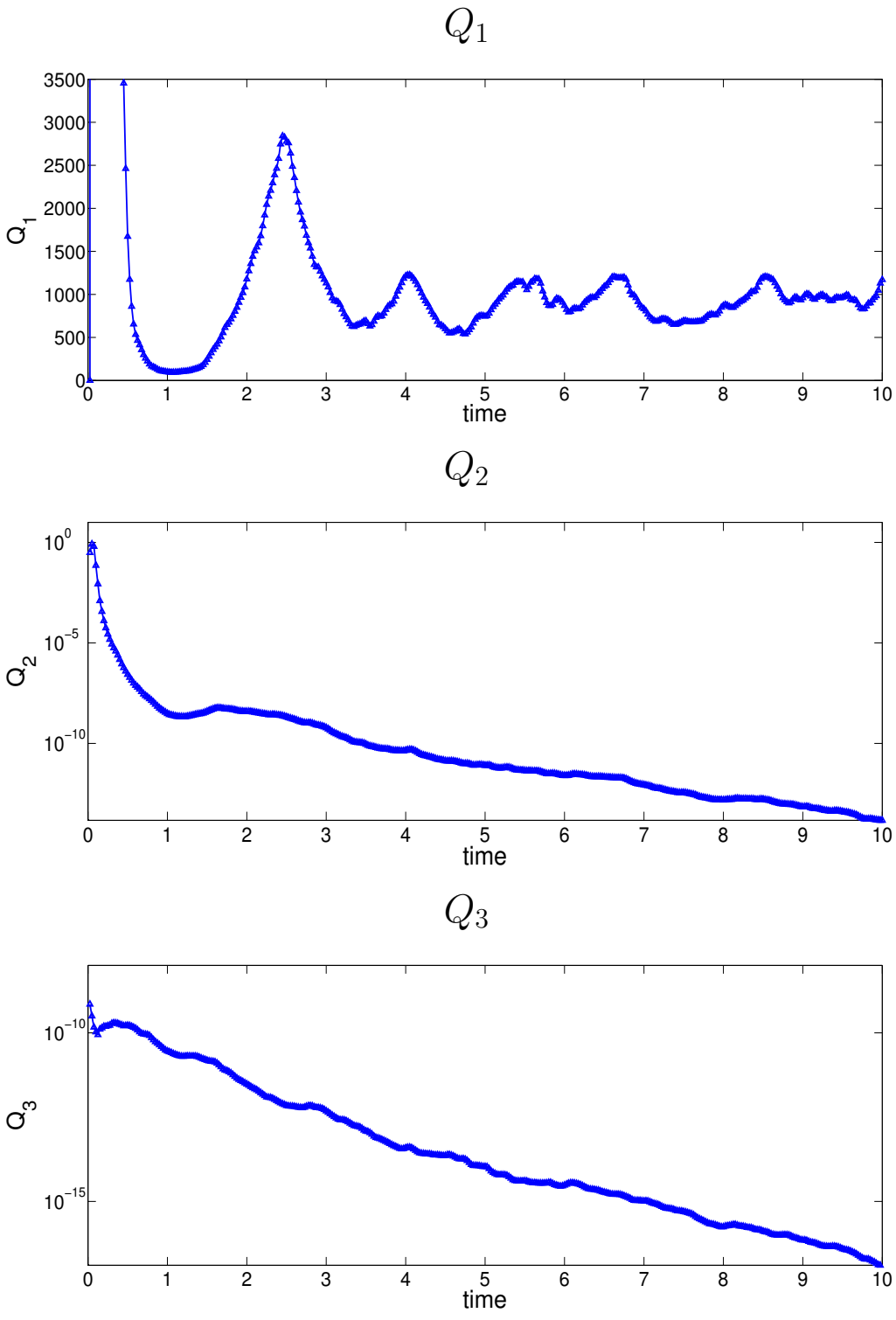

Figure 41: $\nu = 1/800$, $\Delta t = 0.025$, without $u_j' \cdot \nabla u_j$

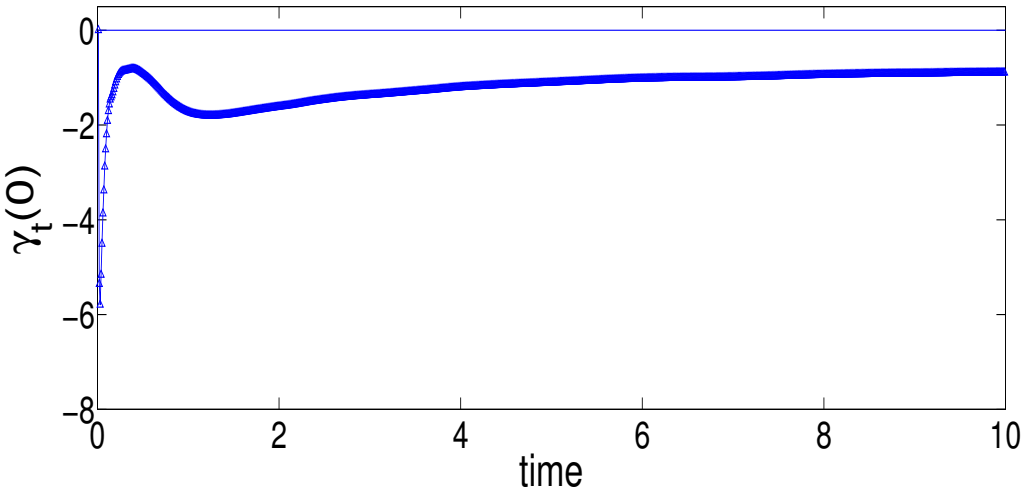

Figure 42: Averaged, effective Lyapunov exponent, $\nu = 1/800$, $\Delta t = 0.01$.

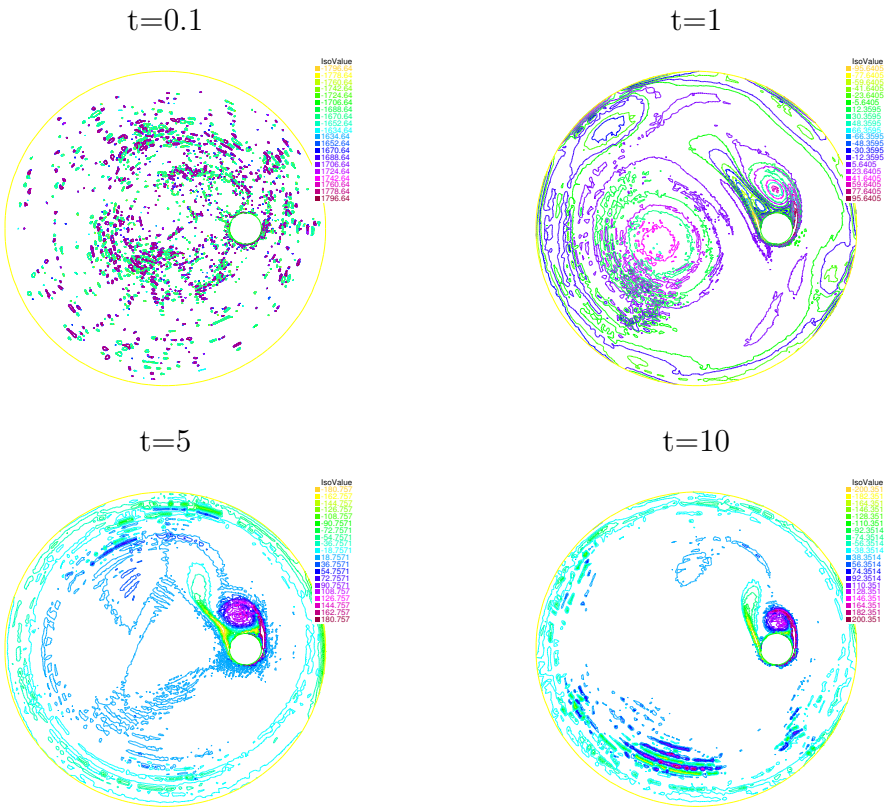

Figure 43: Vorticity, $\nu = 1/800$, $\triangle t = 0.01$.

6.7 CONCLUSIONS AND OPEN QUESTIONS

In fluid dynamics it is uncommon for numerical tests to be unequivocal and not unknown for unequivocal tests to be incorrectly interpreted. With this warning in mind, the initial tests suggest that the method (6.0.1) functions as a very effective conventional turbulence model. Simply adding an EV term to each NSE realization means including the $u_j' \cdot \nabla u_j$ term, [54]. In this case, EV functions as a numerical regularization. There are applications where a CTM solution (at reduced cost) is desired and where information about fluctuations about the mean (obtainable from the numerical regularization approach) are desired. Thus, both are potentially useful and worthy of further study. The theory and the (simple) tests herein show (Figures 39, 40, 42) that the solution remains much closer to the unperturbed solution and converges to a time averaged statistical equilibrium. (Compare the Lyapunov exponents of the model (6.0.1) in Figure 42 herein to those of the regularization, Figure 8 in [55].) Ensemble simulations with different realization equations provide very effective numerical regularizations and conventional turbulence models.

There are applications such as uncertainty quantification and sensitivity analysis in which calculation of an ensemble of solutions is an essential step. With these applications, developing turbulence models from the calculated ensemble (at reduced cost based on block methods) is promising. The methods in this report, as their next step, should be tested in more complex turbulent flow benchmark problems.

7.0 CONCLUSIONS AND FUTURE WORK

The need for ensemble calculations arises in calculation of sensitivities by differences [75], uncertainty quantification [67], stochastic NSE simulations [73], generation of bred vectors and their use in improving forecasting skill, Kalnay [89]. The most efficient way to calculate such an ensemble will vary widely depending on the application, flow, computational resources and code used. In this work we have presented and analyzed an algorithm for computation of an ensemble of solutions such that each step requires the solution of one linear system with multiple right hand sides. We also analyze an efficient ensemble regularization algorithm for under-resolved and convection dominated flows (including ones at higher Reynolds numbers). Computing an ensemble simultaneously allows each realization to access ensemble data. This allows use of means and fluctuations in regularizations used for each realization. The combined approach of ensemble time stepping and ensemble regularizations allows direct calculation of the turbulent viscosity coefficient and gives an unconditionally stable algorithm. It also suggests reconsidering an old but not as well developed definition of the mixing length. This mixing length vanishes at solid walls without van Driest damping, increases stability and improves flow predictions in our preliminary tests.

In applications such as the climate and ocean forecasts, which involve both turbulent flows and long time integration, higher order methods incorporating turbulence models are indispensable. We present a second order method to compute flow ensembles at less cost. The ensemble mean must be adapted to be compatible with the time discretization. Numerical tests indicate its potential use in exploring various aspects of turbulent flows such as turbulence intensity, Dirichlet quotients and effective Lyapunov exponents.

In Chapter 6 we develop an ensemble or statistical eddy viscosity model. The model is parameterized by an ensemble of solutions of an ensemble-Leray regularization. The

combined approach of ensemble time stepping and ensemble eddy viscosity modeling allows direct parametrization of the turbulent viscosity coefficient that gives an unconditionally stable algorithm. We prove that the model's solution approaches statistical equilibrium as $t \to \infty$; the model's variance $\to 0$ as $t \to \infty$. The ensemble method is used to interrogate a rotating flow, testing its predictability by computing effective averaged Lyapunov exponents.

Simply adding an EV term to each NSE realization means including the $u_j' \cdot \nabla u_j$ term. In this case, EV functions as a numerical regularization. There are applications where a CTM solution (at reduced cost) is desired and where information about fluctuations about the mean (obtainable from the numerical regularization approach) are desired. Thus, both are potentially useful and worthy of further study. The theory and the (simple) tests herein show (Figures 39, 40, 42) that the solution remains much closer to the unperturbed solution and converges to a time averaged statistical equilibrium. (Compare the Lyapunov exponents of the model (6.0.1) in Figure 42 herein to those of the regularization, Figure 8 in [55].) Ensemble simulations with different realization equations provide very effective numerical regularizations and conventional turbulence models.

Since this is a very recent topic, many questions and challenges are still open. The following are a few ideas for future research.

- **Simulations with 3D Channel flow:** The ensemble based turbulence models need to be tested with 3D benchmark problems. To develop 3D Channel flow simulation to further explore their strengths and limits is an open problem.
- **Efficiency:** Testing the efficiency of our algorithm with ensemble of large size is an open problem. It requires embedding external code for solving linear systems with multiple right hand sides to our existing FreeFem code.
- **Application in Atmospheric models:** Exploring the use of our algorithm in more complex settings is important. The next step is to study the primitive equations used in Atmospheric models.
- **Ensemble Kalman filter:** The ensemble Kalman filter (EnKF) is a recursive filter suitable for problems with a large number of variables, such as discretizations of partial differential equations in geophysical models. It is now an important data assimilation component of ensemble forecasting. Exploring the connections between my work and

statistical approaches in data assimilation, especially EnKF, which is currently one of the most popular methods, is important.

- **Implementation of Bred Vector algorithm:** The Bred Vector algorithm is commonly used to generate initial conditions in operational weather forecasting. It selects a minimal set of ensemble members capturing maximal spread of the resulting forecast. The combination of this algorithm and our ensemble simulation methods (and its use in climate modeling) is an important open problem.
- **Connection to Model Reduction** Proper Orthogonal Decomposition is now a popular approach for model reduction. It has found its increasing applications in computationally processing large amounts of high-dimensional data with the aim of obtaining low-dimensional descriptions that capture much of the phenomena of interest. Exploring its connections to my work is an open problem.

BIBLIOGRAPHY

[1] U.M. Ascher, S.J. Ruuth and W.T.R. Wetton, *Implicit-explicit methods for time-dependent partial differential equations*, SIAM J. Numer. Anal., 32 (1995), 797-823.

[2] M. Anitescu and W.J. Layton, *Sensitivities in large eddy simulation and improved estimates of turbulent flow functionals*, SIAM Journal of Scientific Computing, 29 (2007), 1650-1667.

[3] G. Alfonsi, *Reynolds-averaged Navier-Stokes equations for turbulence modeling*, Applied Mechanics Reviews, 62 (2009), 1-20.

[4] O. Axelsson, *A survey of preconditioned iterative methods for linear systems of algebraic equations*, BIT, 25 (1985), 166-187.

[5] L.C. Berselli and F. Flandoli, *On a stochastics approach to eddy viscosity models for turbulent flows*, Adv. Math. Fluid Mech., (2010), 55-81.

[6] G. Boffetta, A. Celani, A. Crisanti and A. Vulpiani, *Predictability in two dimensional decaying turbulence*, Physics Fluids, 9 (1997), 724-734.

[7] S. Brenner and R. Scott, *The Mathematical Theory of Finite Element Methods*, Springer, 3rd edition, 2008.

[8] L.C. Berselli, *On the large eddy simulation of the Taylor-Green vortex*, J. Math. Fluid Mech., 7 (2005), 164-191.

[9] J. Borggaard, T. Iliescu and J.P. Roop, *A bounded artificial viscosity large eddy simulation model*, SIAM J. Numer. Anal., 47 (2009), 622-645.

[10] L. Botti and D.A. Di Pietro, *A pressure-correction scheme for convection-dominated incompressible flows with discontinuous velocity and continuous pressure*, J. Comp., Phys., 230 (2010), 572-585.

[11] E. Burman and A. Linke, *Stabilized finite element schemes for incompressible flow using Scott–Vogelius elements*, Applied Numerical Mathematics, 58 (2008), 1704-1719.

[12] L.C. Berselli, T. Iliescu and W. Layton, *Mathematics of Large Eddy Simulation of Turbulent Flows*, Springer, Berlin, 2006.

[13] D. Barbato, L.C. Berselli, and C.R. Grisanti, *Analytical and numerical results for the rational large eddy simulation model*, J. Math. Fluid Mech., 9 (2007), 44-74.

[14] B. Rollin, Y. Dubief and C.R. Doering, *Variations on Kolmogorov flow: turbulent energy dissipation and mean flow profiles*, J. Fluid Mech., 670 (2011), 204-213.

[15] D. Carati, M.M. Rogers and A.A. Wray, *Statistical ensemble of large eddy simulation*, JFM, 455 (2002), 195-212.

[16] A.J. Chorin, *Numerical solution for the Navier-Stokes equations*, Math. Comp., 22 (1968), 745-762.

[17] M. Carney, P. Cunningham, J. Dowling and C. Lee, *Predicting probability distributions for surf height using an ensemble of mixture density networks*, International Conference on Machine Learning, 2005.

[18] S.H. Cheung, T.A. Oliver, E.E. Prudencio, S. Prudhomme, and R.D. Moser, *Bayesian uncertainty analysis with applications to turbulence modeling*, Reliability Engineering And System Safety, 96 (2011), 1137-1149.

[19] B. Cockburn, G. Kanschat and D. Schötzau, *A note on discontinuous Galerkin divergence-free solutions of the Navier-Stokes equations*, J. Sci. Comput., 31 (2007), 61-73.

[20] M. Case, V. Ervin, A. Linke and L. Rebholz, *A connection between Scott-Vogelius elements and grad-div stabilization*, SINUM, 49 (2011), 1461-1481.

[21] T. Chacon-Rebollo and R. Lewandowski, *Mathematical and Numerical Foundations of Turbulence Models and Applications*, Springer, New York, 2014.

[22] A. Cheskidov, D. D. Holm, E. Olson and E. S. Titi, *On a Leray- α model of turbulence*, Royal Society London, Proceedings, Series A, Mathematical, Physical and Engineering Sciences, 461 (2005), 629-649.

[23] A. Du and J. Duan, *A stochastic approach for parameterizing unresolved scales in a system with memory*, Journal of Algorithms and Computational Technology, 3 (2009), 319-405.

[24] J. Duan and B. Nadiga, *Stochastic parameterization for large eddy simulation of geophysical flows*, Proc. American Math. Soc., 135 (2007), 1187-1196.

[25] P.A. Durbin and B.A. Petterson Reif, *Statistical Theory and Modeling for Turbulent Flows*, Second Edition, Wiley, Chichester, 2011.

[26] C.R. Doering and J.D. Gibbon, *Applied Analysis of the Navier-Stokes Equations*, Cambridge U. Press, 1995.

[27] C. Ethier and D. Steinman, *Exact fully 3D Navier-Stokes solutions for benchmarking*, Int. J. Numer. Methods Fluids, 19 (1994), 369-375.

[28] R.M. Errico, R. Langland and D.P. Baumhefner, *The workshop on atmospheric predictability*, Bull. Amer. Meteor. Soc., 74 (2002), 1341-1343.

[29] R.W. Freund and M. Malhotra, *A block QMR algorithm for non-Hermitian linear systems with multiple right-hand sides*, Lin. Alg. Appl., 254 (1997), 119-157.

[30] P.F. Fischer, *Projection techniques for iterative solution of Ax=b with successive right-hand sides*, CMAME, 163 (1998), 193-204.

[31] R.W. Freund and M. Malhotra, *A block QMR algorithm for non-Hermitian linear systems with multiple right-hand sides*, Linear Algebra and its Applications, 254 (1997), 119-157.

[32] Y. T. Feng, D. R. J. Owen and D. Peric, *A block conjugate gradient method applied to linear systems with multiple right hand sides*, Comp. Meth. Appl. Mech. & Engng., 127 (1995), 203-215.

[33] C. Foias, O. P. Manley, R. Rosa, and R. Temam, *Navier-Stokes Equations and Turbulence*, Encyclopedia of Mathematics and its Applications, Vol. 83, Cambridge University Press, Cambridge, 2001.

[34] C. Greif, D. Li, D. Schötzau and X. Wei, *A mixed finite element method with exactly divergence-free velocities for incompressible magnetohydrodynamics*, Comput. Methods Appl. Mech. Engrg., 199 (2010), 2840-2855.

[35] J.D. Giraldo and S.G. García Galiano, *Building hazard maps of extreme daily rainy events from PDF ensemble, via REA method, on Senegal River Basin*, Hydrology and Earth System Sciences, 15 (2011), 3605-3615.

[36] B.J. Geurts and D.D. Holm, *Leray and LANS-α modelling of turbulent mixing*, Journal of turbulence, 7 (2006), 1-33.

[37] V. Girault and P. Raviart, *Finite Element Approximation of The Navier-Stokes Equations*, Lecture Notes in Mathematics, Vol. 749, Springer, Berlin, 1979.

[38] M.D. Gunzburger, *Finite Element Methods for Viscous Incompressible Flows - A Guide to Theory, Practices, and Algorithms*, Academic Press, 1989.

[39] E. Gallopulos and V. Simoncini, *Convergence of BLOCK GMRES and matrix polynomials*, Lin. Alg. Appl., 247 (1996), 97-119.

[40] A.E. Green and G.I. Taylor, *Mechanism of the production of small eddies from larger ones*, Proc. Royal Soc. A., 158 (1937), 499-521.

[41] J.L. Guermond and L. Quartapelle, *On stability and convergence of projection methods based on pressure Poisson equation*, IJNMF, 26 (1998), 1039-1053.

[42] M. Ghil, R. Benzi and G. Parisi, *Turbulence and Predictability in Geophysical Fluid Dynamics and Climate Dynamics*, North Holland, Amsterdam, 1985.

[43] B. J. Geurts and D. D. Holm, *Regularization modeling for large eddy simulation*, Physics of fluids, 15 (2003), 13-16.

[44] J.-L. Guermond and S. Prudhomme, *On the construction of suitable solutions of the Navier-Stokes equations and questions regarding the definition of large eddy simulation*, Physica D, 207 (2005), 64-78.

[45] A. Hasegawa, *Self-organization processes in continuous media*, Adv. Physics, 34 (1985), 1-42.

[46] M. Hairer and J.C. Mattingly, *Ergodicity of the 2D Navier-Stokes equations with degenerate stochastic forcing*, Annals of Math., 164 (2006), 993-1032.

[47] T. J. R. Hughes, L. Mazzei, and K. E. Jansen, *Large eddy simulation and the variational multiscale method*, Computing and Visualization in Science, 3 (2000), 47-59.

[48] E. Hopf, *Statistical hydromechanics and functional calculus*, J. Rational Mech. Anal., 1 (1952), 87-123.

[49] T.M. Hamill, J.S. Whitaker, M. Fiorino, S.E. Koch and S.J. Lord, *Increasing NOAA's computational capacity to improve global forecast modeling*, NOAA White Paper, 19 July 2010.

[50] F. Hecht, *New development in freefem++*, J. Numer. Math. 20 (2012), no. 3-4, 251-265.

[51] V. John, *Large Eddy Simulation of Turbulent Incompressible Flows. Analytical and Numerical Results for a Class of LES Models*, LN in CSE, 34, Springer-Verlag, Berlin, 2004

[52] V. John and W. Layton, *Analysis of numerical errors in large eddy simulation*, SIAM JNA, 40 (2002), 995-1020.

[53] N. Jiang and W. Layton, *An algorithm for fast calculation of flow ensembles*, International Journal for Uncertainty Quantification, 4 (2014), 273-301.

[54] N. Jiang and W. Layton, *Numerical analysis of two ensemble eddy viscosity models of fluid motion*, to appear: Numerical Methods for Partial Differential Equations, 2014, DOI: 10.1002/num.21908.

[55] N. Jiang, *A higher order ensemble simulation algorithm for fluid flows*, to appear: Journal of Scientific Computing, 2014, DOI: 10.1007/s10915-014-9932-z.

[56] N. Jiang, S. Kaya and W. Layton,*Analysis of Model Variance for Ensemble Based Turbulence Modeling*, submitted, 2014, available at: http://www.mathematics.pitt.edu/sites/default/files/ETM24April.pdf.

[57] D. Jackson and B. Launder, *Osborne Reynolds and the publication of his Papers on turbulent flow*, Annu. Rev. Fluid Mech., 39 (2007), 19-35.

[58] G. Karniadakis, M. Israeli and S. Orszag, *High-order splitting methods for the incompressible Navier-Stokes equations*, J. Comput. Phys., 97 (1991), 414-443.

[59] E. Kalnay, *Atmospheric Modelling, Data Assimilation and Predictability*, Cambridge, UK, 2003.

[60] J.M. Lewis, *Roots of ensemble forecasting*, Monthly Weather Rev., 133 (2005), 1865-1885.

[61] W. Layton, L. Rebholz and C. Trenchea, *Modular nonlinear filter stabilization of methods for higher Reynolds number flow*, J. Mathematical Fluid Mechanics, 14 (2012), 325-354.

[62] O.P. Le Maitre and O.M. Kino, *Spectral Methods for Uncertainty Quantification*, Springer, Berlin, 2010.

[63] W. Layton and L. Tobiska, *A two-level method with backtracking for the Navier–Stokes equations*, SINUM, 35 (1998), 2035-2054.

[64] W. Layton, *The 1877 Boussinesq conjecture: Turbulent fluctuations are dissipative on the mean flow*, Technical Report, Department of Mathematics, University of Pittsburgh, March 2014, available at: http://www.mathematics.pitt.edu/sites/default/files/ExpandedBoussinesqHypothesis.pdf.

[65] J. Leray, *Essay sur les mouvements plans d'une liquide visqueux que limitent des parois*, J. Math. Pur. Appl., Paris Ser. IX, 13 (1934), 331-418.

[66] J. Leray, *Sur les mouvements d'une liquide visqueux emplissant l'espace*, Acta Math., 63 (1934), 193-248.

[67] M. Leutbecher and T.N. Palmer, *Ensemble forecasting*, J. Comp. Phys., 227 (2008), 3515-3539.

[68] R. Lewandowski, *The mathematical analysis of the coupling of a turbulent kinetic energy equation to the Navier-Stokes equation with an eddy viscosity*, Nonlinear Analysis, 28 (1997), 393-417.

[69] W. Layton, C. Manica, M. Neda and L. Rebholz, *Numerical analysis and computational testing of a high-order Leray-deconvolution turbulence model*, Numerical Methods for Partial Differential Equations, 24 (2008), 555-582.

[70] W. Layton and R. Lewandowski, *Analysis of an eddy viscosity model for large eddy simulation of turbulent flows*, Journal of Mathematical Fluid Dynamics, 4 (2002), 374-399.

[71] H.K. Moffatt and A. Tsinober, *Helicity in laminar and turbulent flow*, Ann. Rev. Fluid Mech., 24(1992), 281-312.

[72] A. Majda and X. Wang, *Nonlinear Dynamics and Statistical Theories for Basic Geophysical Flows*, Cambridge, UK, 2006.

[73] L. Moriconi and R. Rosa, *Theoretical aspects of homogeneous isotropic turbulence*, J. Braz. Soc. Mech. Sci. & Eng., 26 (2004), 391-399.

[74] A. Majda and X. Wang, *Nonlinear Dynamics and Statistical Theories for Basic Geophysical Flows,* Cambridge, 2006.

[75] W.J. Martin and M. Xue, *Initial condition sensitivity analysis of a mesoscale forecast using very-large ensembles*, Mon. Wea. Rev., 134 (2006), 192-207.

[76] B. Mohammadi and O. Pironneau, *Analysis of the K-Epsilon Turbulence Model*, John Wiley and Sons, New York, 1994.

[77] A.S. Monin and A.M. Yaglom,*Statistical Fluid Mechanics, Mechanics of Turbulence, Vol.1 and Vol. 2*, Dover, Mineola, 1971 and 1975.

[78] D.P. O'Leary, *The block conjugate gradient algorithm and related methods*, Lin. Alg. Appl., 29 (1980), 292-322.

[79] D. P. O'Leary, *The block conjugate gradient algorithm and related methods*, Linear Algebra and its Applications, 29 (1980), 293–322.

[80] M. Olshanskii and A. Reusken, *Grad-Div stabilization for the Stokes equations,* Math. of Comp., 73 (2004), 1699-1718.

[81] M.A. Olshanskii and L.G. Rebholz, *Velocity-vorticity-helicity formulation and a solver for the Navier-Stokes equations*, J. Comp, Phys., 229 (2010), 4291-4303.

[82] S.B. Pope, *Turbulent Flows*, Cambridge Univ. Press, Cambridge, 20002

[83] H.-G. Roos, M. Stynes and L. Tobiska, *Numerical Methods for Singularly Perturbed Differential Equations*, Springer, Berlin, 1996.

[84] R. Rosa, *Some results on the Navier-Stokes equations in connection with the statistical theory of stationary turbulence*, Applications of Mathematics, 47 (2002), 485-516.

[85] P. Sagaut, *Large Eddy Simulation for Incompressible Flows*, Springer, Berlin, 2001.

[86] D. J. Stensrud, *Parameterization Schemes: Keys to Numerical Weather Prediction Models*, Cambridge U. Press, 2009.

[87] G.I. Taylor, *On decay of vortices in a viscous fluid*, Phil. Mag., 46 (1923), 671-674.

[88] D. Tafti, *Comparison of some upwind-biased high-order formulations with a second order central-difference scheme for time integration of the incompressible Navier-Stokes equations*, Comput. & Fluids, 25 (1996), 647-665.

[89] Z. Toth and E. Kalnay, *Ensemble forecasting at NMC: The generation of perturbations*, Bull. Amer. Meteor. Soc., 74 (1993), 2317-2330.

[90] E. van Groesen, *Time-Asymptotics and the self organization hypothesis for the 2d Navier-Stokes equations*, Physica, 48A (1998), 312-320.

[91] J. Varah, *Stability restrictions on second-order, three level finite difference schemes for parabolic equations*, SIAM J. Numer. Anal., 17 (1980), 300-309.

[92] R. Verfürth , *On the constants in some inverse inequalities for finite element functions*, Report, Universität Bochum, May 1999.

[93] X. Wang, *An efficient second order in time scheme for approximating long time statistical properties of the two dimensional Navier-Stokes equations*, Numer. Math., 121 (2012), 753-779.

[94] H. Wan, M.A. Giorgetta, and L. Bonaventura, *Ensemble Held-Suarez test with a spectral transform model: variability, sensitivity and convergence*, Mon. Wea. Rev., 136 (2008), 1075-1092.

[95] O. Walsh, *Eddy solutions of the Navier-Stokes equations*, pp. 306-309, in: *The Navier-Stokes Equations II - Theory and Numerical Methods*, Lecture Notes in Mathematics, Volume 1530, 1992.

[96] F.J. Walburn, H.N. Sabbah and P.D. Stein, *An experimental evaluation of the use of an ensemble average for the calculation of turbulence in pulsatile flow*, Ann Biomed Eng., 11 (1983), 385-399.

[97] S. Zhang, *A family of Qk+1, k×Qk, k+1 divergence-free finite elements on rectangular grids*, SIAM J. Numer. Anal., 47 (2009), 2090-2107.